AD-A190 965 ADAPTIVE SEGMENTATION EVALUATION(U) MARTIN MARIETTA 1/2
AEROSPACE ORLANDO FL R PATTON 24 SEP 87 OR-19130
DAAL02-85-C-0084
UNCLASSIFIED F/G 20/6 NL

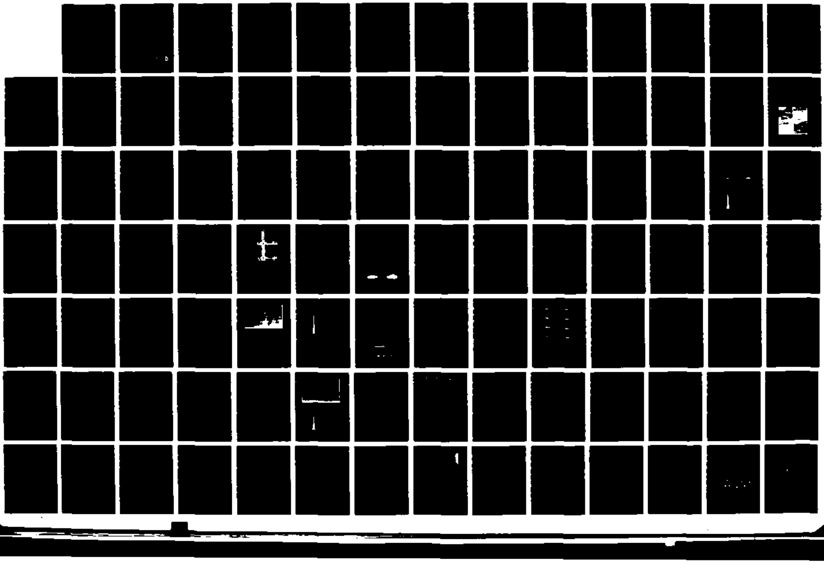

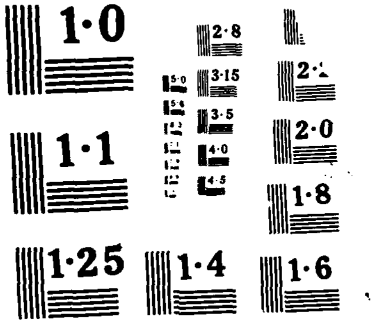
1·0
2·8
3·15
3·5
4·0
4·5
5·0
2·2
2·0
1·1
1·8
1·25
1·4
1·6

(2)

DTIC FILE COPY

ADAPTIVE SEGMENTATION EVALUATION
FINAL REPORT

OR 19,130

January 1988

AD-A190 965

Reporting Period: 1 January 1987 to 31 August 1987

Contract DAAL02-85-C-0084

Expiration Date of Contract: 31 August 1987

Effective Date of Contract: 22 July 1985

Sponsored By:

Defense Advanced Research Projects Agency (DoD)
DARPA Order No.

Monitored By: Joe Kitrosser (CNVEO)

Prepared For:

Center for Night Vision and Electro-Optics
AMSEL-RD-NV-AC-SIPT
Fort Belvoir, Virginia 22060-5677

Distribution of this document is unlimited and unrestricted.
Requests for this document must be referred to:

Director
USA ERADCOM
Night Vision & Electro-Optics Center
ATTN: AMSEL-RD-NV-AC-SIPT
Fort Belvoir, Virginia 22060

The views and conclusions contained in this document are those of the authors and should not be interpreted as necessarily representing the official policies, either expressed or implied, of the Defense Advanced Research Projects Agency or the U.S. Government.

Denmer Baxter (305) 356-3331

Martin Marietta Electronic Systems
P.O. Box 628007
Orlando, Florida 32862-8007

DTIC
ELECTE
FEB 0 2 1988
S D
H

88 1 27 073

UNCLASSIFIED
SECURITY CLASSIFICATION OF THIS PAGE

REPORT DOCUMENTATION PAGE

1a. REPORT SECURITY CLASSIFICATION UNCLASSIFIED

1b. RESTRICTIVE MARKINGS

2a. SECURITY CLASSIFICATION AUTHORITY

2b. DECLASSIFICATION/DOWNGRADING SCHEDULE

3. DISTRIBUTION/AVAILABILITY OF REPORT Unlimited/Unrestricted

4. PERFORMING ORGANIZATION REPORT NUMBER(S) 19, [illegible] 130

5. MONITORING ORGANIZATION REPORT NUMBER(S)

6a. NAME OF PERFORMING ORGANIZATION
Martin Marietta Corporation
Orlando Aerospace

6b. OFFICE SYMBOL *(If applicable)*

7a. NAME OF MONITORING ORGANIZATION Center for Night Vision and Electro-Optics

6c. ADDRESS *(City, State and ZIP Code)*
P.O. Box 628007
Orlando, FL 32862-8007

7b. ADDRESS *(City, State and ZIP Code)*
AMSEL-RD-NV-AC-SIPT
Fort Belvoir, Virginia 22060-5677

8a. NAME OF FUNDING/SPONSORING ORGANIZATION DARPA/CNVEO

8b. OFFICE SYMBOL *(If applicable)*

9. PROCUREMENT INSTRUMENT IDENTIFICATION NUMBER DAAL02-85-C-0084

8c. ADDRESS *(City, State and ZIP Code)*
ATTN: AMSEL-RD-NV-AC-SIPT
Fort Belvoir, VA 22060

10. SOURCE OF FUNDING NOS.

PROGRAM ELEMENT NO.	PROJECT NO.	TASK NO.	WORK UNIT NO.

11. TITLE *(Include Security Classification)* Adaptive Segmentation Evaluation-Unclassified

12. PERSONAL AUTHOR(S) Ron Patton

13a. TYPE OF REPORT Final

13b. TIME COVERED FROM Jan 1987 TO Aug 1987

14. DATE OF REPORT *(Yr., Mo., Day)* 1987, 9, 24

15. PAGE COUNT

16. SUPPLEMENTARY NOTATION

Technical monitor: Joe Kitrosser (CNVEO)

17. COSATI CODES

FIELD	GROUP	SUB. GR.

18. SUBJECT TERMS *(Continue on reverse if necessary and identify by block number)*

Segmenter performance
Characterization metrics
Motion extraction; multiframe data integration.

19. ABSTRACT *(Continue on reverse if necessary and identify by block number)*

Phase 2 of the Adaptive Segmentation contract addressed the issue of improving segmenter performance on military vehicles in IR imagery through the use of temporal processing techniques.

The approach concentrated on developing techniques for image data stabilization through the use of multiframe data integration. The most important aspect of multiframe data integration is its ability to increase frame to frame data stability and reduce noise. These properties have two important consequences: First, the improved signal quality greatly reduces the need for special purpose processing by each ATR component to overcome the image ambiguities found in the raw data. Second, features that represent higher levels of structural detail usually masked by noise can be computed for improved object discrimination and classification performance.

20. DISTRIBUTION/AVAILABILITY OF ABSTRACT
UNCLASSIFIED/UNLIMITED ☐ SAME AS RPT. ☒ DTIC USERS ☐

21. ABSTRACT SECURITY CLASSIFICATION Unclassified

22a. NAME OF RESPONSIBLE INDIVIDUAL Ron Patton

22b. TELEPHONE NUMBER *(Include Area Code)* (305) 356-9516

22c. OFFICE SYMBOL

DD FORM 1473, 83 APR EDITION OF 1 JAN 73 IS OBSOLETE

UNCLASSIFIED
SECURITY CLASSIFICATION OF THIS PAGE

SUMMARY

Task Objectives

Phase 2 of the Adaptive Segmentation Evaluation contract addressed the issue of improving the segmenter performance on military vehicles in ~~IR~~ → [illegible] imagery through the use of temporal processing techniques. The specific objectives were as follows:

1. Develop temporal-based techniques to augment current segmentation algorithms
2. Develop a set of metrics to quantitatively represent segmenter performance in terms of quality and consistency of segmentation
3. Perform a comparative study of performance results between the modified segmentation approach and the unaided approach.

Technical Problems

A study of the usefulness of dynamic scene information is necessary to fully evaluate the options associated with temporal-based segmentation techniques. The purpose of this study is to identify those attributes that are most readily applicable to segmentation. Subsequent modifications to the segmentation algorithm will depend on the type of information available and the optimum point of application.

General Methodology

Two basic approaches for using temporal properties were assessed. Each of these approaches is based on a different definition of the segmentation problem. One definition states that inconsistent segmentation results are due primarily to the inherent sensitivity of the algorithm methodology. For this definition, the solution would be to enhance the

on For
A&I ☑
☐
ed ☐
Distribution/
Availability Codes
Dist | Avail and/or Special
A-1

algorithm. The second definition states that the difficulty in developing an algorithm that generates consistent results is due to the high degree of data variation between frames. For this definition, the solution would be to stabilize the data. An analysis of a single metric, ERIM's TIR^2, computed for two military vehicles (tanks A and B) over a sequence of 20 consecutive frames indicates that data variation (tank B varies over a range of 71.21) not algorithm sensitivity, is the problem (Figure 1).

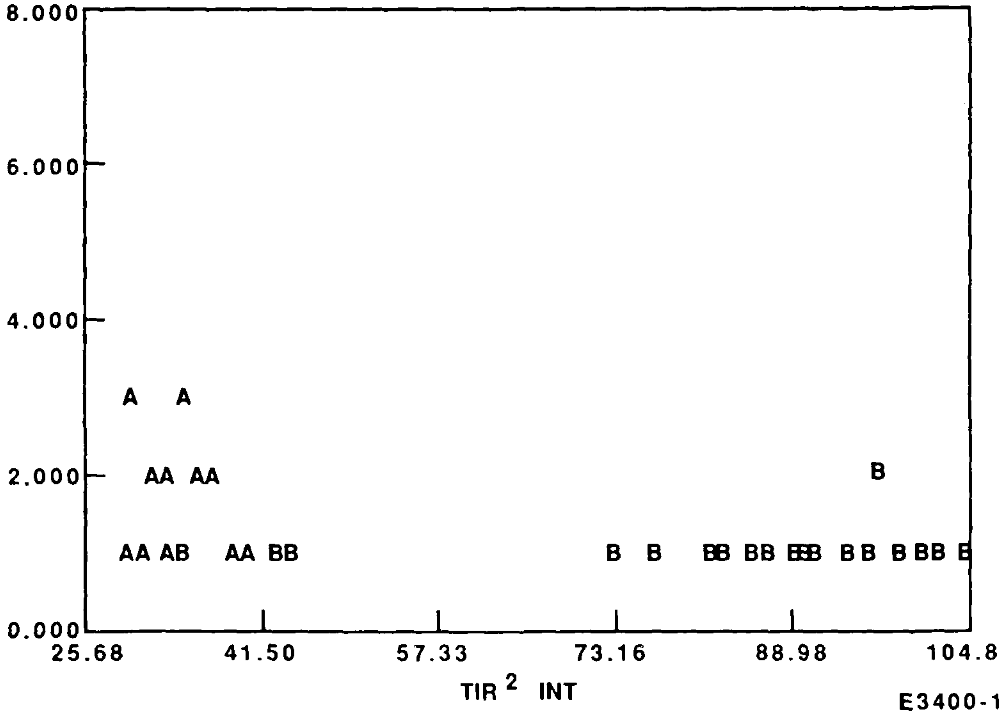

Figure 1. Variations of TIR^2 Over the 20-Frame Set for Tank A and Tank B

For this reason, the methodology concentrated on developing techniques for image data stabilization rather than segmenter enhancement. The justification for adopting this methodology is that a more consistent input signal would obviate the need for special case processing by the segmentor. Image data stabilization was accomplished through the use of multiframe data integration techniques. These techniques attempted to smooth the frame to frame transition of image data by limiting the noise effects and other image ambiguities.

Experimental Methods

A set of experiments was defined to assess the effects of multiframe data smoothing on vehicle signatures and segmenter performance. The experiments consisted of applying a multiframe data smoothing operator and an independent frame enhancement operator to three sets of consecutive sequences of ERIM truthed TI images. The rule directed segmenter was then applied to the raw data, smoothed data, and independently filtered data. Finally, a comparative analysis of segmenter performance was conducted by evaluating the segmenter stability metrics on each of the three data types; and data variations in vehicle signatures were analyzed from the results of the data variation metrics.

The filters used for the multiframe data smoothing experiments were the 1x1x5 median, 1x1x7 median, and 1x1x9 median. Smoothed data from the multiframe mean filter were not significantly different from the median to warrant extensive testing. The 3x3x1 median was used as the independent frame enhancement operator. This operator allowed comparison with a more conventional approach to noise reduction.

Discussion

In general, the experiments conducted on the test data sets confirmed the primary strengths of multiframe smoothing. Both the conventional and multiframe filtering improved segmentation results compared to those with the raw data results. The primary difference was in the behavior of the features computed on the three data types. The features computed on the raw data and conventionally filtered data showed random fluctuations and wide distributions, which is typical for FLIR data. The features computed on the multiframe smoothed data were better clustered and showed increased signal qualities. The improved feature organization and higher response reflect the increase in data stability and noise reduction. These results have two important consequences. First, the improved signal quality greatly reduces the need for special purpose processing by each automatic target recognition (ATR) component to compensate for image ambiguities in the raw data. Second, features that represent higher levels of structural detail, which are usually masked by noise, can be computed for improved object discrimination and classification performance.

Important Findings and Conclusions

The results clearly indicate the advantages of multiframe data smoothing. These results also emphasize the difficulties that exist when image characteristics are not well represented. When a sensor is in motion, scene information must be registered prior to processing. Bland image conditions do not provide sufficient feature information to track with the degree of accuracy required for multiframe integration. This situation represents a constraint of the multiframe approach.

The problem of bland image conditions is not solvable through the use of image enhancement techniques. Such techniques do not improve the fundamental elements represented in the data. These techniques mainly improve the aesthetics of the image. The bland-image problem must be addressed at the system level. A viable solution is to switch between multiframe processing and independent frame processing, based on the success of frame to frame feature tracking.

Implications For Further Research

The most important advantage of multiframe data smoothing is improved signal quality. This improvement increases segmenter performance and, more importantly, feature stability. The increased response and improved clustering of the metrics for the smoothed data images indicate the importance of this technique for object classification. A comparative study of feature selection, feature clustering, feature separability, and object classification between an ATR trained on raw-data images and smoothed-data images would provide a total assessment of multiframe data smoothing.

PREFACE

This report was prepared by Martin Marietta Corporation, Martin Marietta Electronic Systems, P.O. Box 628007, Orlando, Florida 32862-8007, under Contract DAAL02-85-C-0084, with the U.S. Army Center for Night Vision and Electro-Optics. Mr. Joe Kitrosser is the technical monitor for this program.

This evaluation was begun in July 1985 and was completed in August 1987. Ron Patton, (305) 356-9516, was the author and task leader.

TABLE OF CONTENTS

Page

1.0 OBJECTIVES AND APPROACH 1

2.0 OVERVIEW - JANUARY MONTHLY 3
2.1 Definition of Temporal Properties. 3
2.2 Advantage of Temporal Properties 4
2.3 Application of Temporal Properties 4

3.0 METRICS - FEBRUARY 7
3.1 Sensor Variation Metrics 7
3.2 Segmenter Stability Metric 8
3.3 Optical Flow Stability Metrics 9

4.0 SYSTEM APPROACH - MARCH 13
4.1 Extraction of Scene Motion 13
4.2 Flow Vector Selection. 22
4.3 Data Smoothing 23

5.0 EXPERIMENTS - APRIL, MAY, JUNE 26
5.1 Test Set 1 27
5.2 Test Set 2 39
5.3 Test Set 3 62

6.0 CONCLUSIONS AND RECOMMENDATIONS - JULY, AUGUST 77

1.0 OBJECTIVES AND APPROACH

Phase 2 of the Adaptive Segmentation effort was concerned with improving segmenter performance on military vehicles in IR imagery through the use of temporal processing techniques. The approach concentrated on developing methods for image data stabilization rather than segmenter enhancements. The logic being that a more consistent input signal would eliminate the need for special case processing by the segmentation operator. Image data stabilization was accomplished through the use of multiframe data integration techniques. These techniques attempt to smooth the frame to frame transition of image data by limiting the effects of noise and other image ambiguities.

To evaluate multiframe processing, a data base consisting of three sets of consecutive sequences of ERIM truthed TI imagery was created. A multiframe smoothing operator and an independent frame enhancement operator were applied to each of the data sets. A comparative analysis was performed on segmentation results for each set of consecutive sequences of unprocessed (raw) imagery, independently filtered (enhanced) imagery, and multiframe smoothed imagery. The frame-to-frame consistency was analyzed for both the structural properties of the vehicles and the segmentation results for each data set.

To assess the structural stability of a vehicle, a set of local intensity-based metrics was computed for each data type in a test set. The truth silhouettes provided by ERIM were used in computing the metric values. Structural consistencies were assessed by examining the variation in the distributions of each of the metrics. The process used the degree of frame to frame correlation of each metric to determine the structural stability in the data properties represented by the metrics. Variations in signal quality were determined by comparing the metrics for the two filtered image sets to the metrics for the raw imagery. The polarity of their differences indicated an increased or decreased signal response.

To assess segmenter performance, a comparative study was conducted using the rule directed segmenter (RDS) as the control algorithm and the segmentation accuracy metric of binary area cross correlation as the performance measure. For each test set, the RDS was applied to each of the three data types: the raw data, multiframe smoothed data, and independent frame enhanced data. Performance stability was determined by examining the degree of frame to frame consistency in the segmentation accuracy metric. Performance quality was measured by computing the average of the metric. Improvement in segmentation performance was determined by comparing the response of the metric for the two filtered image sets to that computed on the raw imagery.

2.0 TEMPORAL INFORMATION ANALYSIS

2.1 Definition of Temporal Properties

The utility of dynamic scene information is universal, extending to all elements in the target-recognizer system architecture (enhancement, detection, segmentation, feature extraction, and classification), as well as post-processor functions such as target prioritization, tracking, and aimpoint selection. The multiframe approach provides the opportunity to improve component-level performance and, subsequently, ATR performance. The overall utility of multiframe processing and the key attributes of dynamic scene information are summarized in Table 2.1-I. Table 2.1-I shows that two scene attributes, platform motion and temporal statistics, are most readily applicable to segmentation.

TABLE 2.1-I

Summary of Multiframe Processing and Dynamic Scene Information

Dynamic Scene Attribute	Application	Utility
Target motion	Moving target indication (MIT)	Motion as detection, segmentation cue Target velocity for prioritization, prediction, aspect, aimpoint Motion as context
Platform motion	Motion stereo	Scene normalization Passive ranging Terrain and object 3-D relief Navigation
Temporal statistics	Sequential compound decisions	Classification accuracy Consistent segmentation Adaptive preprocessor thresholds
Scene history	Scene prediction	A prior knowledge for next frame Environment evaluation Feedback and global control
All of the above	Intelligent tracking	Multitarget track Track through obscuration Reacquire after breaklock

The effects of platform motion on the imagery can be accurately determined by applying multiframe processing to the sequence of images. Motion is defined in terms of direction and magnitude of displacement. These parameters can be effectively used for frame to frame registration and scene normalization.

Temporal statistics of the dynamic scene improve performance by basing statistical decisions on ensemble data rather than single-event data. This capability provides adaptive optimization of image enhancement parameters and segmentation consistency.

2.2 Advantages of Temporal Properties

To recognize the advantages of using temporal context in image processing, the problems associated with single frame processing must be understood. The two major problems in image processing are data instability and image degradation.

For any given frame of information, an operator, such as a segmenter, determines the optimal result, based on the conditions represented in the data. If data conditions vary significantly from frame to frame, the operator's results will be inconsistent; and these inconsistencies propagate through each component of the ATR system, impacting overall performance.

A second problem associated with single frame processing is image degradation. Atmospheric effects such as attenuation, diffusion, and diffraction can affect image quality. Sensor effects such as lens distortion, focal length, and vibration; and effects associated with the pixelization process, can also affect image quality.

2.3 Application of Temporal Properties

For this application, multiframe data smoothing is defined as the process of operating on a "M" deep stack of registered images to reduce the independent random fluctuations in the data, while improving signal quality and stability. When this process is applied to an image g(x,y) that is formed by the addition of uncorrelated noise n(x,y), the noise component of that image decreases as the number of integrated images increases. The reduction in the random component is specified by the equation:

$$\sigma_{\bar{g}(x,y)} = \frac{1}{\sqrt{M}} \sigma_{n(x,y)}$$

where σ = standard deviation.

This equation shows that the reduction in noise is inversely proportional to the square root of the number of images (M). As the number of noisy images becomes large, the data quality approaches that of an uncorrupted signal. However, the benefits of using large numbers of images for noise reduction are limited by the natural constraints inherent in a moving sensor. Closure, magnification differences, changes in perspective, and information masking limit the number of images that can be effectively integrated. The number of images for multiframe smoothing is therefore determined by the range to the vehicles and the behavior of the sensor (aircraft, tank, etc.).

We have tested three data smoothing techniques: 1x1xn median, 1x1xn mean, and 1x1xn conditional mode-median. The "n" factor in the 1x1xn notation relates to the depth of the filter or number of stacked images.

One advantage of the 1x1xn median filter is that the median is not sensitive to single sample spike, noise, or other extremes that may exist in a sample set. Another advantage is that the number chosen to represent the sample set is a number which exists in the sample set. A third advantage is that the median is also a minimum distance number when computed as

$$\sum_{i=1}^{n} |X_i - A| = \text{MDN} \qquad \text{when } A = \text{median}$$

The 1x1xn mean filter has properties similar to the median when the samples are fairly related. Unlike the median, the mean filter considers all numbers in the sample set when computing a result. For this reason, the mean is sensitive to extremes for small sample sizes, and the number chosen to represent the sample set may not be an original member of the sample set. Like the median, the mean is also a minimum distance number when computed as

$$\sum_{i=1}^{n} (X_i - A)^2 \qquad \text{when } A = \text{mean}$$

The conditional 1x1xn mode-median filter optimizes the sample selection process. The median filter is used when a sample set contains unrelated numbers. When a single value occurs more than once in a sample set, the median result is replaced by the most repeated value or the mode. This process is similar to assigning a probability to each sample value. The selected value is either the highest probability number (mode) or the median (when equal probability exists).

3.0 DEFINITION OF METRICS

A set of metrics that assesses the behavior of information as a function of time were defined. The metrics fall into three general categories: sensor variation metrics, segmenter stability metrics, and optical flow stability metrics.

3.1 Sensor Variation Metrics

The sensor variation metrics statistically represent fluctuations in the raw data prior to any processing. These metrics indicate the degree of instability in the image acquisition process (from sensor to digital format). Since the metrics can only be computed on the digitized images, their results represent the accumulated effects of each processing component in the image acquisition system. System fluctuations are measured from the variations in thermal properties of the vehicles and their local background over a sequence of "n" consecutive images. The thermal properties of the object and the background for any given image are represented by the intensity-based metrics: entropy, contrast, TIR^2, and $TBIR^2$. By computing the variations of these metrics over "n" images, the metrics for entropy variation, contrast variation, TIR^2 variation, and $TBIR^2$ variation are derived. The variation (V) metrics are given by the equation:

$$V = \sqrt{\frac{\sum_{i=1}^{n} (C - \overline{C})^2}{n - 1}}$$

where C are the metric values, $\overline{C}$ is the average metric value, and n is the number of images.

"Characterization of ATR Performance in Relation to Image Measurements" (ATRWG working document 12-12-84) defines these four metrics to represent the fluctuations in object-to-background separability in terms of 1) average intensity (contrast), 2) background intensity variation (TIR^2), and 3) object and background intensity variation ($TBIR^2$ and entropy).

The sensor variation metrics show the effectiveness of data smoothing in stabilizing the signal (noise removal). The degree of data stability is determined by computing the percent change in variation before and after smoothing; (ΔV) which is given by

$$\Delta V = \frac{|C_s - C_r| \times 100\%}{C_r}$$

where C_s is the smoothed-data and C_r is the raw data.

3.2 Segmenter Stability Metric

The segmenter stability metric represents the ability of the segmenter to consistently perform over a sequence of "n" consecutive images. Consistent segmenter performance is defined as a result which is similar to the previously generated segmentation result, independent of the quality of the segmentation. This means that a segmenter, which consistently segments 50 percent of the object, would have a higher stability measure than one that oscillates between 70 and 90 percent. It also means that outputs of segmented objects where one is consistently 40 percent and the other consistently 90 percent have the same stability measure. The average quality of segmentation for each object is also computed. This combination of measures indicates the quality and stability of segmentation for each vehicle.

The segmenter stability metric is determined by computing the variation in the segmentation accuracy measure of binary area cross correlation (BACC) for each object over a sequence of "n" consecutive images. Segmenter stability (SS) is given by

$$SS = \sqrt{\frac{\sum_{x=1}^{n} (BACC - \overline{BACC})^2}{n-1}}$$

The segmenter stability metric is computed over the objects prior to and after data smoothing. The segmenter stability metric provides a good indication of the effectiveness of data smoothing in stabilizing the output segmentation. Success in achieving segmenter stability is determined by examining the values of the variation metric before and after smoothing, while the degree of success is measured by computing their percent of change. The percent change in segmenter stability (ΔSS) is given by

$$\Delta SS = \frac{|SS_s - SS_r| \times 100\%}{SS_r}$$

where SS_r is segmenter stability for smoothed data and SS_s is segmenter stability for raw data.

3.3 Optical Flow Stability Metrics

Optical flow is derived by recording the frame to frame displacement of a set of distinct features distributed throughout the image. A feature is selected according to its uniqueness, relative to other information in its local neighborhood. The type of information that features represent, such as a tree trunk, road segment, or manmade object, is completely scenario dependent. Scenarios that afford a high degree and variety of scene context are ideal for feature selection and matching. However, as scene conditions become indistinguishable, such as in a desert, the process of locating and tracking distinct features becomes very difficult.

The uniqueness factor of a selected feature is an important indicator of the likelihood of the system to correctly track that feature over time (sequence of "n" images). A measure of uniqueness is computed by examining the maximum response of a feature relative to the average response over its local neighborhood. The feature uniqueness (F) is given by

$$F = \frac{\text{maximum feature - mean feature}}{\text{feature variance}}$$

For example, if the feature of interest was contrast, then the local region representing the highest level of contrast would be selected. Feature uniqueness would be determined by computing the difference of highest contrast and average contrast normalized by the contrast variance. The feature-uniqueness metric is a measure of reliability when performing frame to frame registration for data smoothing. Low-uniqueness features have a higher probability of correlation error and subsequently registration error.

Successfully tracking the positional changes of selected features between consecutive images is accomplished by applying full-intensity area correlation. The degree of success in feature matching is indicated by the correlation coefficient [ρ(i,j)], which is given by

$$\rho(i,j) = \frac{\sum_{x,y}^{N,M} [R(x,y) - \bar{R}]\,[L(x-j,\ y-i) - \bar{L}]}{\sqrt{\sum_{x,y}^{N,M} [R(x,y) - \bar{R}]^2 \sum_{x,y}^{N,M} [L(x-j,\ y-i) - \bar{L}]^2}} \,.$$

The average correlation coefficient, which is computed over the "n" consecutive images, is a good indicator of the reliability of the (x,y) to its current location are required. A set of coefficients are computed using all the qualifying features. Each feature is then evaluated using the affine equation with the current set of coefficients. The feature with the greatest error is removed unless that error is less than 3.0, at which time the refinement process has been satisfied. If a feature has an error greater than 3.0, it is removed and the process is repeated with the remaining features. The refinement process terminates if the number of features is reduced to eight. Once the process has concluded, the features that were removed earlier are procesed one last time using the final set of affine coefficients. The quality of flow is derived by computing the average error of divergence D_{av} between the predicted location of each feature (using the affine derived optical flow model) and the actual translated location (Figure 3.3-1).

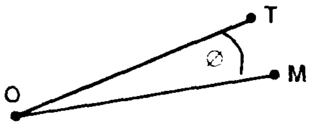

Where
O=Origin of Point
T=True point translation
M=Affine model of translation
∅=Angle of divergence, or affine error (error in pixels)

$$D_{av} = \frac{\sum_{i=1}^{n} \varnothing}{n}$$

Figure 3.3-1. Optical Flow Stability Metrics

correlation operator in solving the correspondence problem. The equation for correlation coefficient (Pa) is

$$P_a = \frac{\sum_{i=1}^{n} \rho}{n} \text{ is the average of this value.}$$

A final measure of optical flow stability is the quality of the global optical flow field. Global quality is expressed in terms of the level of agreement among tracked features in accurately representing the direction and magnitude of motion over the "n" images. The stability of flow is computed by the affine transform, which mathematically models the translation of the selected features over the "n" images. The equations for the transform in two dimensions is given by

$$x' = A_1 x + A_2 y + A_3$$

$$y' = B_1 x + B_2 y + B_3$$

If all features were accurately tracked, the affine transform would exactly model the optical flow field. However, as small inaccuracies in feature tracking occur (due to correlation errors), the affine transform can only approximate the optical flow field.

To determine the quality of optical flow, the affine transform is applied to the optical flow field each time a new image is processed. A record of the optical flow is maintained in a history file, which contains the direction and amount of motion that occurred for each feature being tracked. All features tracked for at least three images are evaluated. Those features that have less than three entries are omitted. The affine is only applied when at least eight features meet the three-image minimum criterion. To solve the affine equation, the location of each feature, which is three images prior to the current image, and the displacement

4.0 SYSTEM APPROACH

The most advantageous attribute of multiframe processing, as compared to independent frame processing, is the ability to integrate information acquired over a continuing sequence of imagery. When a sensor is stationary, the integration problem involves applying a data smoothing operator to stabilize the signal. However, when a sensor is in motion, the problem becomes more difficult. As a sensor moves, the information in the image (field of view) also moves. To accomplish multiframe integration in this context, the image smoothing operator must be preceded by frame to frame registration of the data. Since scenarios for this contract specify moving sensors, our system approach includes the extraction of scene motion followed by frame to frame registration.

To simplify the data registration process and limit registration errors, the data registration operator is only applied to subimage windows that pertain to the vehicle of interest. The window locations are determined by the detection reports generated by the prescreener, while window sizes are based on estimated object size using interpixel distance information (IPD). A point matching operator is used to associate each detection report with a corresponding flow vector containing the x,y displacements for that subregion of the image over the full sequence of images. Once the data registration operator has been run, the final process is the application of a data smoothing operator. Our overall system approach is shown in Figure 4.0-1.

4.1 Extraction of Scene Motion

In regard to motion extraction, scene motion is defined as the frame to frame changes in position of scene information. The system approach for extracting positional changes of scene information consists of using an interest operator, partition/local maximum operator, and an interest point correlation operator (Figure 4.1-1).

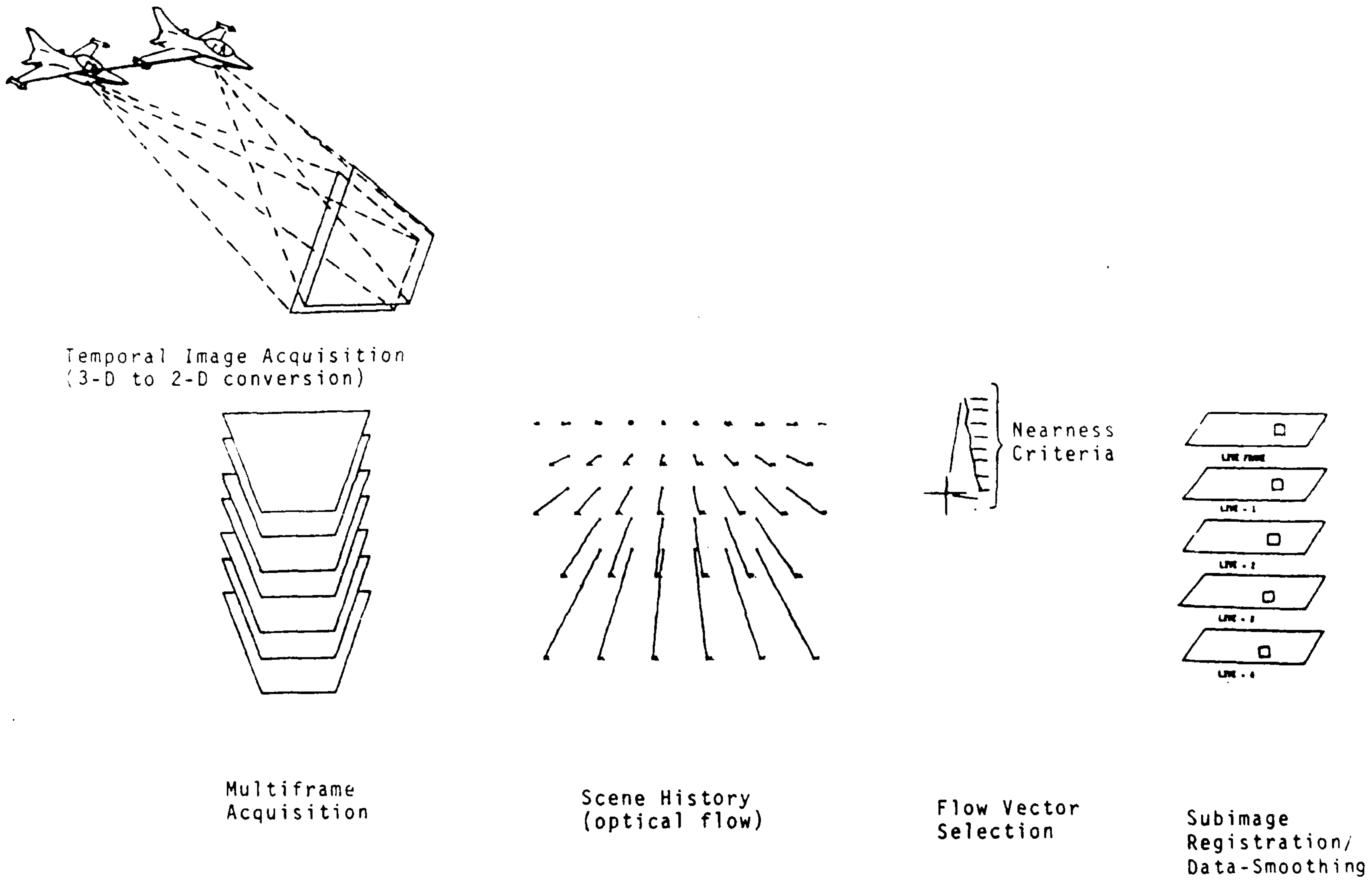
Temporal Image Acquisition
(3-D to 2-D conversion)
Multiframe
Acquisition
Scene History
(optical flow)
Nearness
Criteria
Flow Vector
Selection
LIVE FRAME
LIVE - 1
LIVE - 2
LIVE - 3
LIVE - 4
Subimage
Registration/
Data-Smoothing

Figure 4.0-1. Multiframe Data Smoothing System Overview

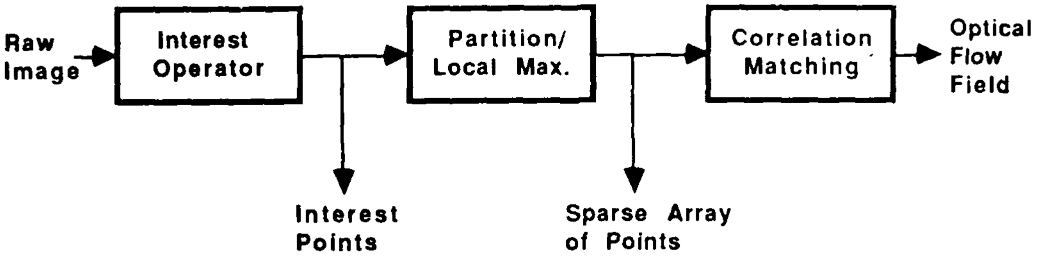
Raw Image
Interest Operator
Partition/ Local Max.
Correlation Matching
Optical Flow Field
Interest Points
Sparse Array of Points

Figure 4.1-1. Optical Flow Generation

Initially, a FLIR sensor is used to transform the three-dimensional scene into a two-dimensional projection of the scene (Figure 4.1-2, upper left corner). Points representing locally distinctive regions within the scene that can be readily matched from frame to frame are then automatically identified, using an interest operator.

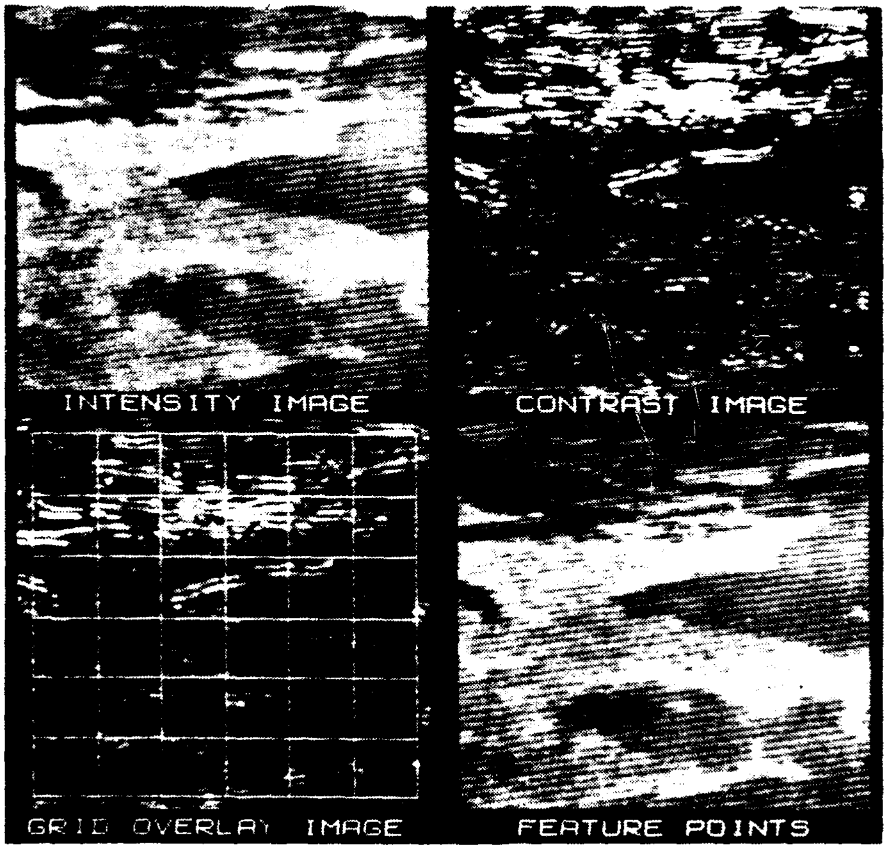
INTENSITY IMAGE
CONTRAST IMAGE
GRID OVERLAY IMAGE
FEATURE POINTS

Figure 4.1-2. Interest Point Nomination Summary

Our current operator is called the size contrast operator (SCO). The SCO (Figure 4.1-3) is designed to measure the level of contrast between an inner size-grated rectangle and an outer surrounding size-grated collar. The difference between the average of the inner window and the outer border region is computed and stored as an image metric for each pixel (Figure 4.1-2, upper right corner). The SCO can function as an edge operator or as a detector for localized regions of high contrast and specified size. The advantage of the SCO is that it accurately locates the centroid of localized features; the major disadvantage is that it is not effective when the scene lacks localized regions of high contrast such as in a desert environment.

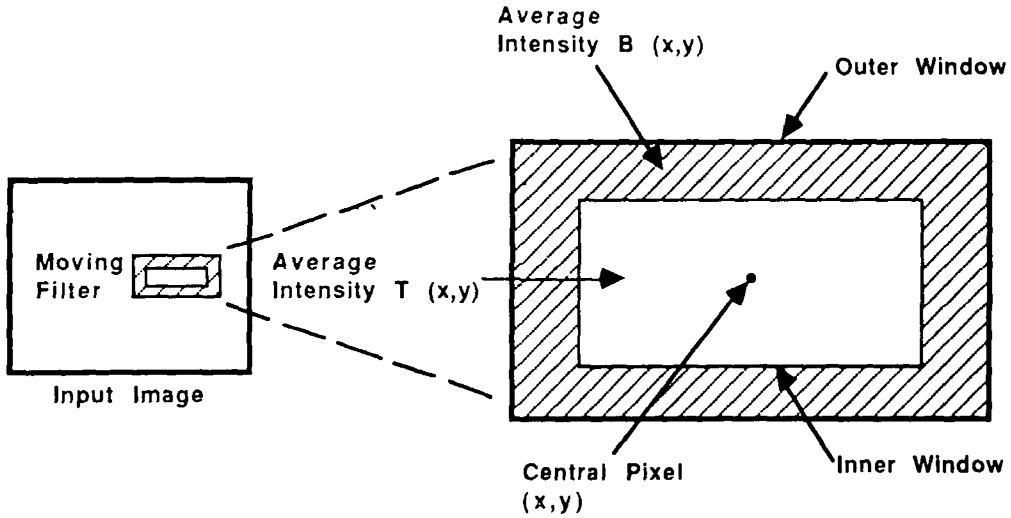

Figure 4.1-3. Size Contrast Window

To reduce the contrast metric image to individual points representing locations of local maximum contrast, a partition and local maximum operator is applied (Figure 4.1-2, lower left corner). The procedure consists of partitioning the metric image into "N" windows (In this representation N = 36) and locating the highest local maximum within each window. The windows are recessed from the edges to avoid nominating points at the edge of the image. This method of point nomination has two basic advantages. First, by nominating the most distinctive location in each partition the local maximum operator maximizes the chances of successful point correlation. Second, the resulting point distribution is by definition, nearly uniform (Figure 4.1-2, lower right corner - selected points overlaid on intensity image).

Establishing frame to frame correspondences is, perhaps, the most difficult step in the multiframe procedure. Occlusion of regions and regions that are not rigid (e.g., smoke or vehicle exhaust) can be difficult to match. Also, because the platform is constantly moving, regions continuously enter and leave the field of view. Full intensity area correlation is a widely used and well understood technique for solving the correspondence problem. Correlation is applied by defining a reference window centered on an interesting point in the earlier frame. A search window which is several pixels larger than the reference window is defined in the current live frame at the same x,y location. A template the size of the reference window is then moved throughout the search window area. The live template that best matches the reference template represents the updated location of the interest point in the live frame. The measure of similarity is the normalized cross-correlation coefficient, which was described previously.

When the live template and reference template match exactly, the probability (p) is 1. When the two templates are exactly inverted, p is -1. If the reference and live templates are totally uncorrelated, p is 0. The row and column in the live frame where the correlation is maximized represent the location where the live template best matches the reference template. This change in location of an interest point between two frames is defined as optical flow. The result of this processing on all interest points, which is called an optical flow field, is a quantification of the frame to frame disparities (Figure 4.1-4).

Credibility of the optical flow field is maintained by establishing a goodness criterion in the form of a correlation threshold. This threshold reduces the risk of tracking low confidence interest points that do not

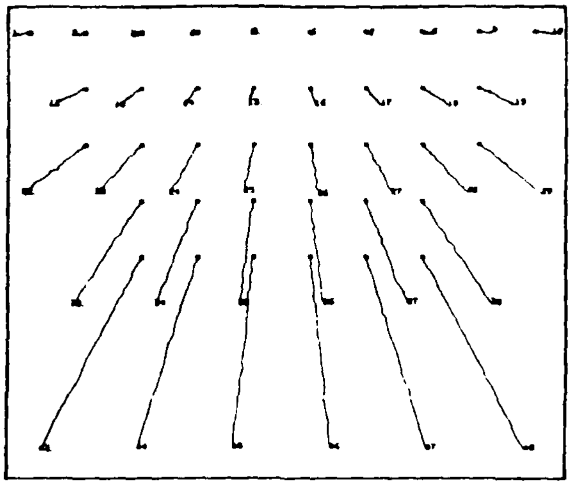

Figure 4.1-4. Synthetic Optical Flow Field

accurately model the true scene motion. However, the correlation threshold will not eliminate those points that do not conform to the global optical flow because of overcorrelation. Overcorrelation can occur when a feature is selected by the interest operator in a window containing very low contrast or cyclical patterns. The correlation coefficient for this type of point equally exceeds the threshold at a number of locations, which causes the maximum to be deterministically assigned. To purge the flow field (Figure 4.1-5) of this type of interest point, the affine transform is used. The affine model is a first-order approximation to the optical flow field. The affine transformation is defined as:

$$x' = A_1x + A_2y + A_3$$

$$y' = B_1x + B_2y + B_3.$$

To derive the affine coefficients, the flow field is least-squares fit to an affine sensor model and the residual error for each point is recorded. The flow point with the worst residual error is discarded, and the

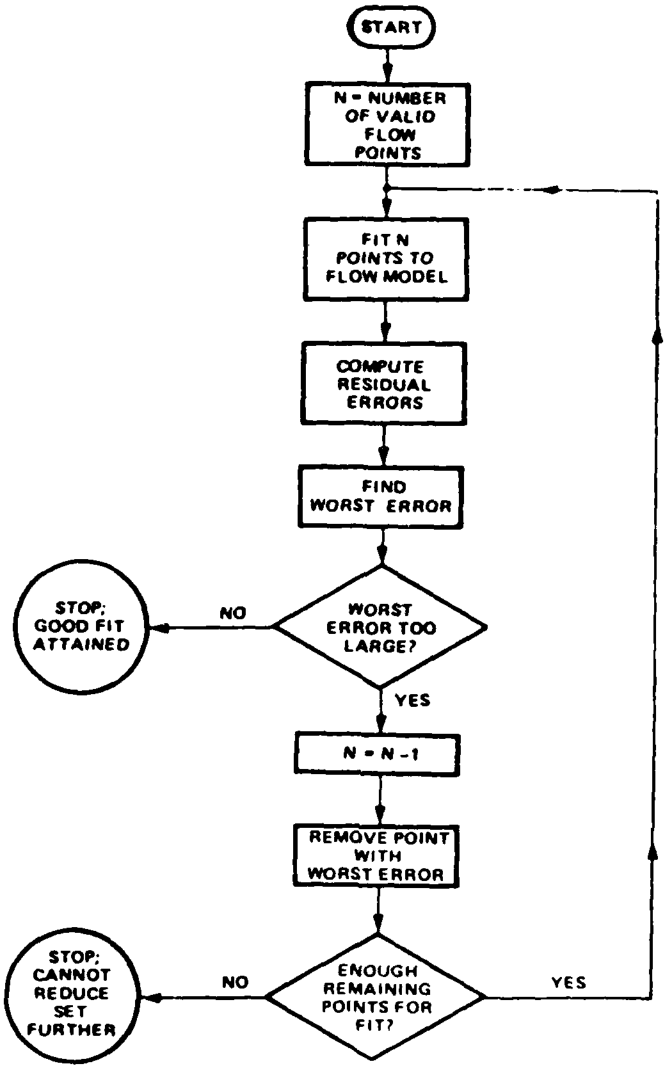
START
N = NUMBER OF VALID FLOW POINTS
FIT N POINTS TO FLOW MODEL
COMPUTE RESIDUAL ERRORS
FIND WORST ERROR
WORST ERROR TOO LARGE?
NO
STOP; GOOD FIT ATTAINED
YES
N = N -1
REMOVE POINT WITH WORST ERROR
ENOUGH REMAINING POINTS FOR FIT?
NO
STOP; CANNOT REDUCE SET FURTHER
YES

Figure 4.1-5. Flow Field Refinement

reduced list is fit to the sensor model and the coefficients recomputed. These iterations continue until either all flow points have an acceptably small residual error, or until further reduction of the list would cause the set to become smaller than a specified minimum number of flow points. Once the final set of affine coefficients has been computed, the residual error for each point in the original set is recomputed. Those points that exceed the maximum affine error threshold (currently 10) are removed from the list and replaced by a new entry.

In the affine model, the residual error is defined as the product of the magnitude of the observed flow and the sine of the angle between the predicted flow vector and the observed flow vector. If the cosine of the angle is less than zero, the residual error is the magnitude of the actual flow.

Accounting and maintenance of the optical flow field are accomplished through the use of a scene history file (Table 4.1-I). The history file provides a mechanism for accumulating interimage information regarding the selected interest point, thereby providing a historical reference of scene history. Key information in the history file includes:

1 KAV - Entry key of this optical flow point (key access value)

2 FRM - Frame number

3 ROW - Row location of point for this frame

4 COL - Column location of point for this frame

5 MET - Metric value of interest point at point selection time

6 AVG - Average of metrics in window partition

7 SDV - Sigma of metrics in window partition

8 MET - Highest correlation coefficient from area correlator

9 DIR - Quantized direction indicating orientation of point change

10 RDS - Row displacement of a point between last and current frame

11 CDS - Column displacement of a point between last and current frame

TABLE 4.1-I

History File Report Data Record

```
23-MAR-87  14:10:04

KAV FRM ROW COL MET AVG SDV MET COD QUD LLR DIR RDS CDS DIS RANGE DRNG  X-MAP  Y-MAP  Z-MAP ATE VOT
--- --- --- --- --- --- --- --- --- --- --- --- --- --- --- ----- ----  -----  -----  ----- --- ---
  2   1 160 382  40   4   5   0   0   0   0   0   0   0   0     0    0      0      0      0   0   0
  2   2 159 382   0   0   0  94  -1   0 100   1  -1   0   1     0    0      0      0      0   0   0
  2   3 159 381   0   0   0  98  25   0  71   7   0  -1   1     0    0      0      0      0   0   3
  2   4 159 380   0   0   0  97  27   0  75   7   0  -1   1     0    0      0      0      0   0   3
  2   5 159 380   0   0   0  98  31   0  75   0   0   0   0     0    0      0      0      0   1   5
  2   6 159 380   0   0   0  95  34   0  75   0   0   0   0     0    0      0      0      0   0   4
  2   7 159 379   0   0   0  98  31   0  79   7   0  -1   1     0    0      0      0      0   0   3
  2   8 159 378   0   0   0  97  26   1  82   7   0  -1   1     0    0      0      0      0   0   4
  2   9 159 378   0   0   0  96  25   1  82   0   0   0   0     0    0      0      0      0   0   4
  2  10 159 378   0   0   0  97  24   1  82   0   0   0   0     0    0      0      0      0   0   5
  2  11 159 377   0   0   0  96  23   2  85   7   0  -1   1     0    0      0      0      0   0   5
  2  12 159 376   0   0   0  98  21   2  87   7   0  -1   1     0    0      0      0      0   0   5
  2  13 159 375   0   0   0  97  18   3  88   7   0  -1   1     0    0      0      0      0   0   5
  2  14 159 374   0   0   0  97  16   4  90   7   0  -1   1     0    0      0      0      0   0   5
  2  15 159 373   0   0   0  97  14   6  91   7   0  -1   1     0    0      0      0      0   0   5
  2  16 159 372   0   0   0  98  13   7  91   7   0  -1   1     0    0      0      0      0   0   5
  2  17 159 371   0   0   0  98  12   9  92   7   0  -1   1     0    0      0      0      0   0   5
  2  18 159 370   0   0   0  98  11  11  93   7   0  -1   1     0    0      0      0      0   0   5
  2  19 159 370   0   0   0  96  11  13  93   0   0   0   0     0    0      0      0      0   0   5
  2  20 159 369   0   0   0  98  10  15  93   7   0  -1   1     0    0      0      0      0   0   5
  2  21 159 368   0   0   0  95  10  17  94   7   0  -1   1     0    0      0      0      0   0   5
  2  22 159 367   0   0   0  95   9  19  94   7   0  -1   1     0    0      0      0      0   0   5
```

12 DIS - Total distance that a point has moved between last and current frame

13 ATE - Current affine transform error of a point.

4.2 Flow Vector Selection

Once a scene history for a consecutive sequence of images has been generated, a process is run that selects the optimum flow vector for each detection report. The locations of the detection reports are extracted from the image header file, which corresponds to the last image processed in the image sequence. The vector selection program computes the distance between each flow vector that has been successfully maintained over the entire sequence, and the detection reports (Figure 4.2-1). The flow vector that is closest to each detection report is used to decompose the frame to frame positional shifts that occurred over the sequence of images during the application of the subimage registration process.

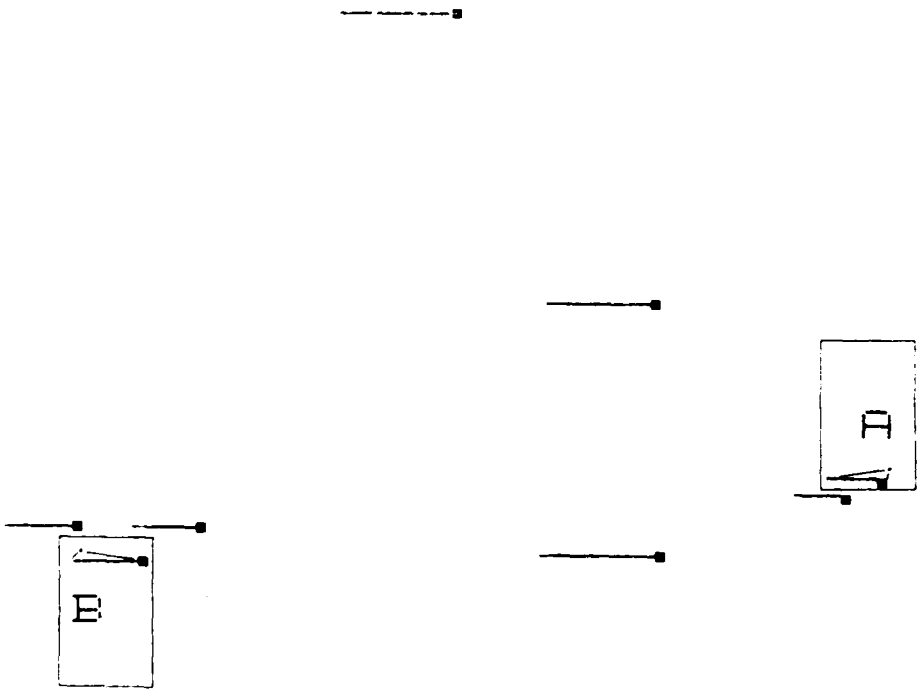

Figure 4.2-1. Flow Vector Selection

4.3 Data Smoothing

The data smoothing algorithm performs multisubimage registration (three to nine images) and applies a pixel smoothing technique between subimage windows. The smoothing process is acccomplished by applying a 1x1xN filter to each pixel in the subimage set, where N equals the number of registered images (depth); the filter type can be a mean or median or other such filter.

A prerequisite for this process is the existence of an optical flow history file generated over the N consecutive images. The history file contains the frame to frame positional changes of scene context that occur over the sequence of images. The positional changes recorded in this file are used to register the subimages extracted from each full frame image.

The smoothed images are generated by working backwards through the history file. The last image written to the history file will be the first image processed. Each vehicle in an image is processed in the same manner. The general concept is as follows:

1 Identify an optical flow vector. Using the optical flow history file, the optical flow vector, closest to a detection report (vehicle) in the last image in the sequence, is identified. The vector must have been tracked through all the images in the sequence. This flow vector is used to register all subimages in the sequence pertaining to this vehicle.

2 Equalize the number of passes. The number of passes (and output smoothed images) equals the total number of images in the test sequence minus the number of images used in the subimage smoothing process (called a cluster) plus 1 (i.e., pass = total - cluster + 1).

3 Read cluster images. For each cluster (such as five images per cluster) the most current image (newest) is the master image (Figure 4.3-1). The images corresponding header file is used to determine the extent of the window needed to fully encompass the detected vehicle and to include enough background for metric computation (subimage includes vehicle and background collar area). Each subsequent image in the cluster is read, and a subimage of equal size to the first is located (using the flow vector to compensate for x,y change) and stored. When all five images have been read, registered, and stored, a 1x1x5 filter is applied. The output filtered subimage is then placed back into the master image. After each vehicle in the image has been processed in this manner, the smoothed master image is written to disk. The next newest image is then read along with its set of four consecutive older images. The process stops when a cluster of five images cannot be formed.

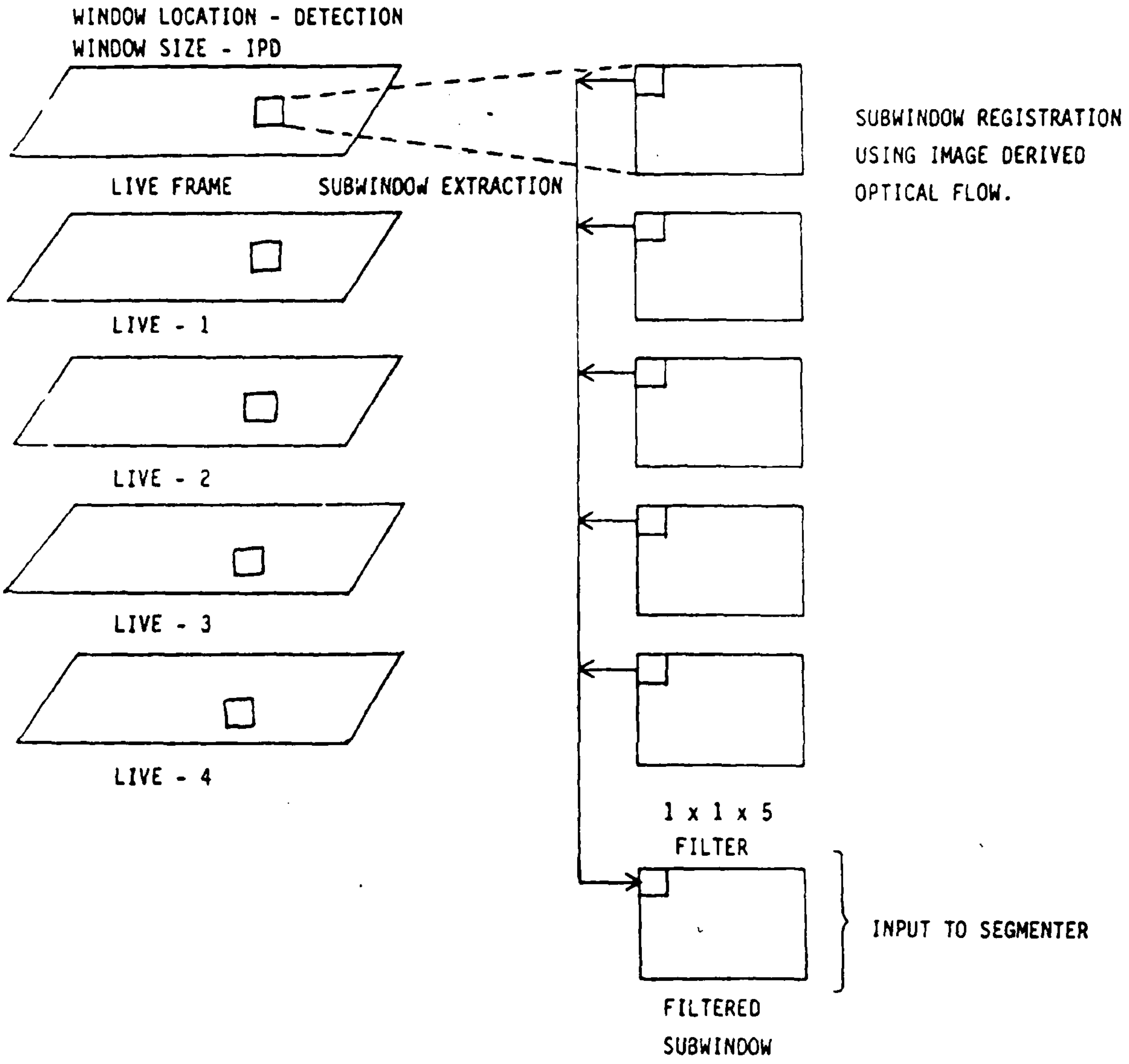
WINDOW LOCATION - DETECTION
WINDOW SIZE - IPD
LIVE FRAME
SUBWINDOW EXTRACTION
SUBWINDOW REGISTRATION USING IMAGE DERIVED OPTICAL FLOW.
LIVE - 1
LIVE - 2
LIVE - 3
LIVE - 4
1 x 1 x 5 FILTER
INPUT TO SEGMENTER
FILTERED SUBWINDOW

Figure 4.3-1. Multiframe Data Smoothing

5.0 EXPERIMENTS

A set of experiments were defined to assess the effects of multiframe data smoothing on vehicle signatures and segmenter performance. The experiments consisted of applying a multiframe data smoothing operator and an independent frame enhancement operator to three sets of consecutive sequences of ERIM truthed TI images. The rule directed segmenter was then applied to the raw data, smoothed data, and independently filtered data. A comparative analysis of segmenter performance was conducted by evaluating the segmenter stability metrics for each data type. Data variations in vehicle signatures were analyzed from the results of the data variation metrics.

The filters used for the multiframe data smoothing experiments were the 1x1x5 median, 1x1x7 median, and 1x1x9 median. The results obtained using the multiframe mean filter were not significantly different from the median to warrent extensive testing. The independent frame enhancement operator was the 3x3x1 median. The inclusion of this operator enabled us to compare the results against a more conventional approach to noise reduction.

The primary difference between the multiframe median and the local median is the method of sample set selection. The multiframe approach uses sample elements (one from each of n consecutive frames), each representing the same local area of information in the image. The integration of this data improves signal quality without jeopardizing organizational detail. The 3x3x1 median uses nine sample elements (from the same frame), each representing a different local area of information in the image. The relationship between the data represented by the nine samples determines whether the result represent signal improvement (all samples are related) or signal degradation (all samples are unrelated). Since both cases occur within the image, the result represents a combination of improved and decreased signal quality. This property of the 3x3x1 median makes it undesirable as a preprocessor for functions that require a precise numerical representation of the data, such as feature extraction. However, the ability of the median to reduce some noise, while preserving step edges, is useful to some types of image segmentation operators. In comparison, the multiframe approach is idealy suited for both signal improvement and feature enhancement.

5.1 Test Set 1

The first data set tested was the image sequence extracted from ERIM data tape number 3014-12, set 4D. The data tape included the raw imagery, ground truth information, metrics, and truth silhouettes. The first 30 images (44 total) in the sequence were removed from the tape, using the ATRWG read software.

The image sequence (Figure 5.1-1) contains two tanks, which will be referenced as tank-1 (the rightmost tank) and tank-2 (the leftmost tank). The images show side views of the tanks with their gun barrels in the combat position. The engines and wheels are hotter than the bodies of the tanks, which indicates that the tanks are either in motion or have recently been moving. Tank-1, a T46, is approximately 1946 meters from the sensor; Tank-2, a T95, is approximately 1919 meters from the sensor. Excluding the tanks, the scene is virtually void of any significant context and only has a gray level range of approximately 30 intensity levels (Figure 5.1-2). The road on which the tanks are positioned is almost nondetectable. There appears to be some sort of runway directly above tank-2. The lack of context in this sequence makes frame to frame feature correspondence very difficult. However, the close range of the tanks permits a better assessment of the effects of multiframe smoothing on the structural detail of the tanks, segmenter performance, and metric behavior.

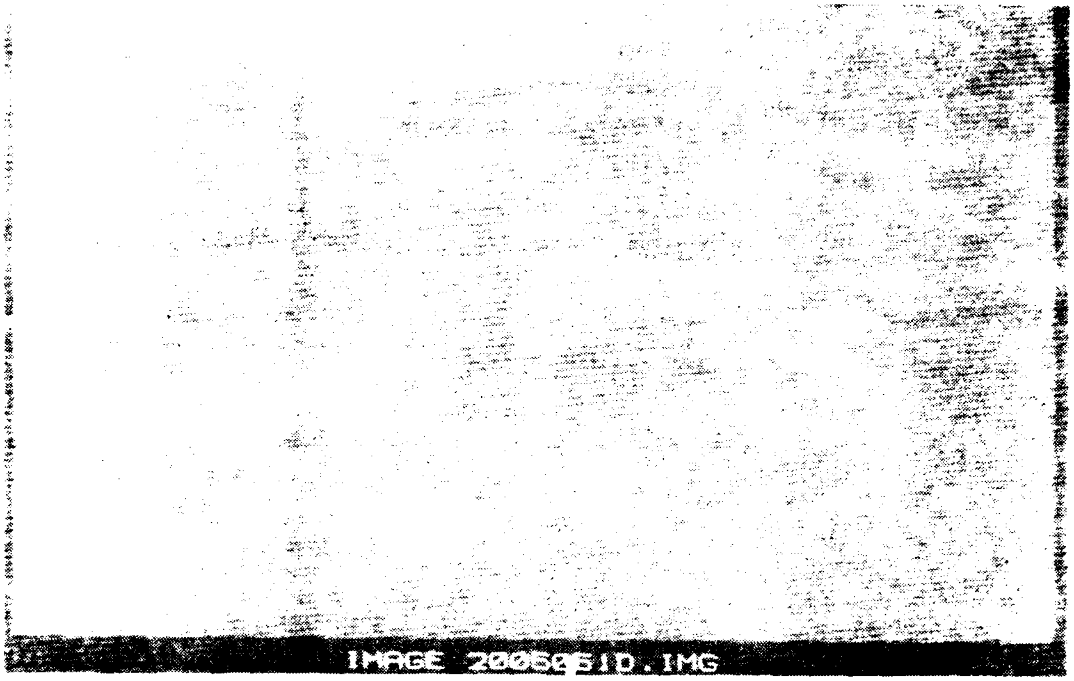
IMAGE 200505ID.IMG

Figure 5.1-1. Tank Image Sequence

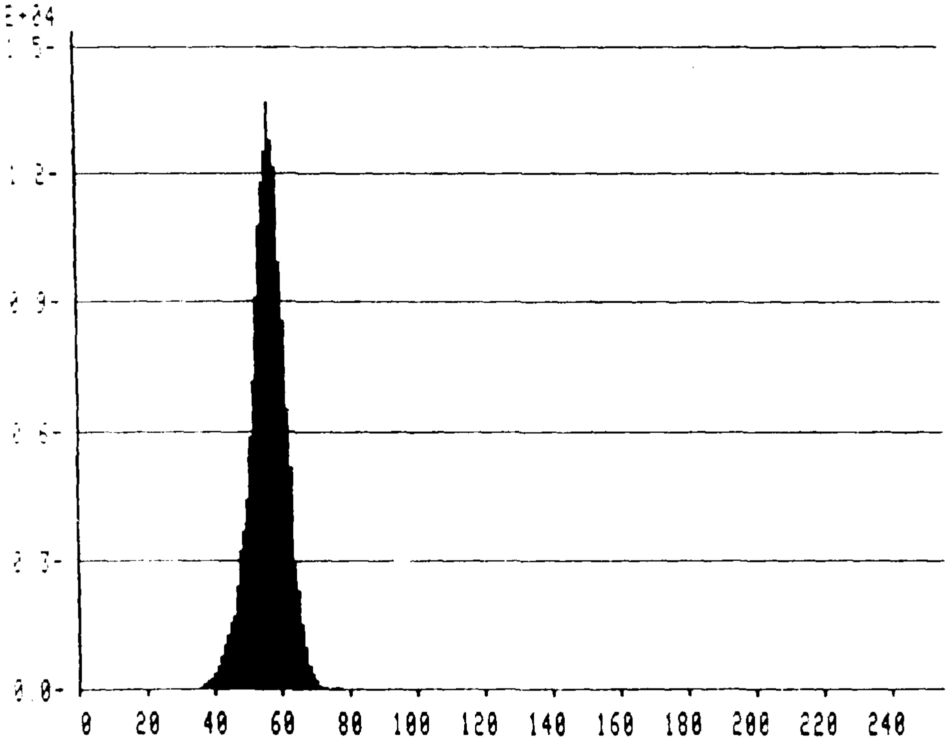

Figure 5.1-2. Intensity Histogram of Channel 1

Scene Motion

The 30-image test set was processed using the scene motion extraction software. The parameters for the point selection and tracking operators were set as follows;

1 Size contrast inner window size: 9 pixels wide, 7 pixels high

2 Partition and local maximum: 6x6 grid surface (36 total points)

3 Correlation coefficient threshold: 0.7 (less than 0.7 is deleted)

4 Affine error threshold: 8.0 (greater than 8.0 is deleted)

The number of feature points tracked for the entire 30-frame sequence consisted of only six points or 16 percent of the initial number selected (Figure 5.1-3). Four of the nominated points pertained to contrast measures between the two tanks and their local background. The high turnover in feature points was due exclusively to poor frame to frame correlation due to bland scene conditions. When points are selected in low contrast areas, the correlation operator is highly influenced by the noise component of the signal. As the data becomes more nearly homogeneous, the correlation process actually attemps to correlate the noise.

The flow vectors selected for performing multi-subimage registration for the two tanks were vectors 3 (Table 5.1-I - for tank-2) and -4 (Table 5.1-II - for tank-1). Assessing the quality of these vectors from the "Optical Flow Metric Report" (Table 5.1-III) indicates a high degree of credibility in accurately tracking the frame to frame positional changes of the two tanks. A visual assessment of the correlation accuracy is shown in

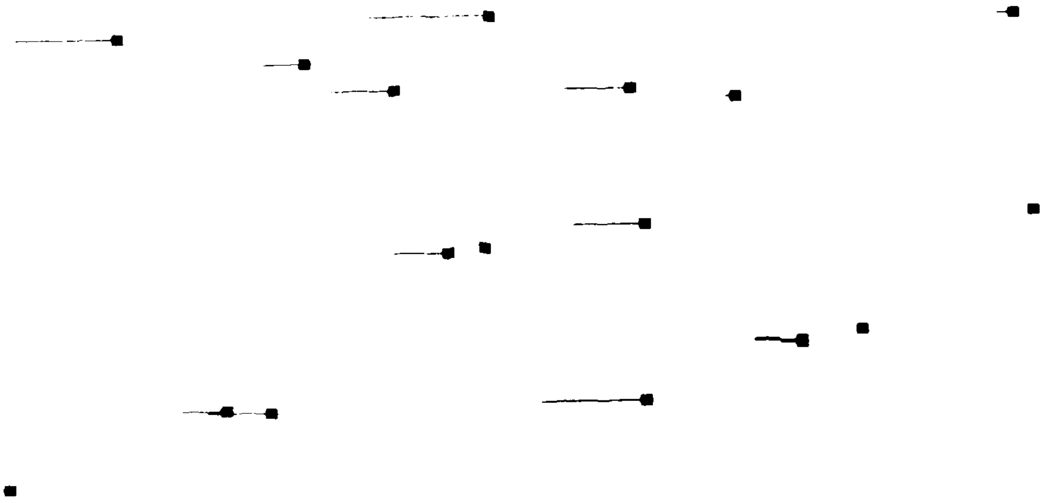

FULL OPTICAL FLOW FIELD

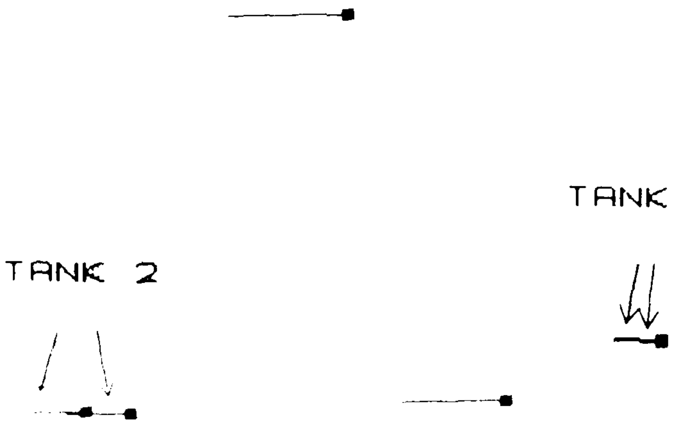

[illegible] OF FEATURES TRACKED FOR THE 30 FRAMES

Figure 5.1-3. Optical Flow Field

TABLE 5.1-I

History File Report Data Record

```
20-APR-87  12:20:22

KAV FRM ROW COL MET AVG SDV MET COD QUD LLR DIR ROS COS DIS RANGE DRNG  X-MAP  Y-MAP  Z-MAP ATE VOT

 3   1 159 382  39   2   3   0   0   0   0   0   0   0   0     0    0      0      0      0   0   0
 3   2 159 382   0   0   0  94  -1   0 100   1  -1   0   1     0    0      0      0      0   0   0
 3   3 159 381   0   0   0  98  25   0  71   7   0  -1   1     0    0      0      0      0   0   3
 3   4 158 380   0   0   0  97  27   0  75   7   0  -1   1     0    0      0      0      0   0   3
 3   5 159 380   0   0   0  98  31   0  75   0   0   0   0     0    0      0      0      0   1   5
 3   6 158 380   0   0   0  95  34   0  75   0   0   0   0     0    0      0      0      0   0   4
 3   7 158 379   0   0   0  98  31   0  79   7   0  -1   1     0    0      0      0      0   0   3
 3   8 158 378   0   0   0  97  26   1  82   7   0  -1   1     0    0      0      0      0   0   4
 3   9 158 378   0   0   0  96  25   1  82   0   0   0   0     0    0      0      0      0   0   4
 3  10 158 375   0   0   0  97  24   1  82   0   0   0   0     0    0      0      0      0   0   5
 3  11 158 377   0   0   0  96  23   2  85   7   0  -1   1     0    0      0      0      0   0   5
 3  12 159 376   0   0   0  98  21   2  87   7   0  -1   1     0    0      0      0      0   0   5
 3  13 158 375   0   0   0  97  18   3  88   7   0  -1   1     0    0      0      0      0   0   5
 3  14 159 374   0   0   0  97  16   4  90   7   0  -1   1     0    0      0      0      0   0   5
 3  15 158 373   0   0   0  97  14   6  91   7   0  -1   1     0    0      0      0      0   0   5
 3  16 159 372   0   0   0  98  13   7  91   7   0  -1   1     0    0      0      0      0   0   5
 3  17 158 371   0   0   0  98  12   9  92   7   0  -1   1     0    0      0      0      0   0   5
 3  18 159 370   0   0   0  98  11  11  93   7   0  -1   1     0    0      0      0      0   0   5
 3  19 158 370   0   0   0  96  11  13  93   0   0   0   0     0    0      0      0      0   0   5
 3  20 159 369   0   0   0  98  10  15  93   7   0  -1   1     0    0      0      0      0   0   5
 3  21 159 368   0   0   0  95  10  17  94   7   0  -1   1     0    0      0      0      0   0   5
 3  22 159 367   0   0   0  95   9  19  94   7   0  -1   1     0    0      0      0      0   0   5
 3  23 158 367   0   0   0  96   9  21  94   0   0   0   0     0    0      0      0      0   0   6
 3  24 158 366   0   0   0  95   9  23  94   7   0  -1   1     0    0      0      0      0   0   6
 3  25 159 365   0   0   0  94   9  26  95   7   0  -1   1     0    0      0      0      0   0   6
 3  26 159 365   0   0   0  97   9  28  95   0   0   0   0     0    0      0      0      0   0   6
 3  27 159 365   0   0   0  95   8  29  95   0   0   0   0     0    0      0      0      0   0   4
 3  28 159 365   0   0   0  93   9  31  95   0   0   0   0     0    0      0      0      0   0   4
 3  29 158 364   0   0   0  97   9  32  95   7   0  -1   1     0    0      0      0      0   0   4
 3  30 158 364   0   0   0  97   9  34  95   0   0   0   0     0    0      0      0      0   0   4
```

TABLE 5.1-II

History File Report Data Record

[illegible]-APR-8[illegible] 12:20:2[illegible]

[illegible]	FRM	ROW	COL	MIT	AVG	SDV	MET	COR	OUT	LIP	DIP	ROT	COS	DIS	RANGE	DRNG	X-MAP	Y-MAP	Z-MAP	ATE	VOT
4	1	185	[illegible]	[illegible]	[illegible]	[illegible]	[illegible]	[illegible]	[illegible]	[illegible]	[illegible]		[illegible]	[illegible]	0	0	0	0	0	0	0
4	2	185	178	0	0	0	96	-1	0	100	7	0	-1	1	0	0	0	0	0	0	0
4	3	185	177	0	0	0	96	-1	0	100	7	0	-1	1	0	0	0	0	0	0	6
4	4	185	176	0	0	0	97	-1	1	100	7	0	-1	1	0	0	0	0	0	0	6
4	5	185	175	0	0	0	96	-1	2	100	7	0	-1	1	0	0	0	0	0	0	6
4	6	185	174	0	0	0	96	-1	2	100	7	0	-1	1	0	0	0	0	0	0	6
4	7	185	173	0	0	0	96	-1	4	100	7	0	-1	1	0	0	0	0	0	0	6
4	8	185	172	0	0	0	96	-1	5	100	7	0	-1	1	0	0	0	0	0	0	6
4	9	185	171	0	0	0	94	-1	6	100	7	0	-1	1	0	0	0	0	0	0	6
4	10	185	171	0	0	0	94	-1	7	100	0	0	0	0	0	0	0	0	0	0	6
4	11	185	170	0	0	0	94	-1	8	100	7	0	-1	1	0	0	0	0	0	0	6
4	12	185	169	0	0	0	96	-1	9	100	7	0	-1	1	0	0	0	0	0	0	6
4	13	185	168	0	0	0	97	-1	11	100	7	0	-1	1	0	0	0	0	0	0	6
4	14	185	167	0	0	0	94	-1	13	100	7	0	-1	1	0	0	0	0	0	0	6
4	15	185	166	0	0	0	97	-1	15	100	7	0	-1	1	0	0	0	0	0	0	6
4	16	185	165	0	0	0	94	-1	17	100	7	0	-1	1	0	0	0	0	0	0	6
4	17	185	164	0	0	0	97	-1	20	100	7	0	-1	1	0	0	0	0	0	0	6
4	18	185	163	0	0	0	92	-1	22	100	7	0	-1	1	0	0	0	0	0	0	6
4	19	185	162	0	0	0	94	-1	25	100	7	0	-1	1	0	0	0	0	0	0	6
4	20	185	161	0	0	0	97	-1	28	100	7	0	-1	1	0	0	0	0	0	0	6
4	21	185	160	0	0	0	96	-1	31	100	7	0	-1	1	0	0	0	0	0	0	6
4	22	185	159	0	0	0	97	-1	35	100	7	0	-1	1	0	0	0	0	0	0	6
4	23	185	158	0	0	0	96	-1	38	100	7	0	-1	1	0	0	0	0	0	0	6
4	24	185	157	0	0	0	96	-1	42	100	7	0	-1	1	0	0	0	0	0	0	6
4	25	185	156	0	0	0	97	-1	46	100	7	0	-1	1	0	0	0	0	0	0	6
4	26	185	155	0	0	0	95	-1	50	100	7	0	-1	1	0	0	0	0	0	0	6
4	27	185	155	0	0	0	95	-1	53	100	0	0	0	0	0	0	0	0	0	0	6
4	28	185	155	0	0	0	93	-1	56	100	0	0	0	0	0	0	0	0	0	0	6
4	29	185	155	0	0	0	98	-1	59	100	0	0	0	0	0	0	0	0	0	0	6
4	30	185	155	0	0	0	97	-1	60	100	0	0	0	0	0	0	0	0	0	0	[illegible]

TABLE 5.1-III

Optical Flow Metric Report

Total frames = 30

Feature number	Current status	Frames tracked	Uniqueness metric	Correlation metric	Affine metric
1	Tracking	30	7.111	95.517	0.000
2	Tracking	30	12.667	96.448	0.038
3	Tracking	30	12.333	96.448	0.038
4	Tracking	30	4.250	95.621	0.000
5	New entry	1	0.000		
6	New entry	1	0.000		
7	New entry	1	0.000		
8	New entry	1	0.000		
9	New entry	1	0.000		
10	Tracking	9	3.000	82.625	0.000
11	Tracking	3	3.000	76.500	
12	New entry	1	0.000		
13	New entry	1	0.000		
14	New entry	1	0.000		
15	New entry	1	5.000		
16	Tracking	4	3.000	77.333	
17	New entry	1	0.000		
18	Tracking	30	3.000	84.897	0.000
19	New entry	1	0.000		
20	Tracking	17	4.000	83.250	0.000
21	New entry	1	0.000		
22	New entry	1	3.000		
23	Tracking	6	3.000	85.400	0.000
24	New entry	1	3.000		
25	New entry	1	0.000		
26	Tracking	5	4.000	85.250	0.000
27	New entry	1	0.000		
28	New entry	1	0.000		
29	Tracking	30	0.000	90.262	0.038
30	Tracking	22	3.000	77.714	0.000
31	Tracking	25	0.000	86.258	0.000
32	Tracking	2	3.000	74.000	
33	Tracking	13	3.000	83.917	0.000
34	Tracking	24	2.000	90.696	0.100
35	New entry	1	3.000		
36	Tracking	[illegible]	2.000	[illegible]	0.000

Figure 5.1.4. The bright white pixel superimposed on the tanks indicates the x,y locations of the selected feature centroids. For tank-2 (above two pictures) the contrast feature selected was in the wheels of the tank. The dominate feature for tank-1 was its engine. The location of the feature centroids in frame 1 compared to their ending position in frame 30, seems to indicate that an accumulation of a one-pixel offset may have occured over the 30-frame sequence. If the correlation drift did occur, it had no detectable effect on the data smoothing results.

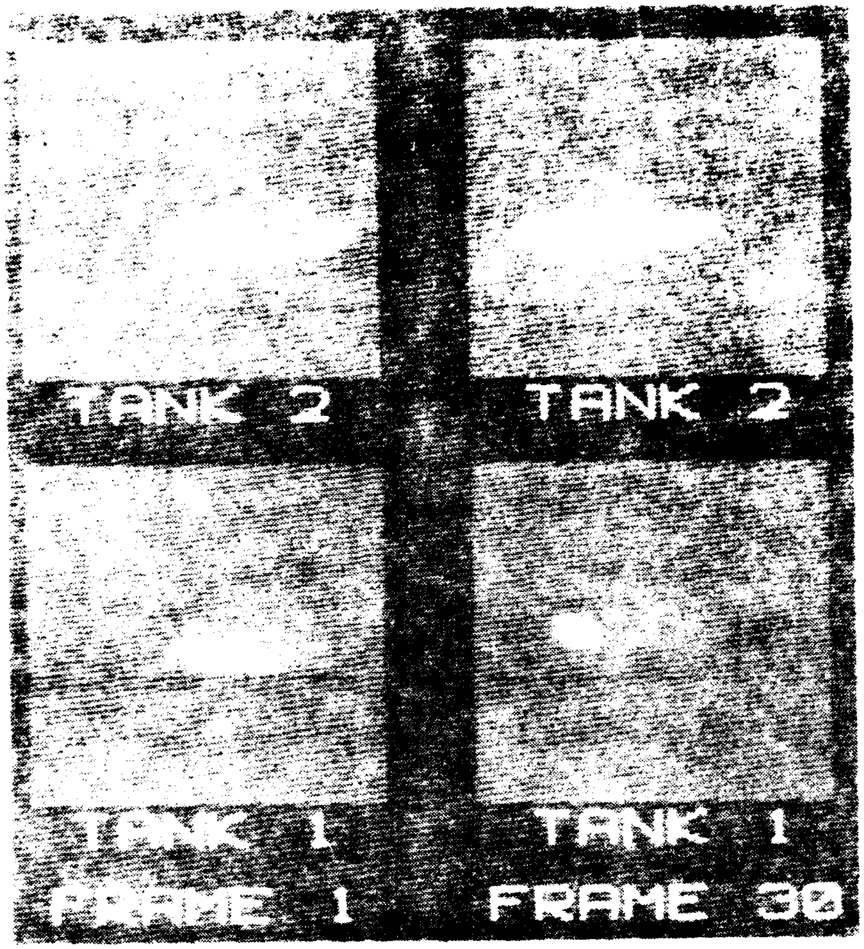

Figure 5.1-4. Scene Correlation

Data Smoothing

The parameters used for multiframe smoothing consisted of registering clusters of five consecutive subimage windows (placed about the vehicles) and applying a 1x1x5 (row by column by depth) median filter. This process generated a data set consisting of 26 images (30 total images - 5 cluster size + 1). These 26 raw data images were also processed using a conventional 3x3x1 median filter.

A visual comparison of the effects of the two enhancement techniques is shown in Figure 5.1-5. The plots depict the intensity structure of a single row of pixels extracted from image 20050510.IMG. The pixels extend

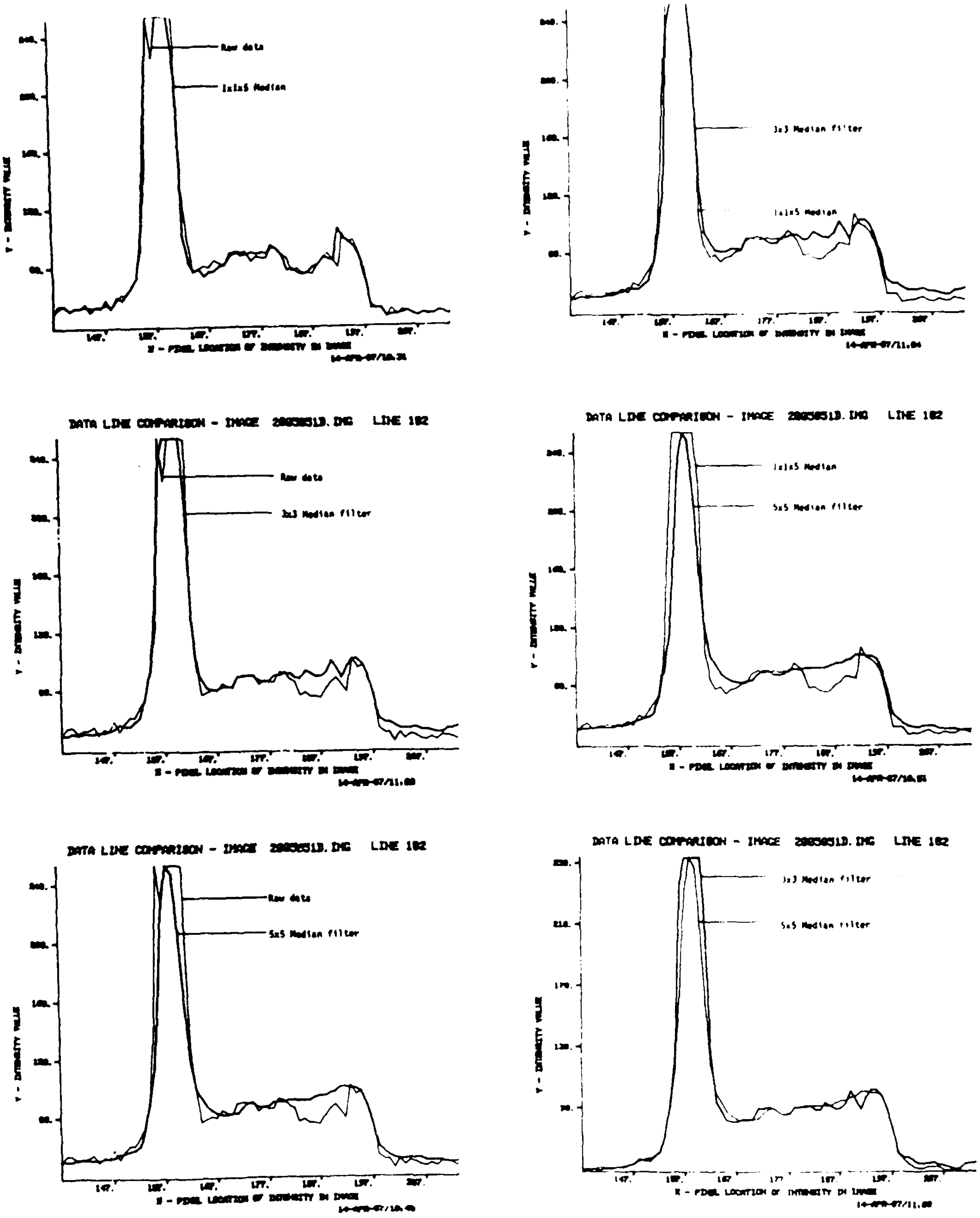

Figure 5.1-5. A Visual Comparison of Enhancement Techniques

across the subimage window of tank-2, passing through the center of the vehicle. The upper left image in Figure 5.1-5 shows how the multiframe approach preserves the detail on the vehicle. The center-left image shows the influences of unrelated information on the filter process. Results from a 5x5x1 median filter were also included for comparison. A more detailed view of the multiframe filter is shown in Figure 5.1-6. The 3-D projection shows the ability of the filter to preserve surface detail on the vehicle, while suppressing noise (most visible in the background data). An improvement in the organization of the tank wheels and engine compartment can be seen in the gray level picture of the tank.

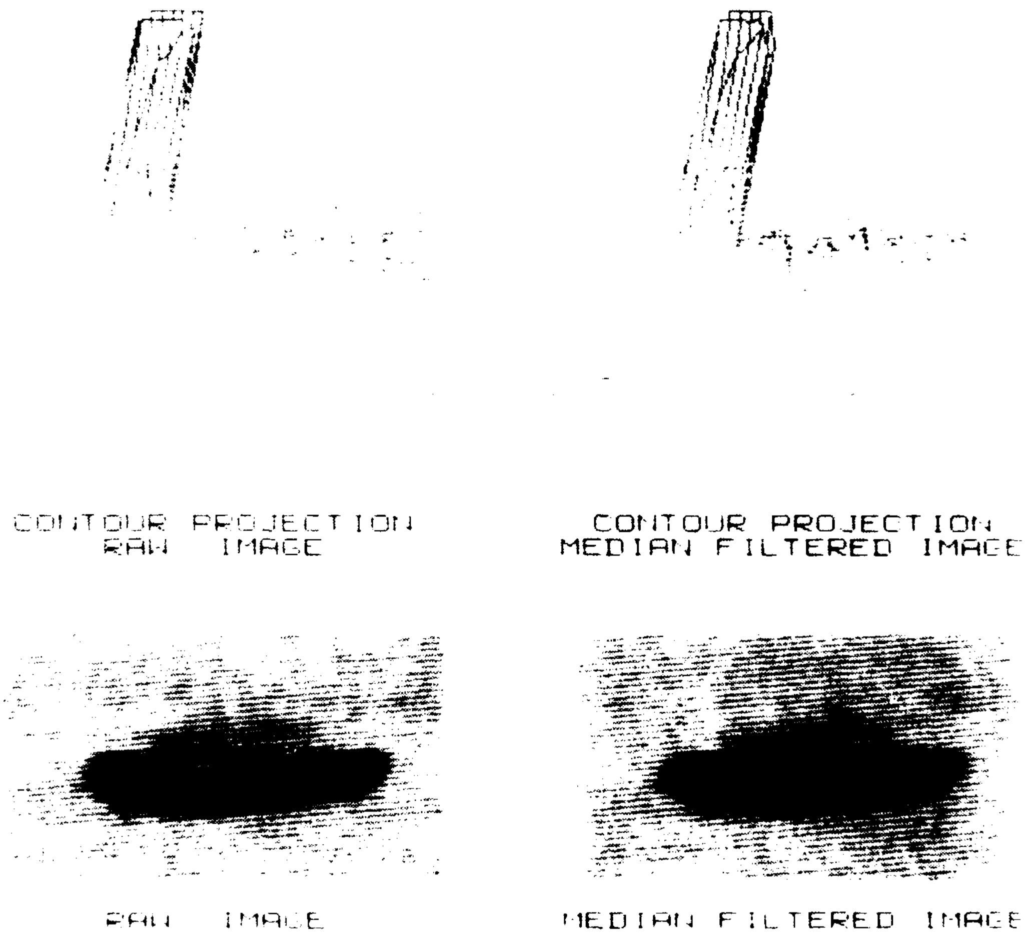

Figure 5.1-6. Noise Reduction Via Multiframe Median Filter

To determine the effects of the two enhancement techniques on segmenter performance, the 1x1x5 smoothed data set, 3x3x1 median-filtered data set, and raw data set were processed using the rule directed segmenter (Figure 5.1-7). The results indicated that both enhancement techniques improved segmenter performance. The segmentation accuracy metric, BACC, for tank-2 (Figure 5.1-8) reveals that the level of improvement is almost identical for both techniques. This implies that both techniques have properties that are beneficial to segmentation.

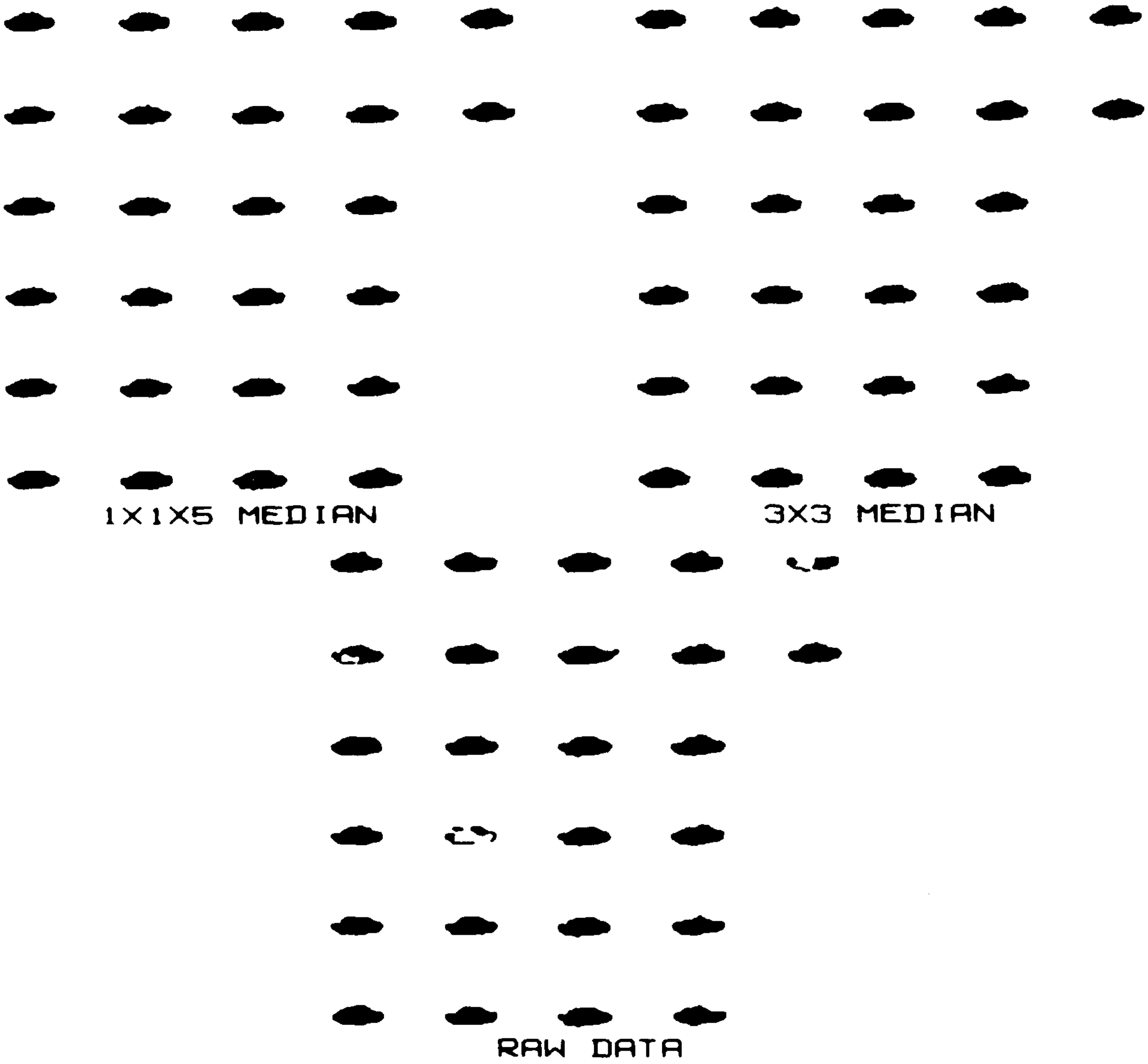

Figure 5.1-7. Segments (RDS) from 26 Consecutive Frames (Tank 2)

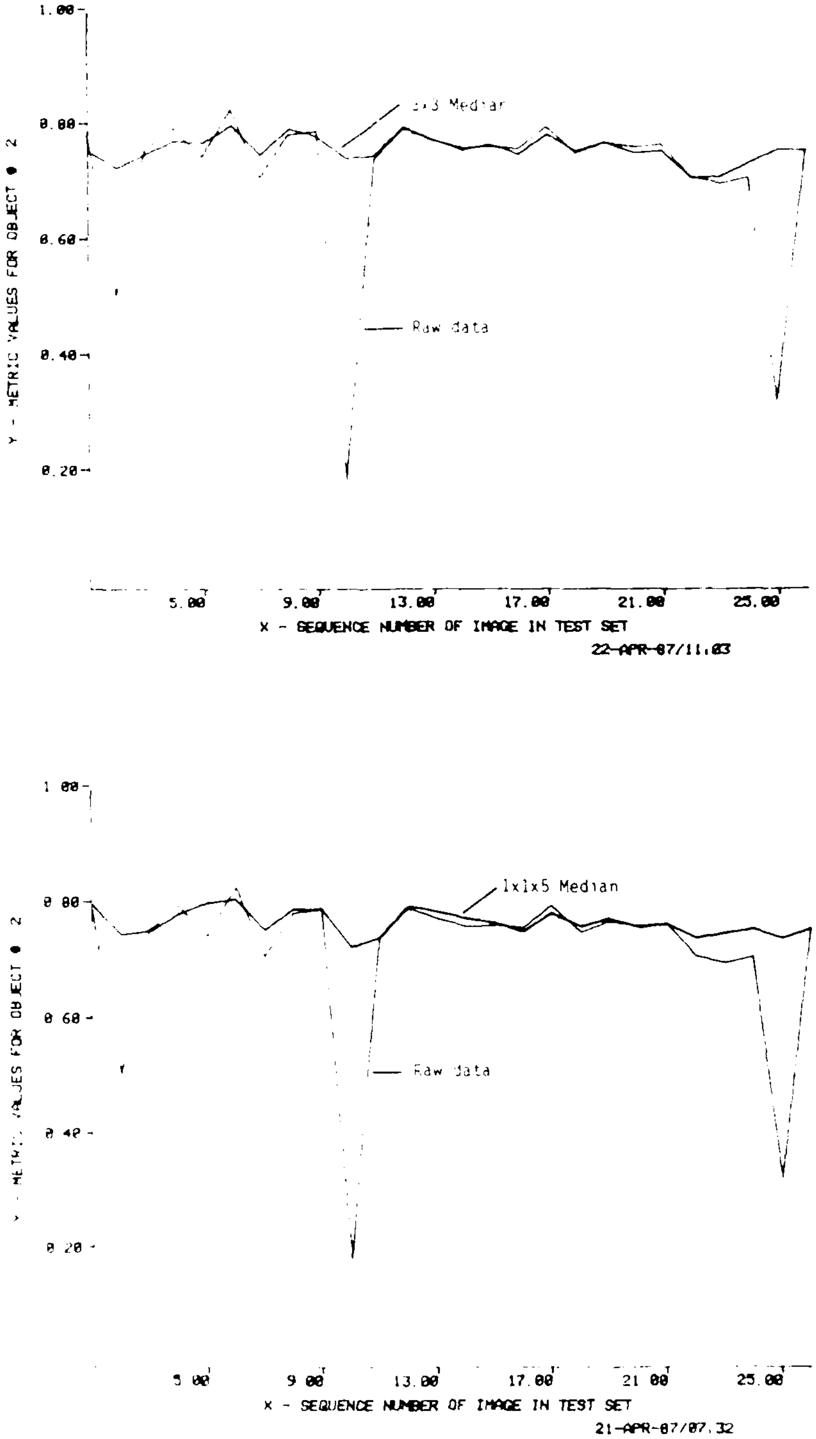

Figure 5.1-8. Metric Comparison of Binary Area Cross Correlation

To understand how the two enhancement techniques improved performance, it is necessary to determine how each technique altered the data. This can be accomplished by comparing the intensity-based metrics computed on the two enhanced data sets to those computed on the raw data set. A summary of those results is presented in Table 5.1-IV (1x1x5 median versus raw data) and Table 5.1-V (3x3x1 median versus raw data). A more visual examination of the intensity-based contrast metric is given in Figure 5.1-9. The plots compare the values of the enhanced data metrics to the raw data metrics computed on tank-2 (y axis) for each of the 26 images (x axis) in the data sets. A study of the two plots shows that the 3x3x1 median behaves as a low pass filter, suppressing the high-frequency information and subsequently reducing the metric values. The general profile of the median graph is very similar to the raw data graph with the exception of a scale factor. Conversely, the graph of the 1x1x5 median filter shows a reduction in the range (vertical extent) of the metric with no decrease in metric response. The results demonstrate the ability of multiframe filters to reduce noise and improve signal stability. A summary of all five intensity based metrics is given in Figures 5.1-10 through -14. The plots depict the distribution of the metrics for the two tanks (1 and 2) for each of the three 26 image data sets. In general, the important aspects of the plots are the organizational features of the metric distributions such as range, level of response, and clustering. The graphs reflect the overall superiority of the multiframe smoothing approach to that of the independent frame filter.

5.2 Test Set 2

The second data set tested was the image sequence extracted from ERIM data tape number 3015-12, set 4D. The data tape included raw imagery, ground truth information, metrics, and truth silhouettes. The first 30 images (34 available in sequence) were removed from the tape, using the ATRWG read software. The image sequence (Figure 5.2-1) contains three military vehicles: a truck (the leftmost object, object-1), a T95 Tank (the center object, object-2), and a T32 Tank (the rightmost object,

TABLE 5.1-IV

Temporal Variation Metrics (1x1x5)

Number of images in this sequence = [illegible]
Number of objects per image = [illegible]
Type of data smoothing used = Median
Number of images per cluster = [illegible]

Object number	Object type	Name of object metric	Standard Deviation Of Metric Raw data	Standard Deviation Of Metric Smoothed data	Difference	% of change	Central Tendency
1	Tank	Contrast (intensity based)	0.572	0.705	0.133	23.20	Decreased
		Contrast (entropy)	0.010	0.009	0.001	11.39	Improved
		TIP-Squared (intensity based)	4.741	5.012	0.271	5.72	Decreased
		TEIP-Squared (intensity based)	0.457	0.544	0.087	19.01	Decreased
		Binary Area Cross Correlation	0.022	0.026	0.004	20.14	Decreased
2	Tank	Contrast (intensity based)	1.000	0.743	0.257	25.73	Improved
		Contrast (entropy)	0.008	0.007	0.001	12.33	Improved
		TIP-Squared (intensity based)	16.889	12.081	4.808	28.47	Improved
		TEIP-Squared (intensity based)	1.094	0.541	0.554	50.59	Improved
		Binary Area Cross Correlation	0.149	0.022	0.127	85.41	Improved

Object number	Object type	Name of object metric	Average Value Of Metric Raw data	Average Value Of Metric Smoothed data	Difference	% of change	Position on X axis
1	Tank	Contrast (intensity based)	20.897	20.649	0.248	1.18	Lower
		Contrast (entropy)	0.199	0.224	0.025	12.42	Increased
		TIP-Squared (intensity based)	32.135	46.563	14.428	44.90	Increased
		TEIP-Squared (intensity based)	5.906	7.183	1.277	21.62	Increased
		Binary Area Cross Correlation	0.733	0.729	0.004	0.56	Unaffected
2	Tank	Contrast (intensity based)	36.029	35.818	0.211	0.59	Unaffected
		Contrast (entropy)	0.257	0.286	0.029	11.43	Increased
		TIP-Squared (intensity based)	87.197	126.293	39.096	44.82	Increased
		TEIP-Squared (intensity based)	9.276	11.222	1.945	20.97	Increased
		Binary Area Cross Correlation	0.718	0.773	0.055	7.63	Increased

TABLE 5.1-V

Temporal Variation Metrics (3x3x1)

Number of images in this sequence = [illegible]
Number of objects per image = 2
Type of data smoothing used = 3x3 Median
Number of images per cluster = 1

Object number	Object type	Name of object metric	Standard Deviation Of Metric Raw data	 Smoothed data	Difference	% of change	Central Tendency
1	Tank	Contrast (intensity based)	0.572	0.605	0.033	5.70	Decreased
		Contrast (entropy)	0.010	0.014	0.004	38.10	Decreased
		TIR-Squared (intensity based)	4.741	9.801	5.060	106.74	Decreased
		TBIR-Squared (intensity based)	0.457	0.735	0.278	60.83	Decreased
		Binary Area Cross Correlation	0.022	0.034	0.012	55.36	Decreased
2	Tank	Contrast (intensity based)	1.000	1.086	0.086	8.57	Decreased
		Contrast (entropy)	0.008	0.011	0.003	36.01	Decreased
		TIR-Squared (intensity based)	16.589	27.548	10.659	63.11	Decreased
		TBIR-Squared (intensity based)	1.094	1.116	0.022	2.00	Decreased
		Binary Area Cross Correlation	0.149	0.023	0.126	84.54	Improved

Object number	Object type	Name of object metric	Average Value Of Metric Raw data	 Smoothed data	Difference	% of change	Position on X axis
1	Tank	Contrast (intensity based)	20.897	19.994	0.903	4.32	Lower
		Contrast (entropy)	0.199	0.234	0.034	17.11	Increased
		TIR-Squared (intensity based)	32.135	63.735	31.599	98.33	Increased
		TBIR-Squared (intensity based)	5.906	8.696	2.790	47.24	Increased
		Binary Area Cross Correlation	0.733	0.721	0.012	1.67	Lower
2	Tank	Contrast (intensity based)	36.029	34.373	1.655	4.59	Lower
		Contrast (entropy)	0.257	0.296	0.039	15.36	Increased
		TIR-Squared (intensity based)	87.197	172.426	85.229	97.74	Increased
		TBIR-Squared (intensity based)	9.276	13.573	4.297	46.32	Increased
		Binary Area Cross Correlation	0.718	0.763	0.045	6.27	Increased

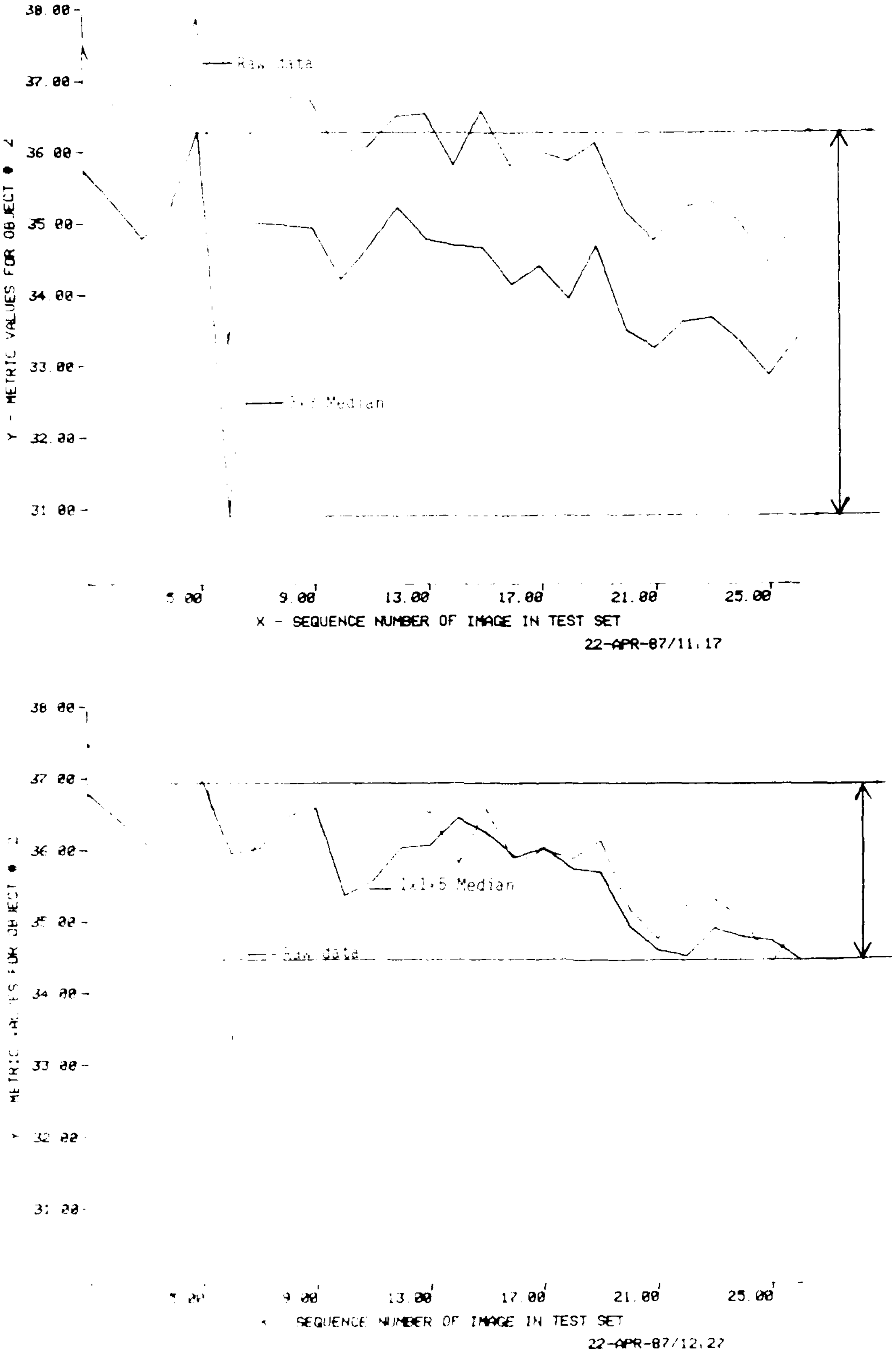

Figure 5.1-9. Metric Comparison of Contrast
(Intensity Based)

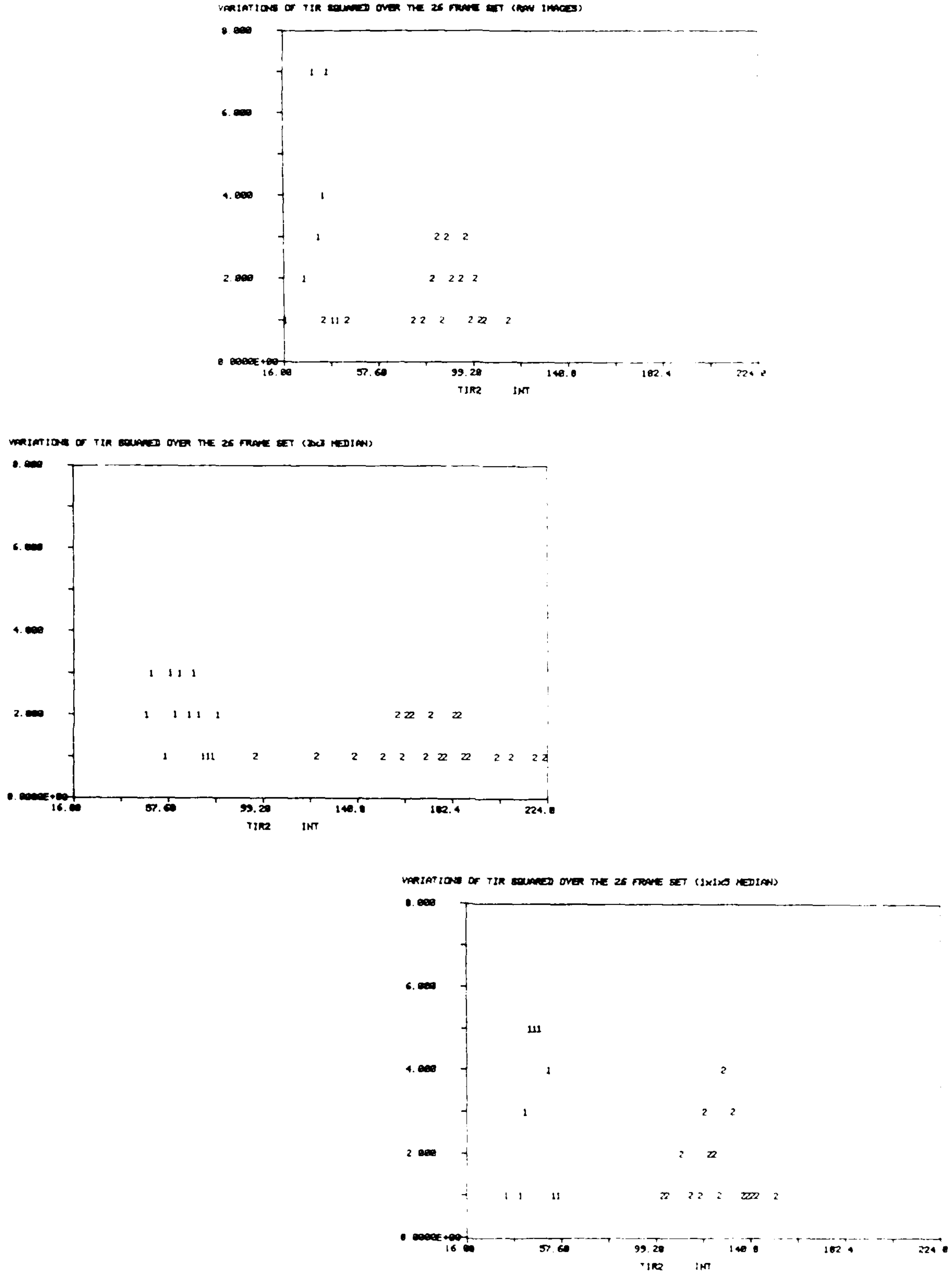

Figure 5.1-10. Feature Histogram Image Sequence of 26 Consecutive Frames (TI Data) Histogram of Intensity Based TIR Squared for two Tanks (1 and 2)

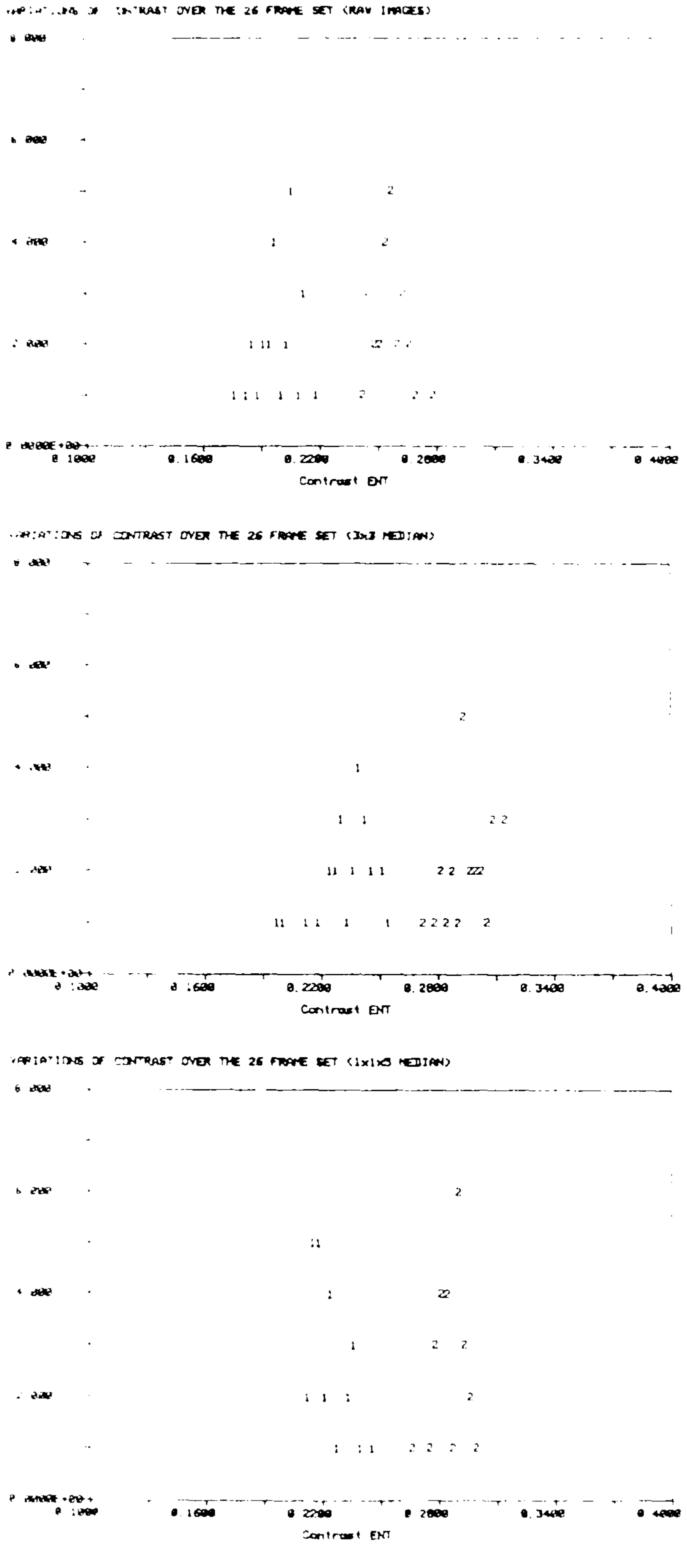

Figure 5.1-11. Feature Histogram Image Sequence of 26 Consecutive Frames (TI Data) Histogram of Entropy Based Contrast for Two Tanks (1 and 2)

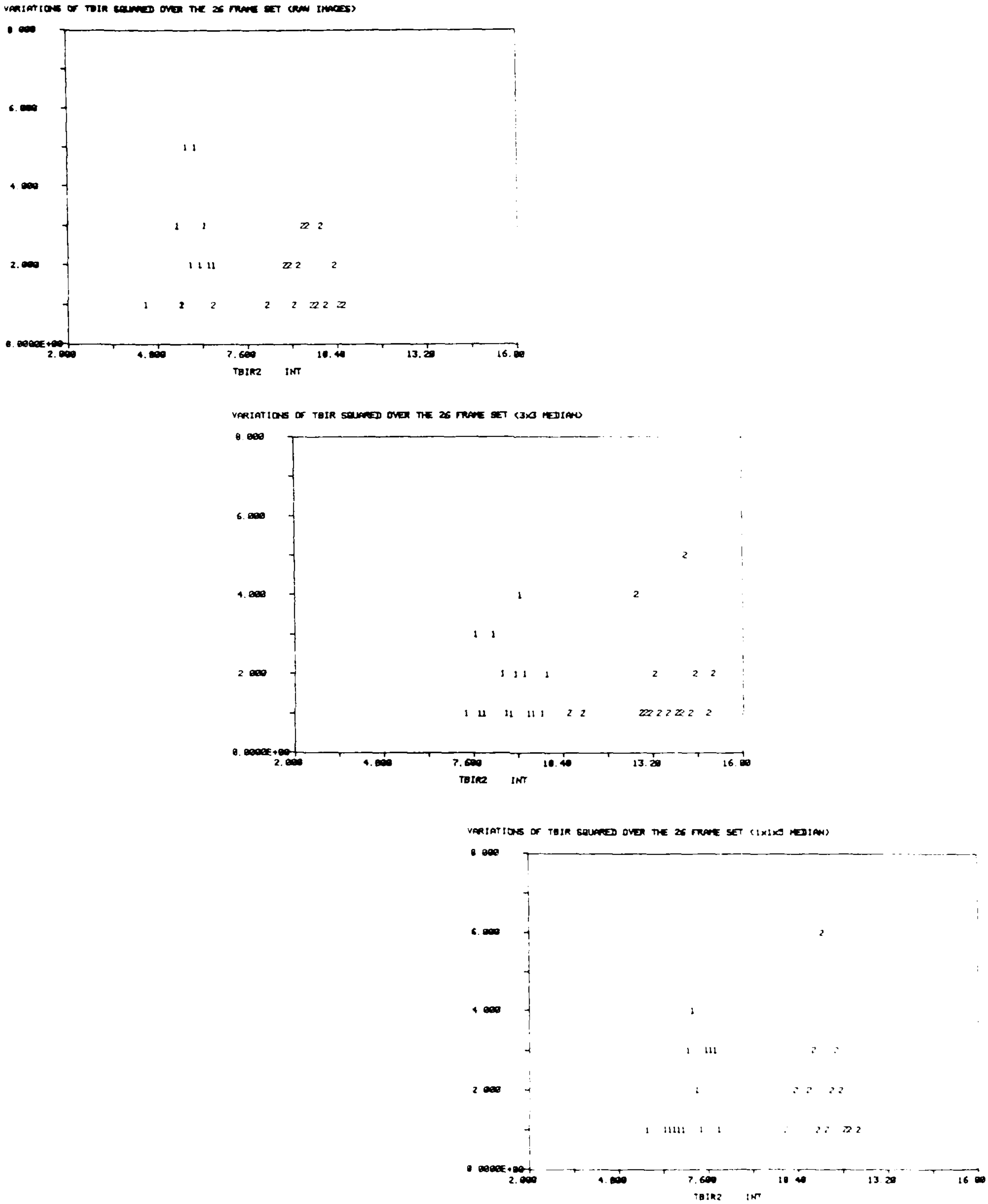

Figure 5.1-12. Feature Histogram Image Sequence of 26 Consecutive Frames (TI Data) Histogram of Intensity Based TBIR Squared for Two Tanks (1 and 2)

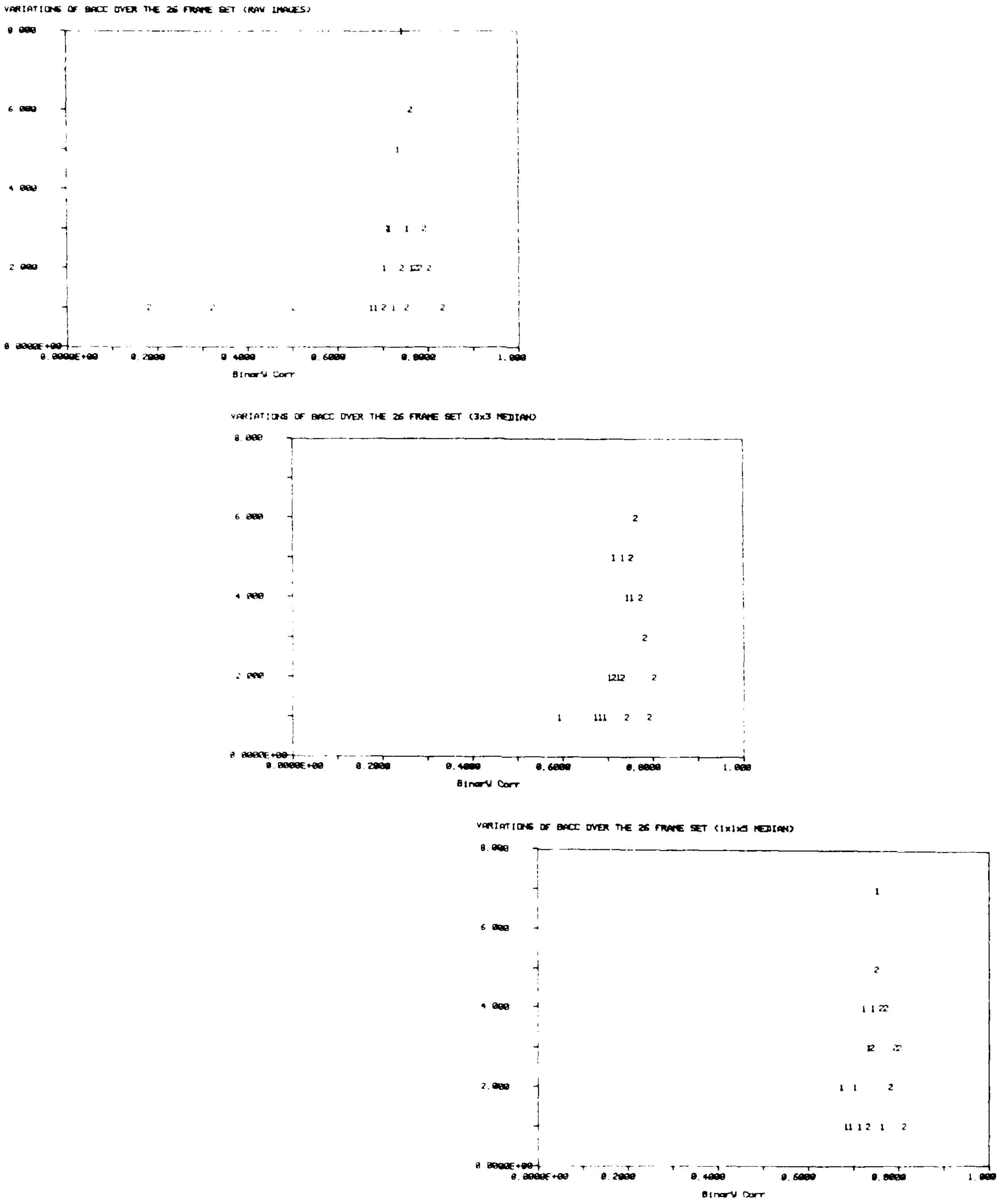

Figure 5.1-13. Feature Histogram Image Sequence of 26 Consecutive Frames (TI Data) Histogram of Binary Area Cross Correlation for Two Tanks (1 and 2)

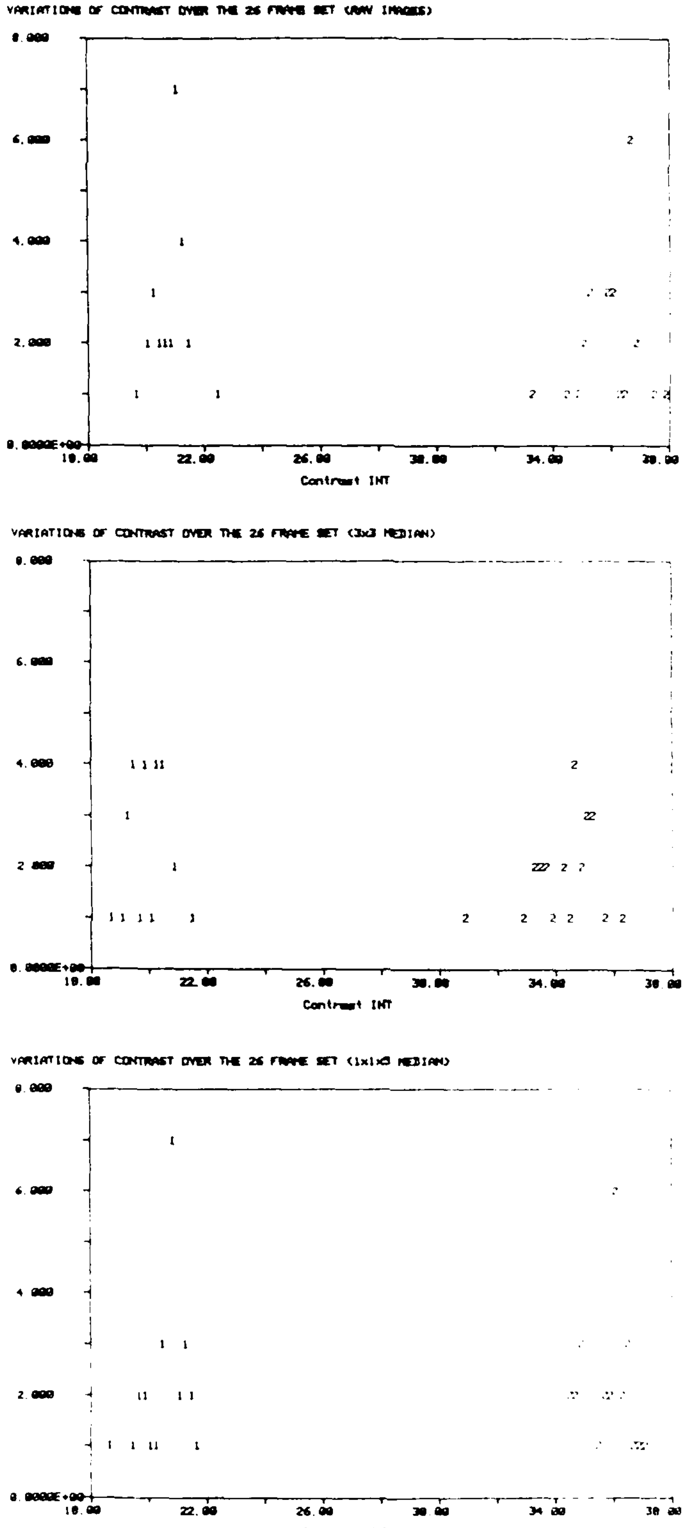

Figure 5.1-14. Feature Histogram Image Sequence of 26 Consecutive Frames (TI Data) Histogram of Intensity Based Contrast for Two Tanks (1 and 2)

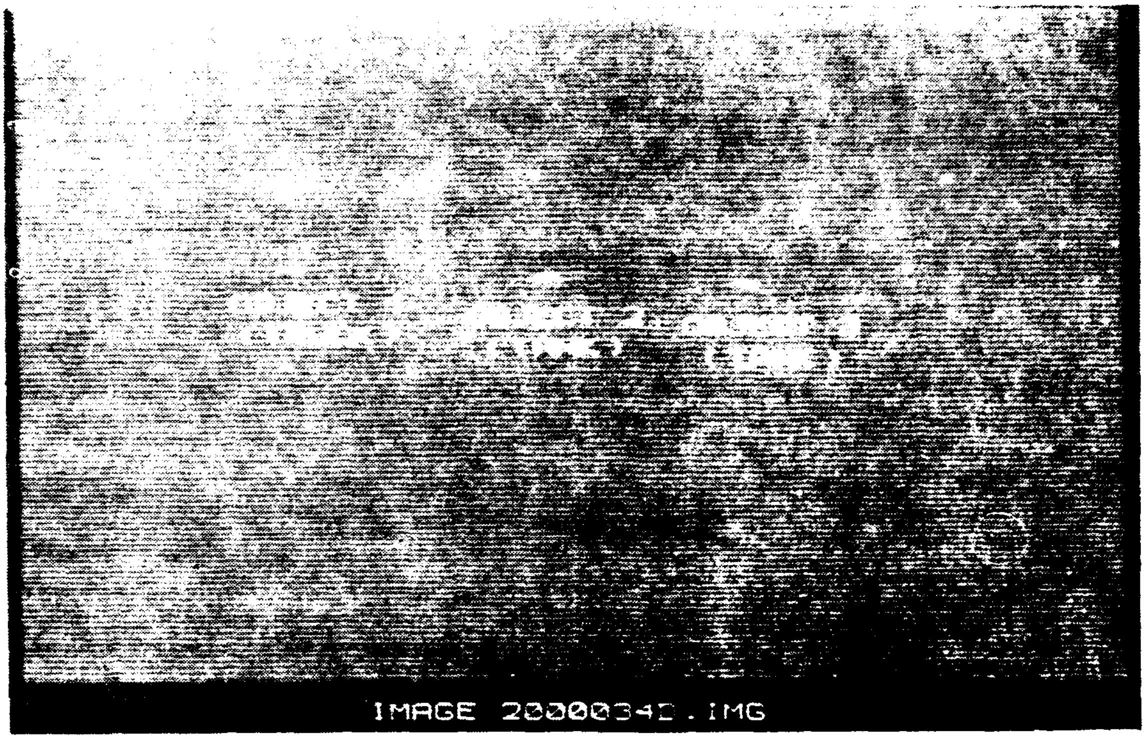

Figure 5.2-1. Image Sequence

object-3). All three vehicles are positioned at approximately side view aspects. Object-1, which is 5000 meters from the sensor, has the lowest contrast of the three vehicles. Object-2, approximately 4965 meters from the sensor, has the best organized structure (most visible) of the three vehicles. Object-3, approximately 4945 meters from the sensor, has structural characteristics that are between the other two vehicles. Excluding the three vehicles, the scene is void of any significant context and has only a gray-level range of approximately 20 intensity levels (Figure 5.2-2).

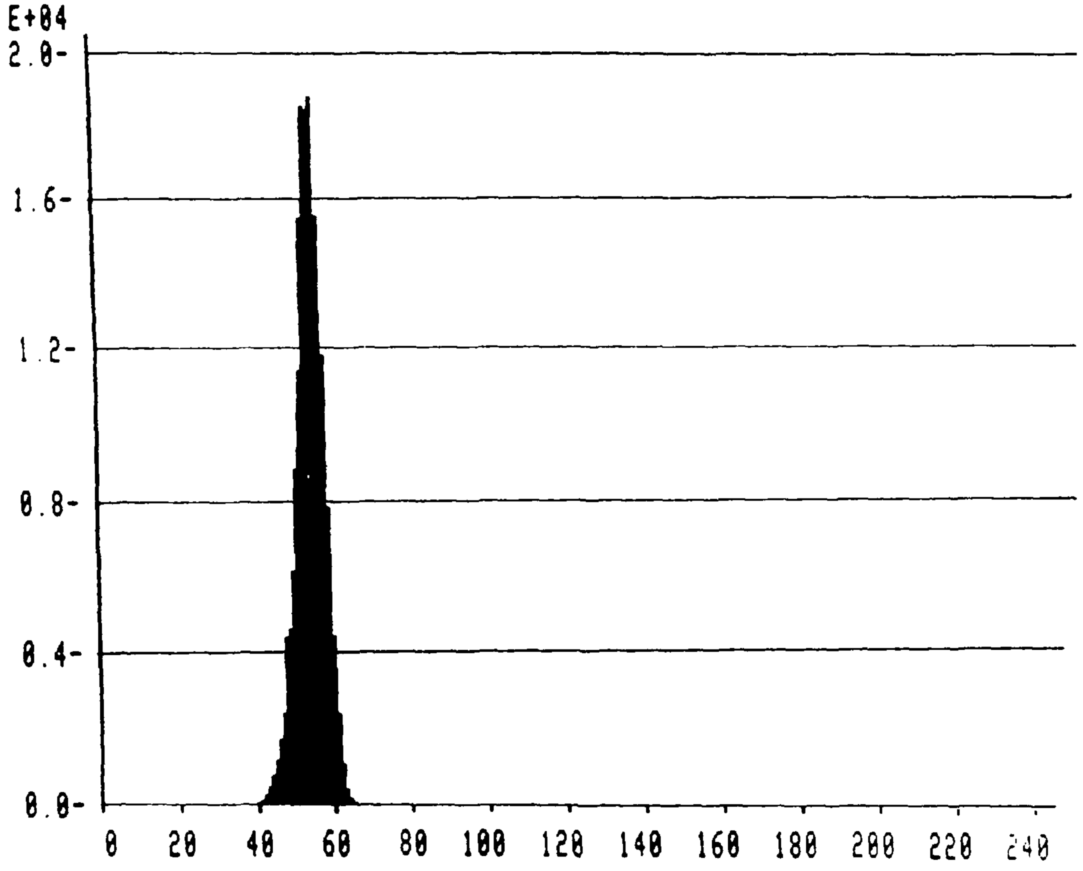

Figure 5.2-2. Intensity Histogram of Channel 1

Scene Motion

The 30-image test set was processed using the scene motion extraction software. Parameters for the point selection and tracking operators were set as follows;

1 Size contrast inner window size: 5 pixels wide, 3 pixels high

2 Partition and lcoal maximum: 8x8 grid surface (64 total points)

3 Correlation coefficient threshold: 0.7 (less than 0.7 is deleted)

4 Affine error threshold: 8.0 (greater than 8.0 is deleted).

The number of feature points tracked for the entire 30-frame sequence consisted of only two points, or 3 percent of the initial number selected. The two points pertained to contrast measures between the two tanks and their local background. The low contrast of the truck made it impossible for the frame to frame correlator to track. A visual review of the tank flow vectors indicated that correlation drift made them unreliable for multiframe smoothing. The lack of a reliable optical flow history file for the 30-frame set made it necessary to create one manually (Figure 5.2-3). Manual generation of the optical flow history file was accomplished by displaying the images on a monitor and noting the x,y positional change of each vehicle, using a cursor which controlled a minimum encompassing object box. The process was applied using a zoom factor of 4 on the images to minimize registration errors. The manual tracking process revealed the extensive level of frame to frame structural variation of the vehicles. These structural variations, along with the low contrast, made the manual tracking process about 75 percent reliable.

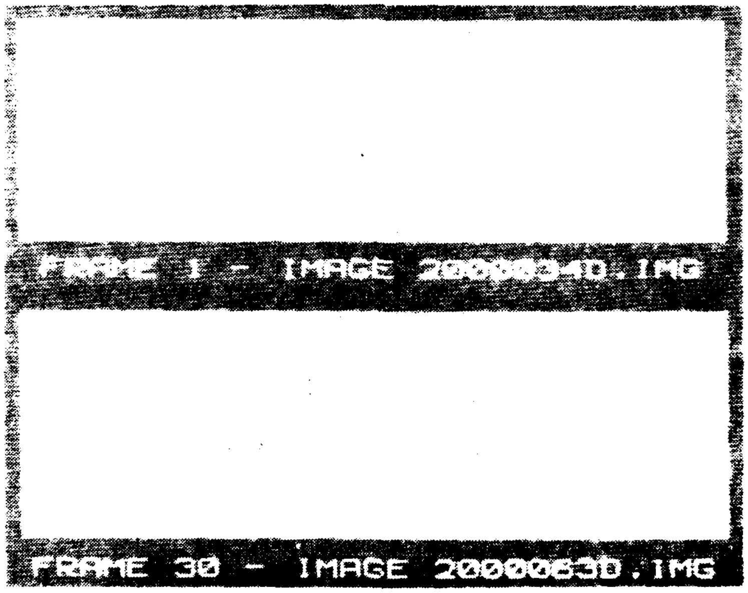

Figure 5.2-3. Optical Flow Vectors Created For Each Object

Data Smoothing

The parameters used for multiframe smoothing consisted of registering clusters of five consecutive subimage windows (placed about the vehicles) and applying a 1x1x5 median filter. This process generated a data set consisting of 26 images (30 total images - 5 cluster size +1). A second multiframe smoothing operator, which registered clusters of nine consecutive subimage windows and applied a 1x1x9 median filter, was also used. This process generated a data set consisting of 22 images. The consideration of nine samples in place of five attempts to further compensate for the low contrast image conditions. In addition, the same 26 raw data images were processed using a conventional 3x3x1 median filter.

To determine the effects of the enhancement techniques on segmenter performance, the 1x1x5 smoothed data set, 1x1x9 smoothed data set, 3x3x1 median filtered data set, and raw data set were processed using the rule directed segmenter. An assessment of the segmenter performance results (measured using the BACC evaluation metric) indicated that none of the techniques has a significant effect on performance. They also showed that each vehicle was affected differently.

Object-1 (the truck - Figure 5.2-4) had a small decrease in segmentation accuracy for the two data smoothing filters (1x1x5 and 1x1x9), while the local median (3x3x1) improved performance slightly (2 percent). The effect of the 1x1x5 median filter on object-1 can be seen in Figure 5.2-5, where a gray level threshold of 61 was applied to the first four images of the 1x1x5 median-filtered object and the raw-data images. The threshold represented the best number for object to background separation for both data sets. A greater level of structural consistency can be seen in the multiframe filtered images. However, for this object at this range, the changes in performance were still negligable.

Object-2 (the center tank - Figure 5.2-6) had the highest segmentation accuracy scores, which averaged 76 percent. The multiframe smoothing filters had a positive effect, reducing the degree of frame to frame performance variation for this vehicle, but no effect on increasing the

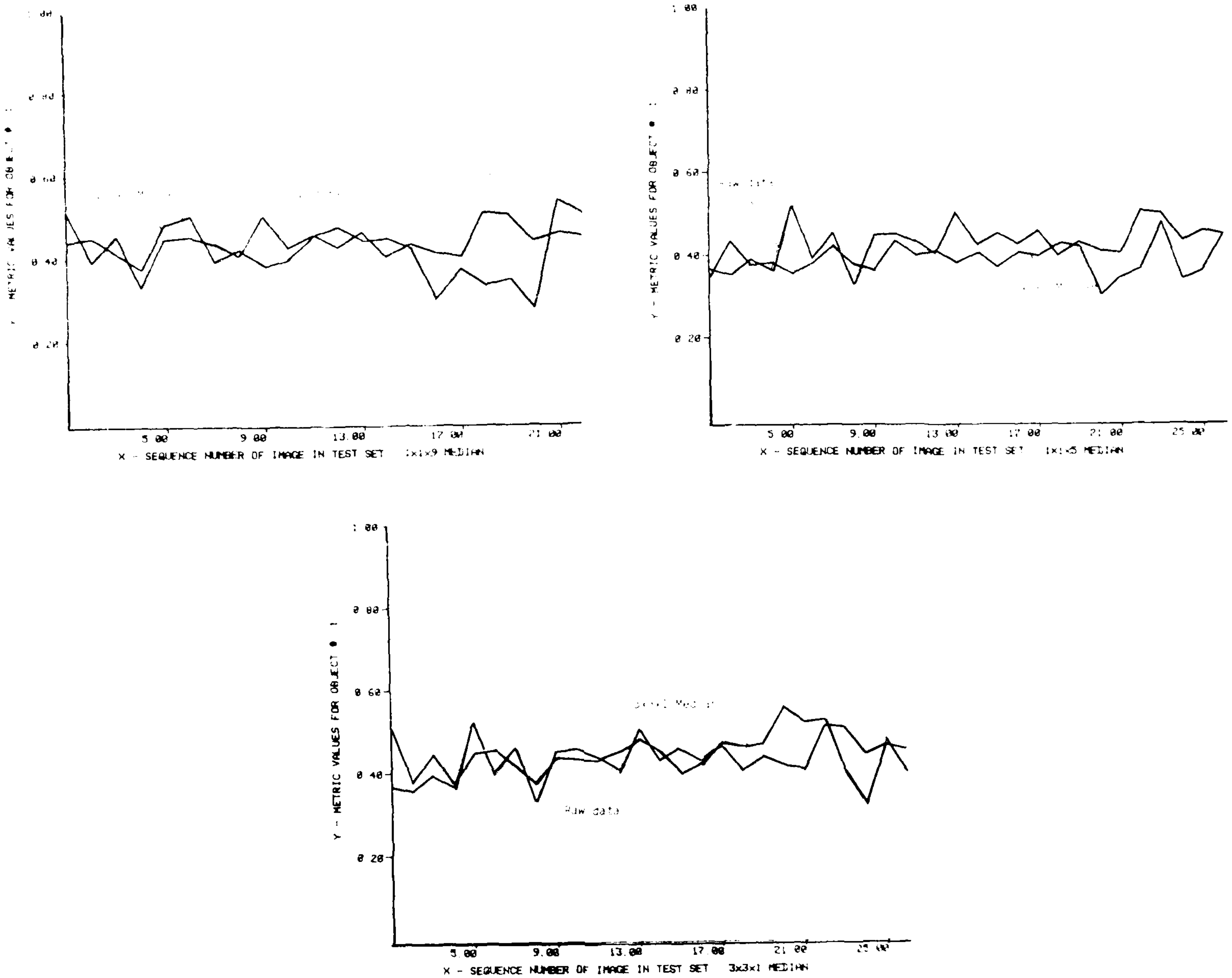

Figure 5.2-4. Comparison of Segmentation Accuracy (BACC)

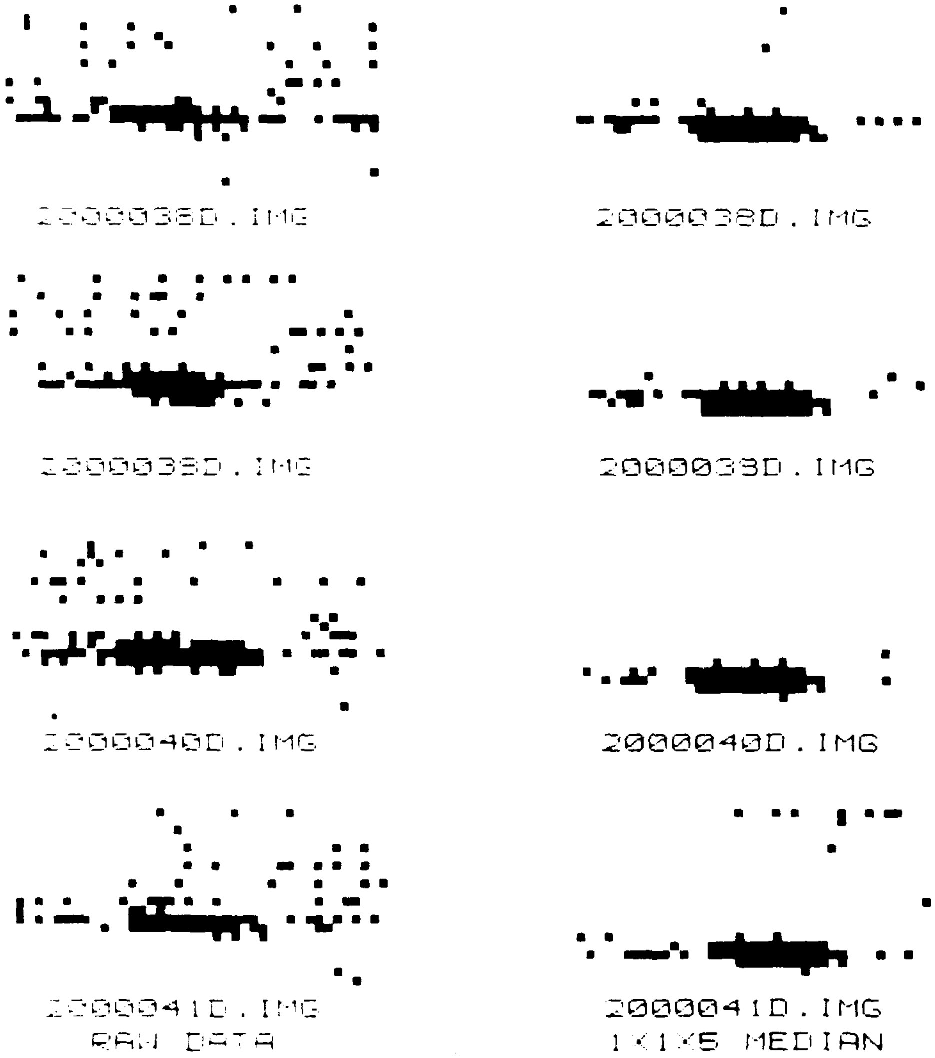
2000038D.IMG
2000038D.IMG
2000039D.IMG
2000039D.IMG
2000040D.IMG
2000040D.IMG
2000041D.IMG
RAW DATA
2000041D.IMG
1X1X5 MEDIAN

Figure 5.2-5. Truck Thresholded at 61 (Raw vs Median)

overall segmenter performance. The 3x3x1 filter had less of an effect on performance stabilization, but managed to increase the overall performance average by 1 percent.

Object-3 (the rightmost tank - Figure 5.2-7) produced results more typical of the first set of experiments. The multiframe smoothing filters increased segmenter performance and improved the frame to frame structural stability of the object. The 3x3x1 filter also improved segmenter performance, but did not improve structural stability.

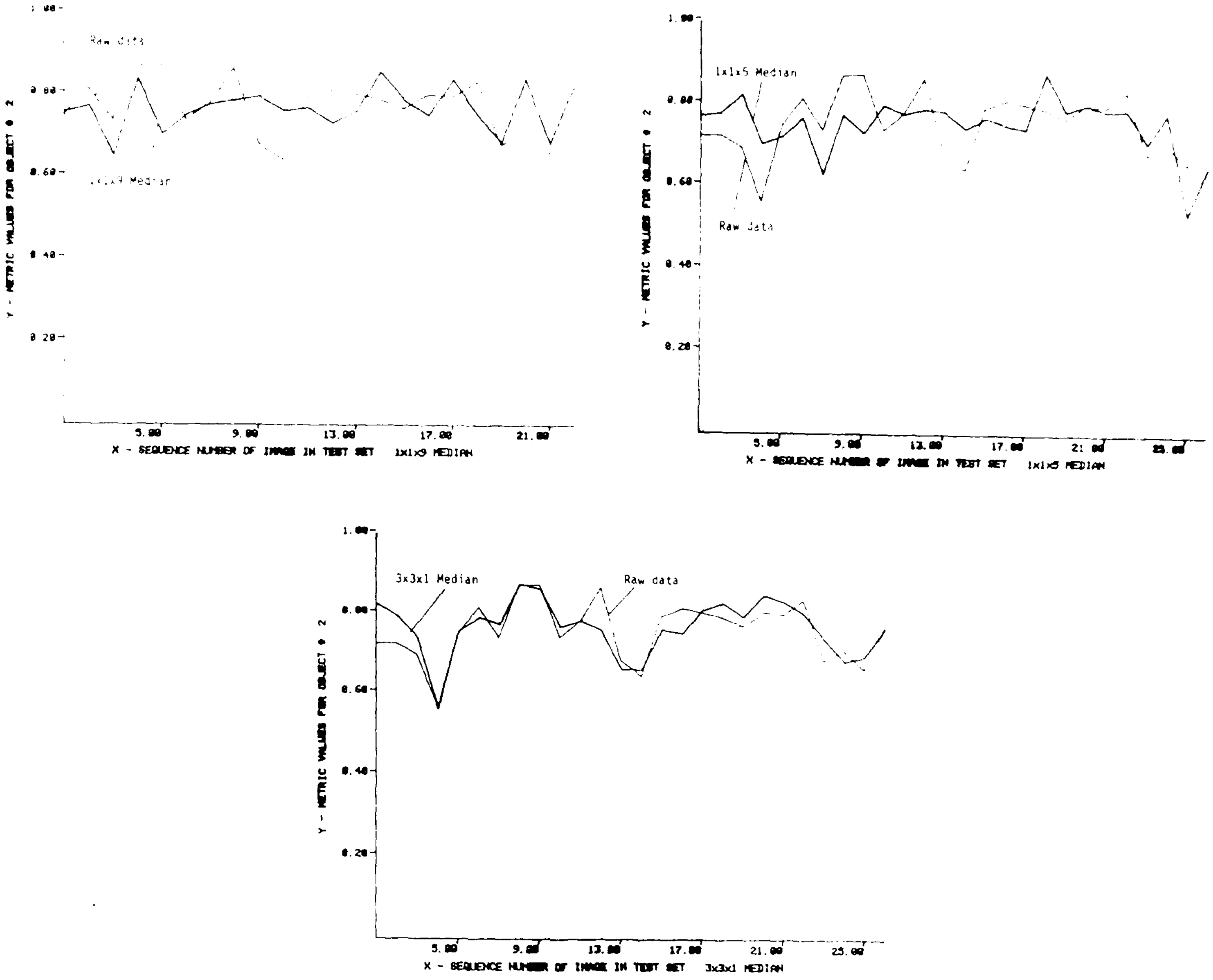

Figure 5.2-6. Metric Comparison of Binary Area Cross Correlation

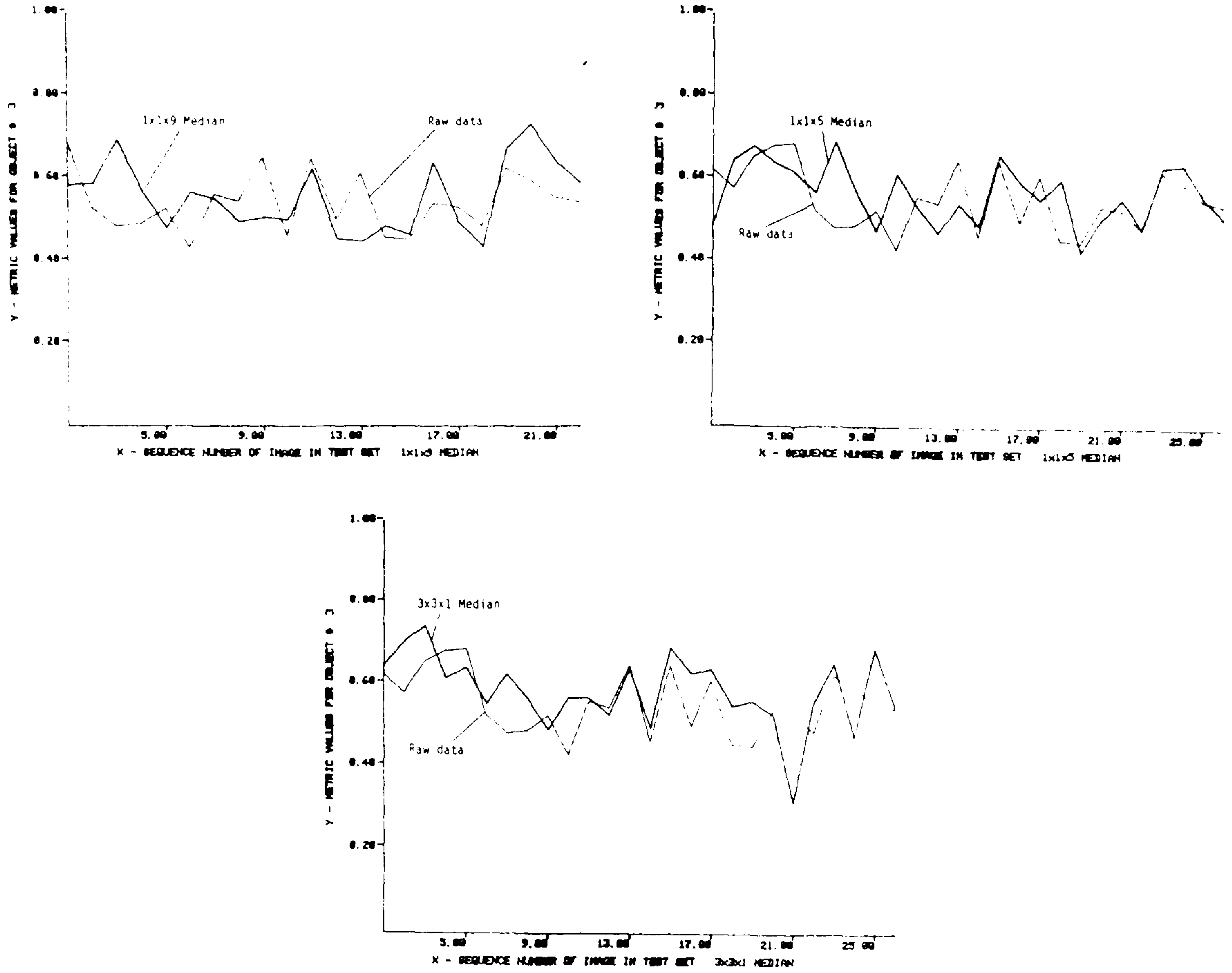

Figure 5.2-7. Metric Comparison of Binary Area Cross Correlation

The difficulty in obtaining consistent improvement in segmenter performance and frame to frame structural stability when applying the multiframe smoothing filters is due primarily to the manually derived optical flow history that was created for this data set. To confirm this, four attempts were made at tracking the frame to frame positional changes of each of the three vehicles through the 30-frame test set. Each attempt produced a slightly different flow history, which caused the performance results to differ. Due to the small size of the objects, minor inaccuracies in determining the x,y vehicle displacements significantly affected the outcome of the smoothing process. Misregistrations can be more easily tolerated when object features are spatially large; however, when a vehicles engine consists of only a few pixels, a one-pixel offset is significant. From the variations accumulated among the four manually derived optical-flow history files, a registration error of approximately 25 percent was estimated. This flow error makes an accurate evaluation of the multiframe smoothing operator difficult for this data set.

Despite the frame to frame registration problems, we were able to extract positive tendencies of the data smoothing operators. A complete comparison of each of the three enhancement methods (1x1x5, 1x1x9, and 3x3x1) is shown in the temporal variation metric listings (Tables 5.2-I through -III). The different responses for each of the three vehicles substantiate the difficulities in generating accurate optical flow history for this test set. Nevertheless, general improvements in metric response and stability are evident in the frame to frame changes in several of the metrics. A comparison of the entropy-based contrast metric for object-3 (Figure 5.2-8) shows an increase in metric response and stability for the multiframe smoothing filters, while the 3x3x1 local filter is still very unstable. This trend is also apparent to a lesser degree in the intensity-based TIR^2 metric for object-2 (Figure 5.2-9). This ability to improve vehicle characteristics indicates that an accurate extraction of optical flow should produce more favorable results than those currently generated. The results also indicate the importance of deriving accuate optical flow history, especially for vehicles at these ranges and beyond.

TABLE 5.2-I

Temporal Variation Metrics

Number of images in this sequence = 26
Number of objects per image = 3
Type of data smoothing used = 3x3 Median
Number of images per cluster = 1

Object number	Object type	Name of object metric	Standard Deviation Of Metric		Difference	% of change	Central Tendency
			Raw data	Smoothed data			
1	Truck	Contrast (intensity based)	0.645	0.658	0.013	2.09	Decreased
		Contrast (entropy)	0.040	0.042	0.002	4.76	Decreased
		TIR-Squared (intensity based)	1.223	3.324	2.101	171.79	Decreased
		TBIR-Squared (intensity based)	0.973	1.764	0.791	81.24	Decreased
		Binary Area Cross Correlation	0.049	0.054	0.005	10.93	Decreased
2	Tank	Contrast (intensity based)	0.563	0.473	0.091	16.12	Improved
		Contrast (entropy)	0.035	0.047	0.013	37.18	Decreased
		TIR-Squared (intensity based)	5.179	34.631	29.452	568.65	Decreased
		TBIR-Squared (intensity based)	1.664	5.578	3.915	235.29	Decreased
		Binary Area Cross Correlation	0.075	0.071	0.004	5.85	Improved
3	Tank	Contrast (intensity based)	0.835	0.758	0.076	9.16	Improved
		Contrast (entropy)	0.035	0.054	0.019	55.26	Decreased
		TIR-Squared (intensity based)	5.079	12.706	7.627	150.18	Decreased
		TBIR-Squared (intensity based)	1.553	2.591	1.038	66.80	Decreased
		Binary Area Cross Correlation	0.076	0.090	0.014	18.38	Decreased

Object number	Object type	Name of object metric	Average Value Of Metric		Difference	% of change	Position on X axis
			Raw data	Smoothed data			
1	Truck	Contrast (intensity based)	6.656	5.539	1.117	16.78	Lower
		Contrast (entropy)	0.058	0.082	0.024	41.89	Increased
		TIR-Squared (intensity based)	5.246	9.769	4.522	86.20	Increased
		TBIR-Squared (intensity based)	3.932	6.343	2.411	61.33	Increased
		Binary Area Cross Correlation	0.437	0.446	0.009	2.07	Increased
2	Tank	Contrast (intensity based)	12.080	10.923	1.157	9.58	Lower
		Contrast (entropy)	0.151	0.235	0.083	54.88	Increased
		TIR-Squared (intensity based)	24.310	81.769	57.459	236.36	Increased
		TBIR-Squared (intensity based)	11.054	21.359	10.305	93.23	Increased
		Binary Area Cross Correlation	0.756	0.764	0.008	1.07	Increased
3	Tank	Contrast (intensity based)	9.974	8.530	1.444	14.48	Lower
		Contrast (entropy)	0.211	0.260	0.049	23.15	Increased
		TIR-Squared (intensity based)	14.588	38.914	24.326	166.75	Increased
		TBIR-Squared (intensity based)	5.141	9.543	4.402	85.62	Increased
		Binary Area Cross Correlation	0.556	0.585	0.029	5.26	Increased

TABLE A2-11

Temporal Variation Metrics

Number of images in this sequence = 26
Number of objects per image = 3
Type of data smoothing used = Median
Number of images per cluster = 5

Object number	Object type	Name of object metric	Standard Deviation Of Metric Raw data	Standard Deviation Of Metric Smoothed data	Difference	% of change	Central Tendency
1	Truck	Contrast (intensity based)	0.645	0.986	0.341	52.89	Decreased
		Contrast (entropy)	0.040	0.050	0.009	23.11	Decreased
		TIR-Squared (intensity based)	1.223	2.876	1.653	135.16	Decreased
		TBIR-Squared (intensity based)	0.973	2.066	1.093	112.29	Decreased
		Binary Area Cross Correlation	0.049	0.039	0.010	19.61	Improved
2	Tank	Contrast (intensity based)	0.563	0.562	0.002	0.29	Unaffected
		Contrast (entropy)	0.035	0.051	0.017	48.16	Decreased
		TIR-Squared (intensity based)	5.179	21.580	16.401	316.66	Decreased
		TBIR-Squared (intensity based)	1.664	3.891	2.227	133.87	Decreased
		Binary Area Cross Correlation	0.075	0.068	0.008	10.03	Improved
3	Tank	Contrast (intensity based)	0.835	0.685	0.150	17.94	Improved
		Contrast (entropy)	0.035	0.029	0.006	17.08	Improved
		TIR-Squared (intensity based)	5.079	6.162	1.083	21.33	Decreased
		TBIR-Squared (intensity based)	1.553	1.431	0.122	7.86	Improved
		Binary Area Cross Correlation	0.076	0.072	0.003	4.55	Improved

Object number	Object type	Name of object metric	Average Value Of Metric Raw data	Average Value Of Metric Smoothed data	Difference	% of change	Position on X axis
1	Truck	Contrast (intensity based)	6.656	6.365	0.291	4.37	Lower
		Contrast (entropy)	0.058	0.080	0.022	37.99	Increased
		TIR-Squared (intensity based)	5.246	8.147	2.901	55.29	Increased
		TBIR-Squared (intensity based)	3.932	5.584	1.652	42.01	Increased
		Binary Area Cross Correlation	0.437	0.397	0.041	9.33	Lower
2	Tank	Contrast (intensity based)	12.080	11.831	0.249	2.06	Lower
		Contrast (entropy)	0.151	0.230	0.078	51.58	Increased
		TIR-Squared (intensity based)	24.310	55.767	31.457	129.40	Increased
		TBIR-Squared (intensity based)	11.054	17.167	6.114	55.31	Increased
		Binary Area Cross Correlation	0.756	0.751	0.005	0.68	Unaffected
3	Tank	Contrast (intensity based)	9.974	9.533	0.441	4.42	Lower
		Contrast (entropy)	0.211	0.268	0.056	26.64	Increased
		TIR-Squared (intensity based)	14.588	25.515	10.927	74.90	Increased
		TBIR-Squared (intensity based)	5.141	6.993	1.852	36.02	Increased
		Binary Area Cross Correlation	0.556	0.568	0.012	2.18	Increased

TABLE 5.2-III

Temporal Variation Metrics

Number of images in this sequence = 22
Number of objects per image = 3
Type of data smoothing used = Median
Number of images per cluster = 9

Object number	Object type	Name of object metric	Standard Deviation Of Metric Raw data	Standard Deviation Of Metric Smoothed data	Difference	% of change	Central Tendency
1	Truck	Contrast (intensity based)	0.573	0.739	0.166	28.96	Decreased
		Contrast (entropy)	0.040	0.044	0.004	9.19	Decreased
		TIR-Squared (intensity based)	1.107	2.235	1.128	101.91	Decreased
		TBIR-Squared (intensity based)	0.778	1.635	0.857	110.18	Decreased
		Binary Area Cross Correlation	0.044	0.067	0.023	51.78	Decreased
2	Tank	Contrast (intensity based)	0.601	0.482	0.118	19.66	Improved
		Contrast (entropy)	0.036	0.040	0.004	12.14	Decreased
		TIR-Squared (intensity based)	5.483	22.374	16.891	308.07	Decreased
		TBIR-Squared (intensity based)	1.731	3.774	2.043	118.03	Decreased
		Binary Area Cross Correlation	0.067	0.054	0.013	18.97	Improved
3	Tank	Contrast (intensity based)	0.875	0.523	0.352	40.21	Improved
		Contrast (entropy)	0.037	0.026	0.012	30.71	Improved
		TIR-Squared (intensity based)	5.483	10.660	5.176	94.41	Decreased
		TBIR-Squared (intensity based)	1.655	1.562	0.093	5.62	Improved
		Binary Area Cross Correlation	0.071	0.086	0.015	21.19	Decreased

Object number	Object type	Name of object metric	Average Value Of Metric Raw data	Average Value Of Metric Smoothed data	Difference	% of change	Position on X axis
1	Truck	Contrast (intensity based)	6.668	6.428	0.240	3.60	Lower
		Contrast (entropy)	0.057	0.091	0.034	58.84	Increased
		TIR-Squared (intensity based)	5.369	8.876	3.506	65.30	Increased
		TBIR-Squared (intensity based)	4.053	6.043	1.989	49.08	Increased
		Binary Area Cross Correlation	0.448	0.422	0.027	5.92	Lower
2	Tank	Contrast (intensity based)	12.045	11.726	0.319	2.65	Lower
		Contrast (entropy)	0.154	0.261	0.107	69.17	Increased
		TIR-Squared (intensity based)	24.450	74.964	50.515	206.61	Increased
		TBIR-Squared (intensity based)	11.027	20.345	9.318	84.51	Increased
		Binary Area Cross Correlation	0.771	0.767	0.004	0.50	Unaffected
3	Tank	Contrast (intensity based)	9.970	9.392	0.577	5.79	Lower
		Contrast (entropy)	0.211	0.295	0.083	39.37	Increased
		TIR-Squared (intensity based)	14.319	32.366	18.047	126.03	Increased
		TBIR-Squared (intensity based)	5.043	7.747	2.704	53.63	Increased
		Binary Area Cross Correlation	0.541	0.554	0.013	2.44	Increased

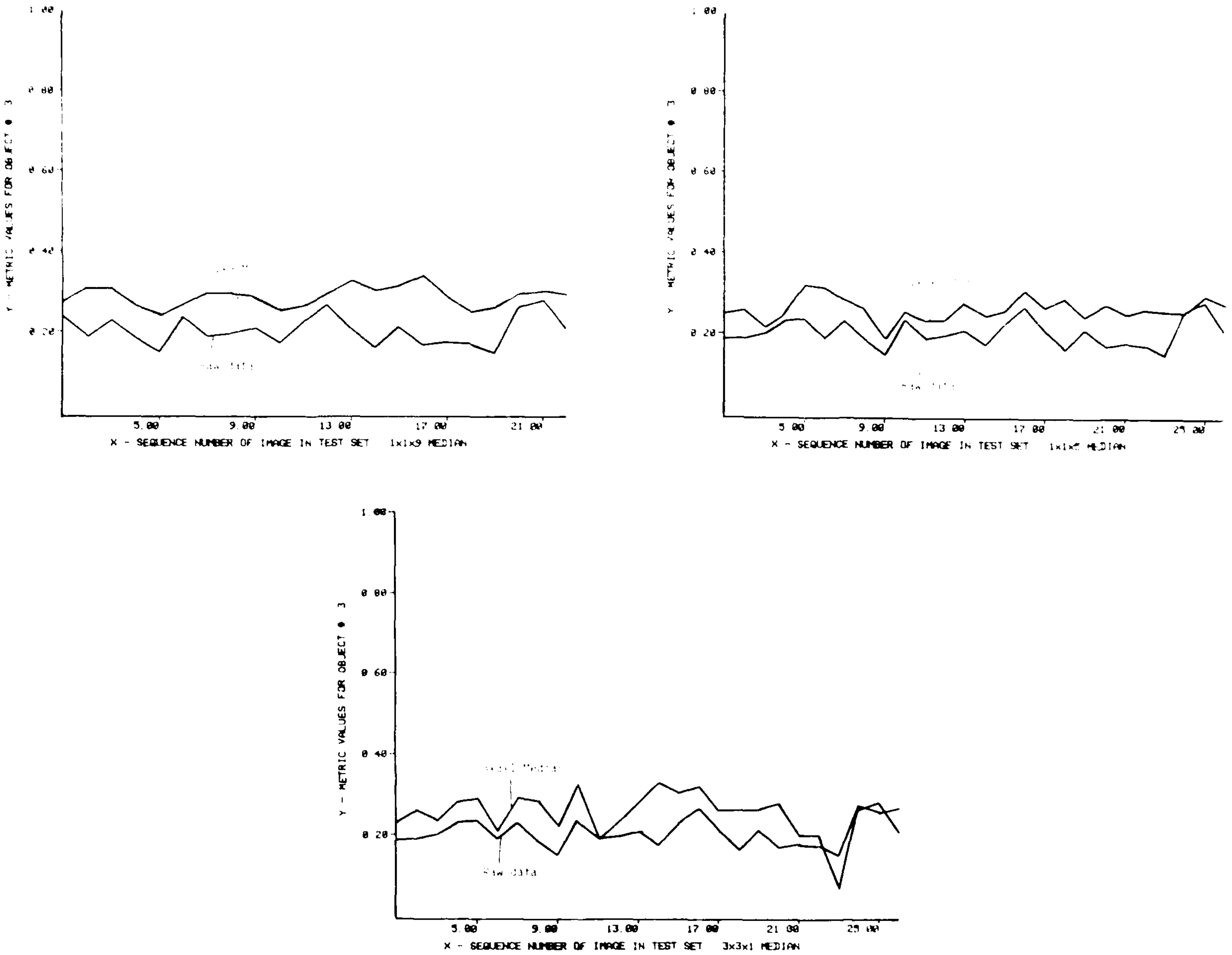

Figure 5.2-8. Metric Comparison of Contrast (Entropy)

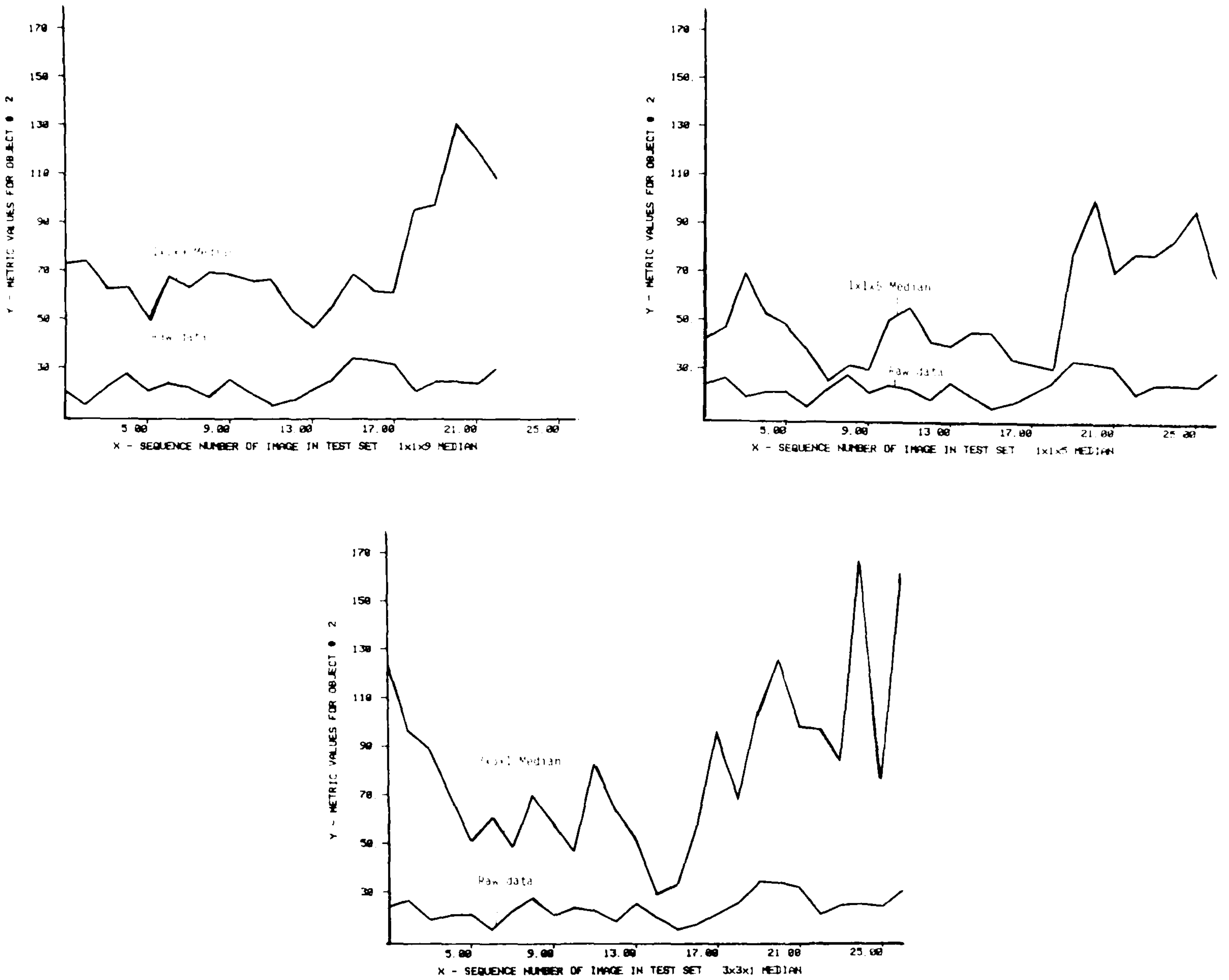

Figure 5.2-9. Metric Comparison of TIR Squared (Intensity Based)

5.3 Test Set 3

The third data set tested was an image sequence from ERIM data tape number 3031-10, set 40. The data tape included raw imagery, ground truth information, metrics, and truth silhouettes. The first 22 images on the tape were noncontinuous, unrelated frames of data taken at various times of the day, which made them inappropriate for testing. The next 21 frames consisted of consecutive sequences of images digitized at 1-second intervals, with the exception of 2 frames, which were 2 seconds apart. The 21 frames of data (Table 5.3-I) were removed from tape using the ATRWG read software.

TABLE 5.3-I
Image List for Experiment 3

2020000D	2020007D	2020015D
2020023D	2020031D	2020039D
2020047D	2020055D	2020063D
2020071D	2020079D	2021007D
2021015D	2021023D	2021031D
2021039D	2021047D	2021055D
2021063D	2021071D	2021079D

The image sequence (Figure 5.3-1) contains three military vehicles: a jeep (the leftmost object, object-1), an APC (the center object, object-2), and a truck (the rightmost object, object-3). All three vehicles are positioned at side view aspects. Objects-1, which is approximately 6341 meters from the sensor, has the most uniformly distributed intensity contrast of the three vehicles. Object-2, approximately 6366 meters from the sensor, has the best organized structure (most visibly distinguishable) of the three vehicles. Object-3, approximately 6415 meters from the sensor, has bimodel structural characteristics. Excluding the three vehicles, the scene is void of any significant context and only has a gray level range of approximately 20 intensity levels (Figure 5.3-2).

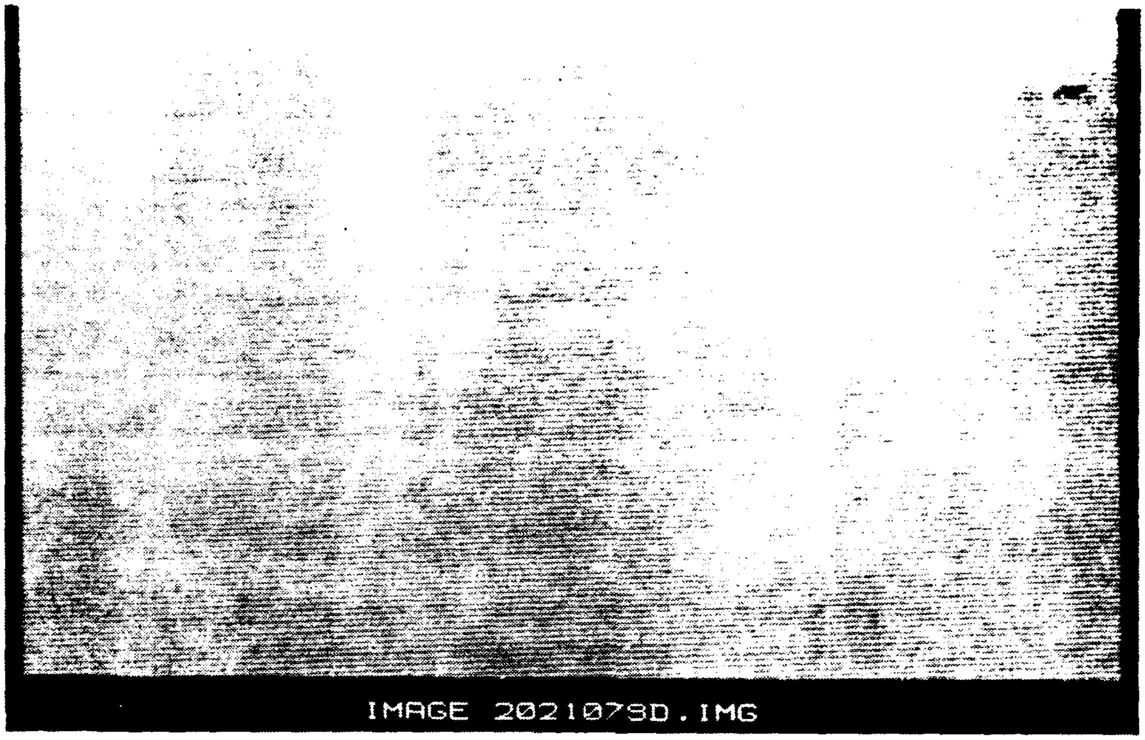
IMAGE 2021079D.IMG

Figure 5.3-1. Image Sequence

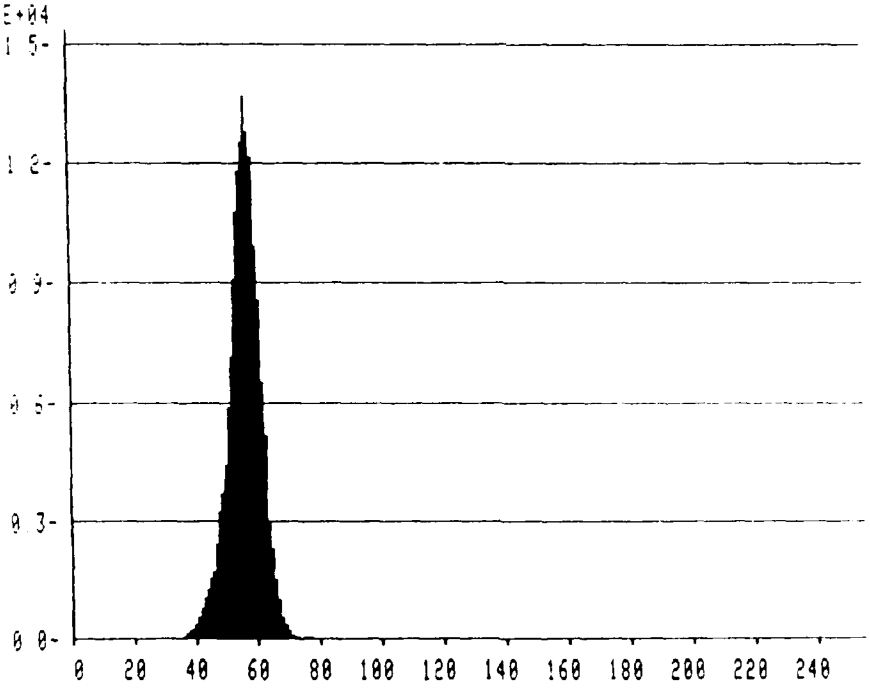

Figure 5.3-2. Intensity Histogram of Channel 1

Scene Motion

The 21-image test set was processed using the scene motion extraction software. The parameters for the point selection and tracking operators were set as follows:

1 Size contrast inner window size: 5 pixels wide, 3 pixels high

2 Partition and local maximum: 8x8 grid surface (64 total points)

3 Correlation coefficient threshold: 0.7 (less than 0.7 is deleted)

4 Affine error threshold: 8.0 (greater than 8.0 is deleted)

The feature tracking software was unsuccessful in maintaining the positional changes of any of the features selected for tracking. This failure was due to the low contrast of the imagery and the 1-second spacing between frames, which allowed object signatures to change significantly. The lack of an optical flow history file for the 21-frame set made it necessary to create one manually (Figure 5.3-3). Manual generation of the optical flow history file was accomplished by displaying truth images on a monitor and noting the x,y positional change of each vehicle, using a cursor that controlled a minimum encompassing object box. The process was applied on the images using a zoom factor of 4 to minimize registration errors.

Truth images were used in place of raw data images in an attempt to improve tracking accuracy and to avoid dealing with the low level contrast conditions of the raw data. The manually derived optical flow field depicts the significant amount of positional change for each vehicle over the 21-frame set. The low contrast conditions of the imagery and the manual tracking process gives the derived optical flow field a reliability rating of about 75 percent.

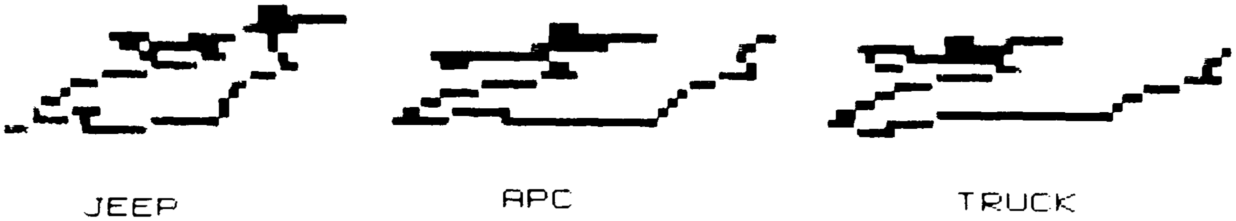

Figure 5.3-3. Optical Flow Vectors Created for Each Object

Data Smoothing

Parameters used for multiframe smoothing consisted of registering clusters of five consecutive subimage windows (placed about the vehicles) and applying a 1x1x5 median filter. This process generated a data set consisting of 17 images (21 total - 5 cluster size + 1). A second multiframe smoothing operator, which registered clusters of seven consecutive subimage windows and applied a 1x1x7 median filter, was also used. This process generated a data set consisting of 15 images. The consideration of 7 samples in place of 5 attempts to further compensate for the low contrast and attempts to further reduce the degree of frame to frame variation. In addition, the same 17 raw data images were processed using a conventional 3x3x1 median filter.

To determine the effects of the enhancement techniques on segmenter performance, the 1x1x5 smoothed data set, 1x1x7 smoothed data set, 3x3x1 median filtered data set, and raw data set were processed using the rule directed segmenter. The segmenter (measured using the BACC evaluation metric) improved performance accuracy for two of the vehicles, with only a slight decrease in performance for the third vehicle. The results also revealed that each vehicle was affected differently by each of the enhancement techniques.

Object-1 (the jeep - Figure 5.3-4) had the largest increase in segmenter performance of the three vehicles in this data set. The best response was to the 1x1x7 data smoothing filter, which increased performance accuracy by an average of 44 percent. All but one of the 1x1x7 smoothed images, processed by the rule directed segmenter, had improved

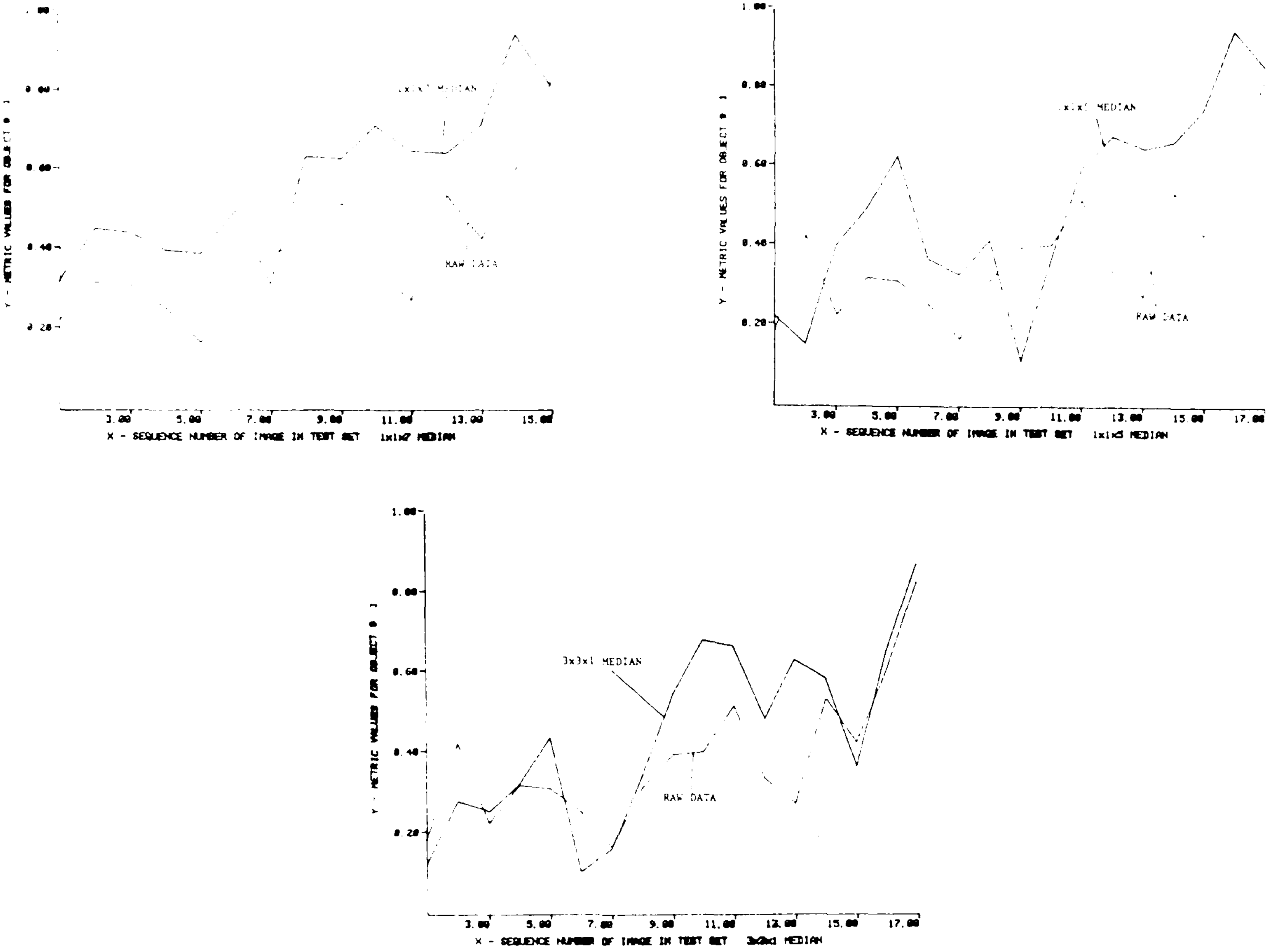

Figure 5.3-4. Metric Comparison of Binary Area Cross Correlation

accuracy. The least successful filter was the conventional 3x3x1 median, which still improved performance accuracy by 14 percent. The 1x1x5 data smoothing filter increased performance accuracy by 32 percent, but was less stable than the 1x1x7 filter. The improved performance is due to a more accurate frame to frame object registration than the last data set tested.

Object-2 (the APC - Figure 5.3-5) also had improved segmentation accuracy scores after data smoothing. The 1x1x5 filter and 1x1x7 filter showed a 24 percent and 22 percent average improvement in performance over the raw data results, while the conventional 3x3x1 median showed a 5 percent increase. Although the 1x1x7 filter had a 2% lower performance gain than the 1x1x5 filter, it still exhibits a high degree of frame to frame stability. The benefits of multiframe data smoothing can be seen by comparing the variations on structural characteristics of the APC for five consecutive frames. (Figure 5.3-6, raw data; Figure 5.3-7, 1x1x7 smoothed data; Figure 5.3-8, 3x3x1 smoothed data). The highest degree of structural similarity is seen between the 1x1x7 smoothed data images. The 3x3x1 filtered images show the smoothing effect, but lack the frame to frame consistency seen in the 1x1x7 results.

Object-3 (the truck - Figure 5.3-9) had lower performance scores than the other two vehicles. A reduction performance accuracy was generated for both of the multiframe smoothing operators and the conventional 3x3x1 median which produced the worst results. Although the average segmenter performance of the 1x1x7 median-smoothed data set was 12 percent lower than the raw data results, an increase of 15 percent was achieved in frame to frame stability of results. The stability factor, an important property of the multiframe smoothing approach, is also extremely beneficial during the feature mapping process used for object classification.

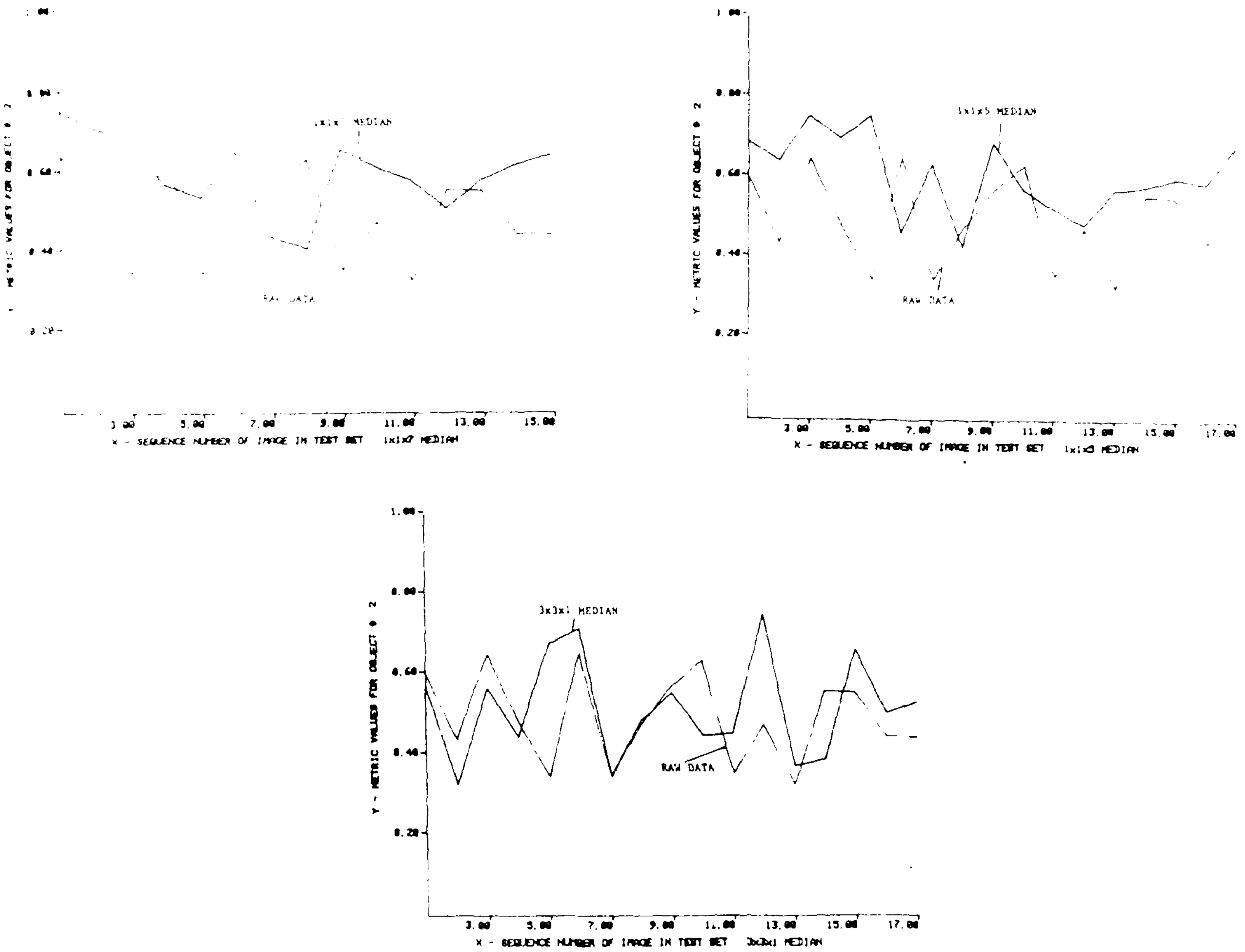

Figure 5.3-5. Metric Comparison of Binary Cross Area Correlation

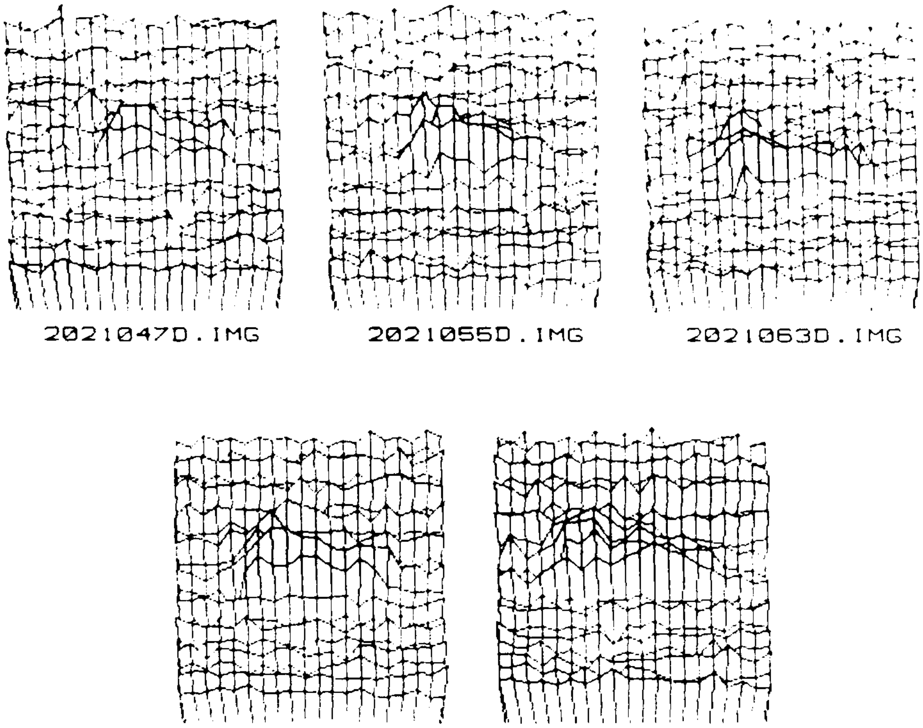
2021047D.IMG 2021055D.IMG 2021063D.IMG

2021071D.IMG 2021079D.IMG

Figure 5.3-6. Object (APC) Variations Over 5 Frames (Raw Data)

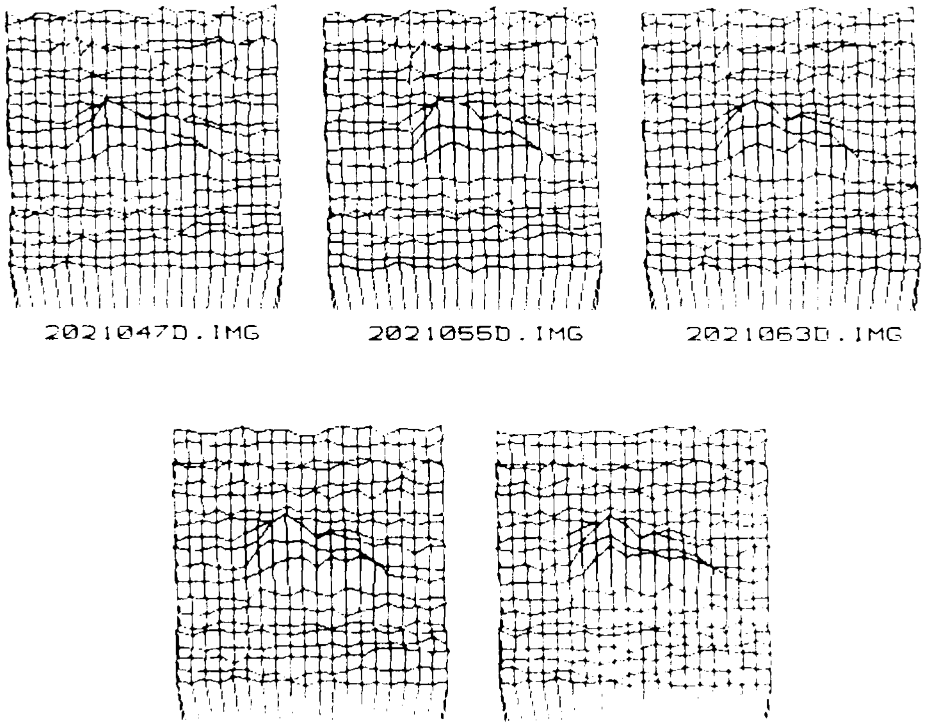
2021047D.IMG 2021055D.IMG 2021063D.IMG

2021071D.IMG 2021079D.IMG

Figure 5.3-7. Object (APC) Variations Over 5 Frames After 1x1x7 Median Smoothing

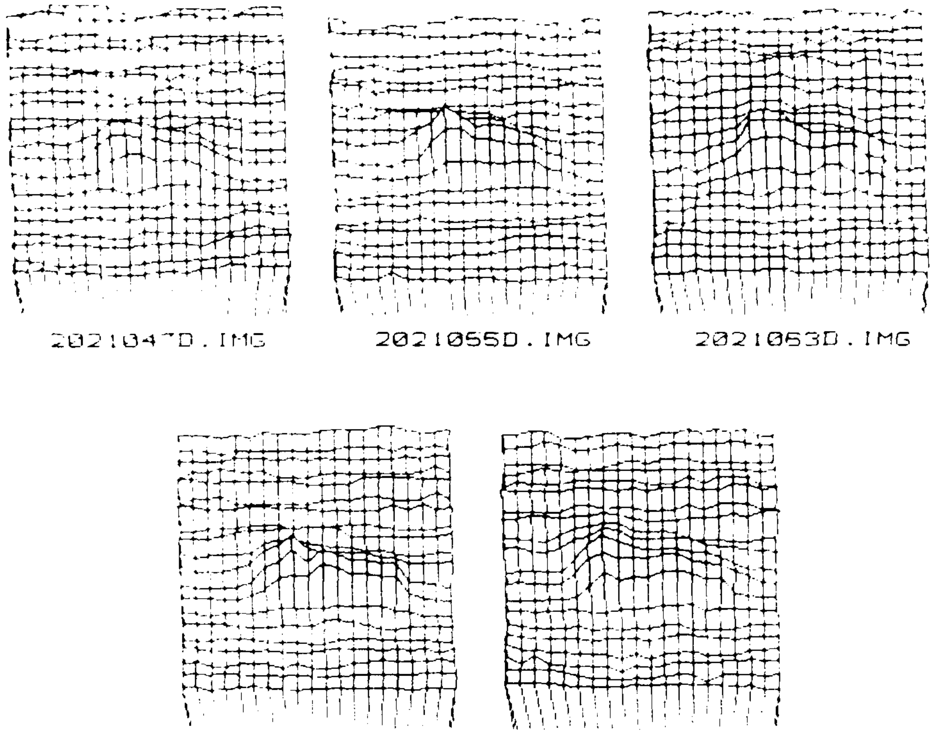

2021047D.IMG 2021055D.IMG 2021063D.IMG

2021071D.IMG 2021079D.IMG

Figure 5.3-8. Object (APC) Variations Over 5 Frames After 3x3x1 Median Smoothing

The difficulty in obtaining consistent improvement in segmenter performance and frame to frame structural stability when applying the multiframe smoothing filters is due to the errors in the manually derived optical flow history and the larger time intervals between image samples (1 to 2 seconds). The frame to frame misregistration errors, along with the structural variations of the vehicles which occur when the image samples are 1 second apart and the sensor is moving, make it difficult to obtain global improvement in performance.

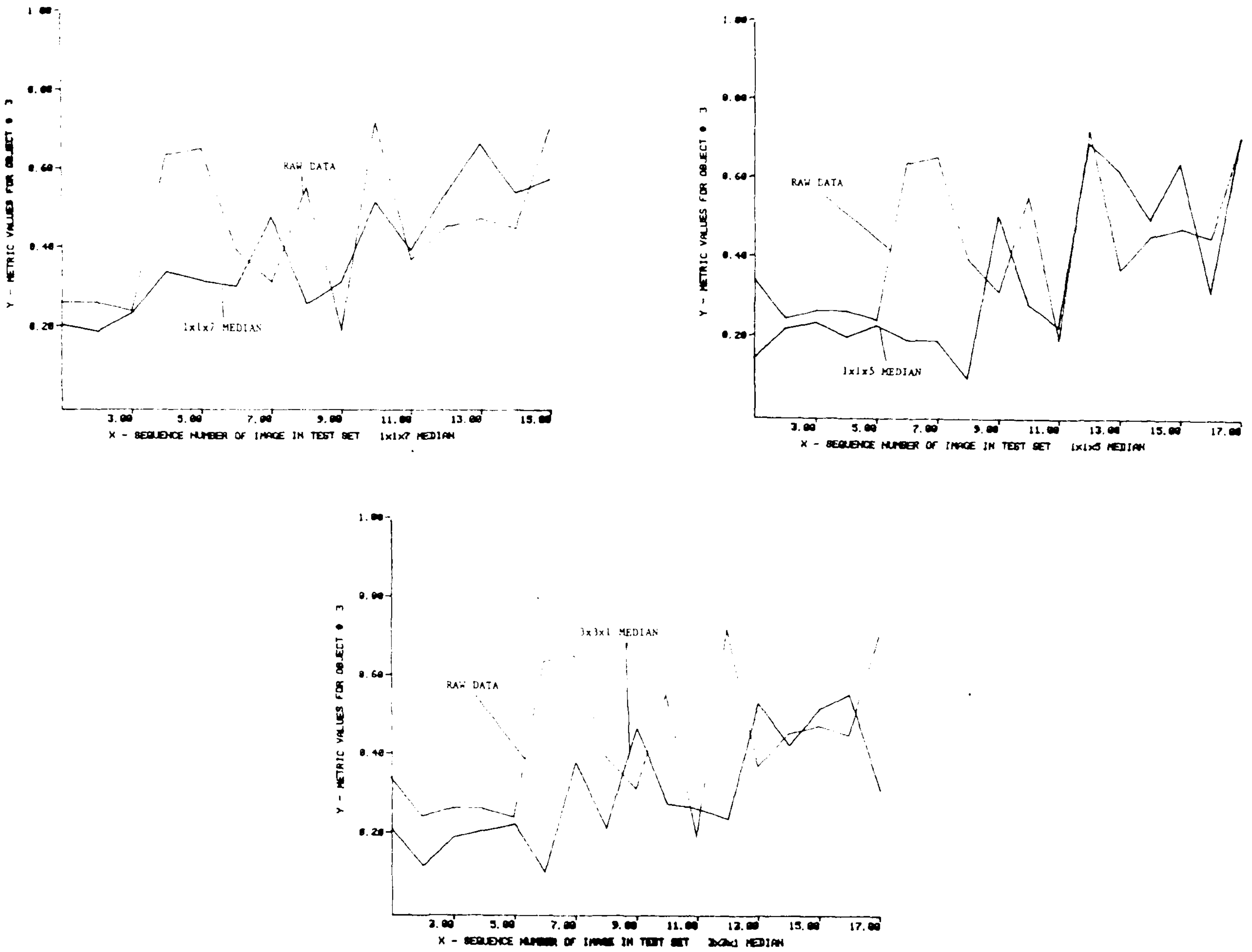

Figure 5.3-9. Metric Comparison of Binary Area Cross Correlation

Nevertheless, we were still able to extract positive tendencies of the data smoothing operators. A comparison of each of the three data enhancement methods is shown in Tables 5.3-II through -IV. The different responses for each of the three vehicles point out the difficulties in generating accurate optical flow history for this test set. However, general improvements in metric response and stability can be seen in the frame to frame changes in several of the metrics. For example, a comparison of the intensity-based TIR^2 metric for object-2 (Figure 5.8-10) shows an increase in metric response and stability for the multiframe smoothing filters, while the 3x3xl median filter shows an increase in metric response and a decrease in metric stability. The increased metric response and stability reflect the beneficial characteristics of the multiframe smoothing operator.

These test results support the conclusions expressed in the second experiment evaluation, which emhpasized the importance of obtaining an accurate optical flow history, especially for vehicles at these ranges.

TABLE 5.3-II

Temporal Variation Metrics

Number of images in this sequence = 17
Number of objects per image = 3
Type of data smoothing used = Median
Number of images per cluster = 5

Object number	Object type	Name of object metric	Standard Deviation Of Metric Raw data	Standard Deviation Of Metric Smoothed data	Difference	% of change	Central Tendency
1	Jeep	Contrast (intensity based)	1.729	1.257	0.473	27.33	Improved
		Contrast (entropy)	0.108	0.102	0.005	5.10	Improved
		TIR-Squared (intensity based)	11.097	27.658	16.561	149.23	Decreased
		TBIR-Squared (intensity based)	3.555	3.661	0.106	2.97	Decreased
		Binary Area Cross Correlation	0.166	0.239	0.073	43.82	Decreased
2	APC	Contrast (intensity based)	1.121	0.590	0.531	47.36	Improved
		Contrast (entropy)	0.034	0.039	0.004	12.73	Decreased
		TIR-Squared (intensity based)	0.914	2.007	1.093	119.66	Decreased
		TBIR-Squared (intensity based)	0.616	0.658	0.043	6.90	Decreased
		Binary Area Cross Correlation	0.111	0.098	0.013	11.77	Improved
3	Truck	Contrast (intensity based)	1.052	0.769	0.282	26.85	Improved
		Contrast (entropy)	0.061	0.054	0.007	12.07	Improved
		TIR-Squared (intensity based)	1.542	2.316	0.774	50.19	Decreased
		TBIR-Squared (intensity based)	0.594	0.674	0.080	13.52	Decreased
		Binary Area Cross Correlation	0.173	0.207	0.034	19.91	Decreased

Object number	Object type	Name of object metric	Average Value Of Metric Raw data	Average Value Of Metric Smoothed data	Difference	% of change	Position on X axis
1	Jeep	Contrast (intensity based)	7.656	6.565	1.091	14.25	Lower
		Contrast (entropy)	0.157	0.193	0.036	22.87	Increased
		TIR-Squared (intensity based)	12.285	25.928	13.643	111.05	Increased
		TBIR-Squared (intensity based)	4.814	6.955	2.141	44.48	Increased
		Binary Area Cross Correlation	0.387	0.511	0.124	32.05	Increased
2	APC	Contrast (intensity based)	3.781	3.297	0.484	12.80	Lower
		Contrast (entropy)	0.060	0.093	0.033	55.67	Increased
		TIR-Squared (intensity based)	1.820	3.705	1.886	103.63	Increased
		TBIR-Squared (intensity based)	1.385	2.163	0.778	56.19	Increased
		Binary Area Cross Correlation	0.491	0.610	0.119	24.27	Increased
3	Truck	Contrast (intensity based)	3.474	2.514	0.960	27.63	Lower
		Contrast (entropy)	0.074	0.082	0.008	10.32	Increased
		TIR-Squared (intensity based)	2.249	2.525	0.276	12.27	Increased
		TBIR-Squared (intensity based)	0.953	1.151	0.198	20.78	Increased
		Binary Area Cross Correlation	0.433	0.356	0.077	17.74	Lower

TABLE 5.3-III

Temporal Variation Metrics

Number of images in this sequence = 15
Number of objects per image = 3
Type of data smoothing used = Median
Number of images per cluster = 7

Object number	Object type	Name of object metric	Standard Deviation Of Metric Raw data	Standard Deviation Of Metric Smoothed data	Difference	% of change	Central Tendency
1	Jeep	Contrast (intensity based)	1.805	1.176	0.629	34.83	Improved
		Contrast (entropy)	0.090	0.160	0.070	78.38	Decreased
		TIR-Squared (intensity based)	11.796	31.231	19.434	164.75	Decreased
		TBIR-Squared (intensity based)	3.796	4.217	0.421	11.09	Decreased
		Binary Area Cross Correlation	0.169	0.186	0.017	9.97	Decreased
2	APC	Contrast (intensity based)	1.102	0.485	0.618	56.02	Improved
		Contrast (entropy)	0.028	0.049	0.022	78.67	Decreased
		TIR-Squared (intensity based)	0.625	0.735	0.110	17.64	Decreased
		TBIR-Squared (intensity based)	0.509	0.442	0.068	13.29	Improved
		Binary Area Cross Correlation	0.114	0.096	0.017	15.28	Improved
3	Truck	Contrast (intensity based)	1.064	0.860	0.204	19.17	Improved
		Contrast (entropy)	0.065	0.066	0.001	1.13	Decreased
		TIR-Squared (intensity based)	1.622	1.801	0.179	11.05	Decreased
		TBIR-Squared (intensity based)	0.627	0.718	0.090	14.40	Decreased
		Binary Area Cross Correlation	0.175	0.149	0.026	14.94	Improved

Object number	Object type	Name of object metric	Average Value Of Metric Raw data	Average Value Of Metric Smoothed data	Difference	% of change	Position on X axis
1	Jeep	Contrast (intensity based)	7.596	5.918	1.678	22.09	Lower
		Contrast (entropy)	0.146	0.210	0.063	43.42	Increased
		TIR-Squared (intensity based)	12.652	33.666	21.014	166.09	Increased
		TBIR-Squared (intensity based)	4.822	7.297	2.475	51.33	Increased
		Binary Area Cross Correlation	0.397	0.572	0.175	44.15	Increased
2	APC	Contrast (intensity based)	3.902	3.125	0.777	19.90	Lower
		Contrast (entropy)	0.058	0.092	0.034	59.65	Increased
		TIR-Squared (intensity based)	1.731	3.201	1.470	84.91	Increased
		TBIR-Squared (intensity based)	1.349	2.052	0.703	52.09	Increased
		Binary Area Cross Correlation	0.487	0.596	0.109	22.34	Increased
3	Truck	Contrast (intensity based)	3.358	2.215	1.143	34.03	Lower
		Contrast (entropy)	0.075	0.078	0.003	4.01	Increased
		TIR-Squared (intensity based)	2.297	2.439	0.143	6.22	Increased
		TBIR-Squared (intensity based)	0.924	1.168	0.244	26.38	Increased
		Binary Area Cross Correlation	0.451	0.395	0.056	12.45	Lower

TABLE 5.3-IV

Temporal Variation Metrics

Number of images in this sequence = 17
Number of objects per image = 3
Type of data smoothing used = 3x3 Median
Number of images per cluster = 1

Object number	Object type	Name of object metric	Standard Deviation Of Metric Raw data	Smoothed data	Difference	% of change	Central Tendency
1	Jeep	Contrast (intensity based)	1.729	1.137	0.592	34.26	Improved
		Contrast (entropy)	0.108	0.134	0.026	24.35	Decreased
		TIR-Squared (intensity based)	11.097	98.537	87.439	787.93	Decreased
		TBIR-Squared (intensity based)	3.555	6.254	2.698	75.89	Decreased
		Binary Area Cross Correlation	0.166	0.222	0.055	33.17	Decreased
2	APC	Contrast (intensity based)	1.121	0.913	0.207	18.51	Improved
		Contrast (entropy)	0.034	0.050	0.015	44.52	Decreased
		TIR-Squared (intensity based)	0.914	3.605	2.692	294.59	Decreased
		TBIR-Squared (intensity based)	0.616	1.724	1.108	179.99	Decreased
		Binary Area Cross Correlation	0.111	0.128	0.016	14.80	Decreased
3	Truck	Contrast (intensity based)	1.052	0.878	0.174	16.53	Improved
		Contrast (entropy)	0.061	0.065	0.004	6.02	Decreased
		TIR-Squared (intensity based)	1.542	1.618	0.075	4.89	Decreased
		TBIR-Squared (intensity based)	0.594	1.203	0.609	102.66	Decreased
		Binary Area Cross Correlation	0.173	0.144	0.028	16.43	Improved

Object number	Object type	Name of object metric	Average Value Of Metric Raw data	Smoothed data	Difference	% of change	Position on X axis
1	Jeep	Contrast (intensity based)	7.656	4.101	3.555	46.44	Lower
		Contrast (entropy)	0.157	0.143	0.014	8.89	Lower
		TIR-Squared (intensity based)	12.285	35.050	22.764	185.30	Increased
		TBIR-Squared (intensity based)	4.814	6.598	1.785	37.07	Increased
		Binary Area Cross Correlation	0.387	0.442	0.056	14.35	Increased
2	APC	Contrast (intensity based)	3.781	3.368	0.414	10.94	Lower
		Contrast (entropy)	0.060	0.076	0.016	26.40	Increased
		TIR-Squared (intensity based)	1.820	5.468	3.649	200.53	Increased
		TBIR-Squared (intensity based)	1.385	3.339	1.954	141.10	Increased
		Binary Area Cross Correlation	0.491	0.515	0.024	4.84	Increased
3	Truck	Contrast (intensity based)	3.474	1.572	1.902	54.76	Lower
		Contrast (entropy)	0.074	0.080	0.006	7.58	Increased
		TIR-Squared (intensity based)	2.249	1.882	0.367	16.32	Lower
		TBIR-Squared (intensity based)	0.953	1.357	0.404	42.44	Increased
		Binary Area Cross Correlation	0.433	0.312	0.121	27.87	Lower

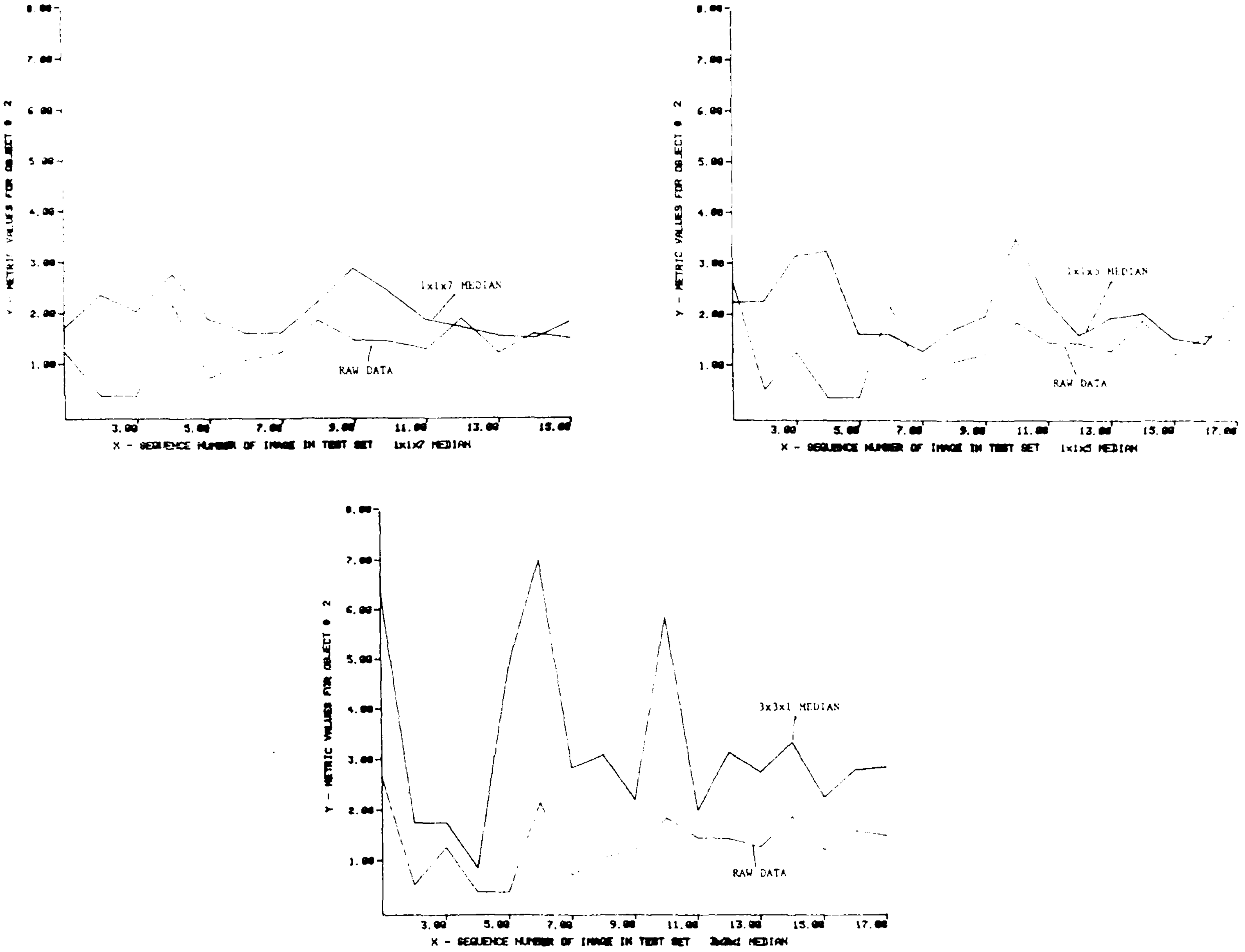

Figure 5.3-10. Metric Comparison of TBIR Squared (Intensity Based)

6.0 CONCLUSIONS AND RECOMMENDATIONS

The temporal processing system used in multiframe integration was designed to solve the two major conceptual problems. The most difficult of the two problems is the extraction of accurate scene motion, defined as the frame to frame positional changes of scene information. More specifically, scene motion entails recording the x,y location of specific scene context as a function of time. The accumulated scene-motion information is used to align subimage windows extracted from a discrete number of consecutive data frames. The second problem is determination of an effective technique for integrating the stack of registered subimage windows. The integration technique must reduce the independent random fluctation in the imagery and improve signal quality and stability. In this section, we present our conclusions and make recommendations for the scene-motion extraction and multiframe-integration software designed under this contract.

Scene Motion Extraction

The implemented system for extracting scene motion consists of an interest point operator, a partition and local maximum operator, an intensity-based area correlator, and an optical flow noise filter (Figure 6.0-1).

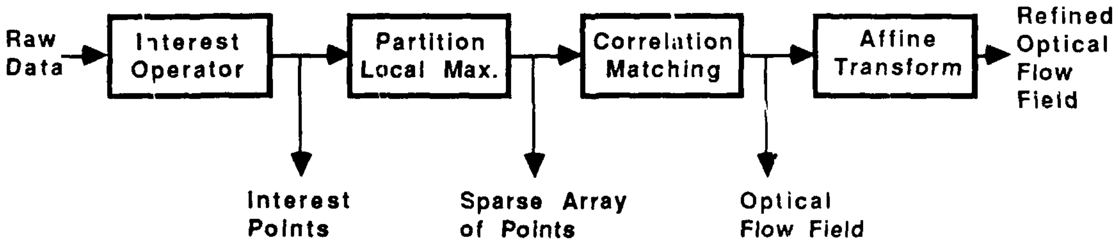
Raw Data
Interest Operator
Partition Local Max.
Correlation Matching
Affine Transform
Refined Optical Flow Field
Interest Points
Sparse Array of Points
Optical Flow Field

Figure 6.0-1. System for Extracting Scene Motion

1 Size contrast operator

The size contrast operator (Figure 6.0-2) emphasizes unique local regions, based on intensity information. The uniqueness feature of the operator is contrast. Contrast is a fundamental feature; texture, gradient, variance, and other image features are dependent upon contrast. This constraint provided the motivation for the use of this feature.

The size contrast operator has the advantage of being size adjustable. This feature allows it to be gated for specific image context. In our experiment, the inner window was set to object size to maximize the potential for nominating vehicles as the feature points to be tracked. Tracking vehicles is highly desirable since the multiframe-integration registration process requires a flow vector near each vehicle. When the flow vector directly represents the temporal transformation of a vehicle, misregistration errors are minimized. In addition to the size criterion, the size contrast metric provides information about the integrity of each feature (Figure 6.0-3). Locations where the metric forms high sharp peaks represent well organized contrast regions, which are well suited for feature tracking. Locations where the metric is low or where the metric is constant over a large area represent low confidence regions.

The overall performance of the size contrast operator for the data sets was very good, considering the characteristics of the imagery. The close-range image data set was almost void of any detail, with the exception of the two military vehicles. For this data set, both vehicles were selected as local points of maximum interest. Both vehicles were sucessfully tracked through the entire image sequence. The two-long range image data sets were void of any detail and contained very low contrast vehicles. Neither of these images sets contained characteristics that favored feature

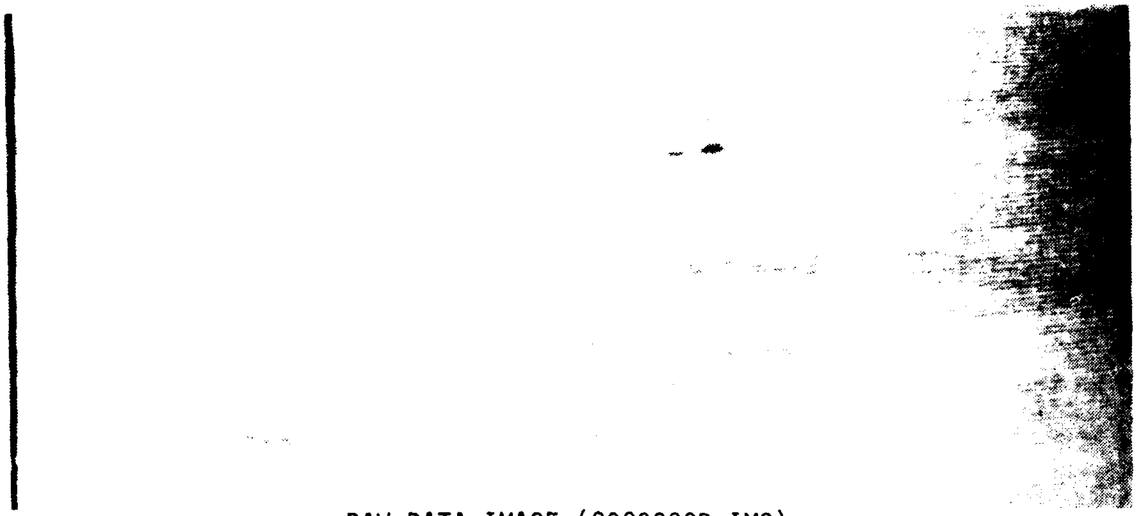

RAW DATA IMAGE (2020000D.IMG)

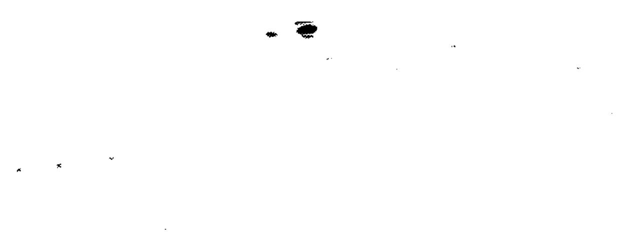

Figure 6.0-2. Size Contrast Metric Image

tracking. Although the size contrast windows were optimized for long range vehicles, the metric responses were low and not well organized. As a result the selected features could not be tracked throught either of the two image sets.

Results from the experiments indicate that a constraint exists when image characteristics are not well represented. Bland image conditions do not provide feature information considered significant enough to track with the degree of accuracy required for multiframe

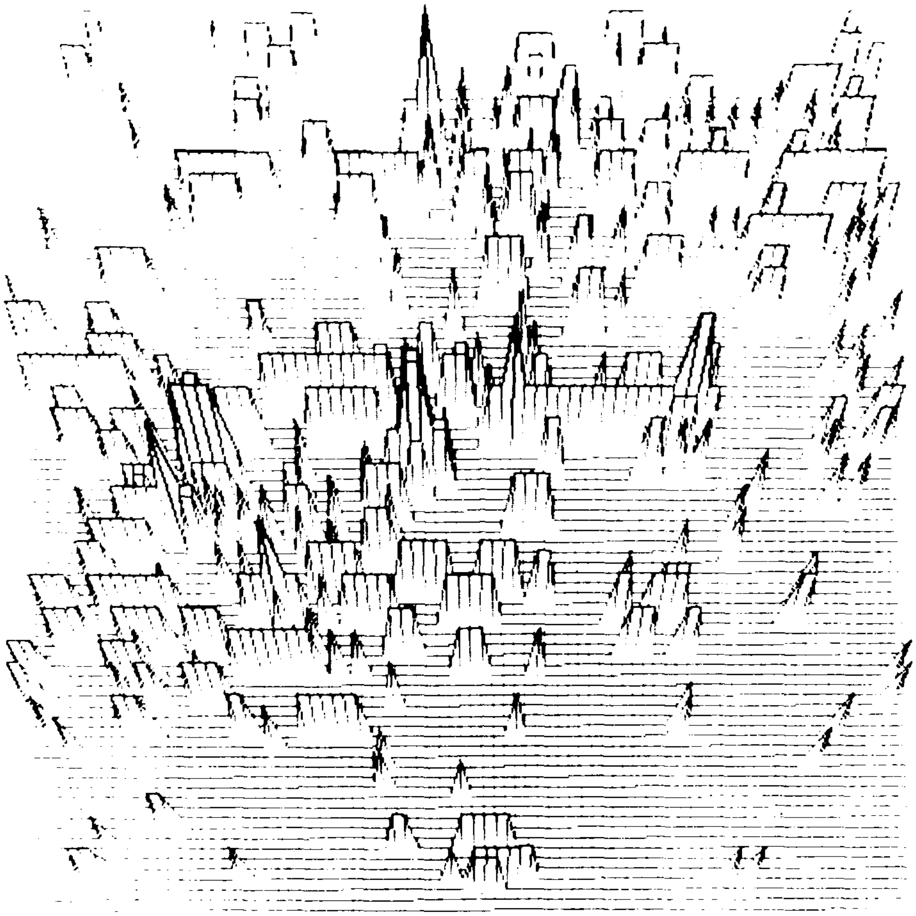

Figure 6.0-3. Size-Contrast Metric Image

integration. Image enhancement techniques such as histogram stretching are not practical for improving contrast because such techniques do not improve the fundamental elements represented in the data. Such techniques mainly improve the aesthetics of the image.

The results of the size contrast operator must be correctly interpreted to manage the interest point extraction function. Currently, we record contrast metrics, average metric, and standard deviation of the metrics for each partitioned window. Based on these values, a determination of whether to select a feature from a partitioned window can be made. In addition, when features are sparse in a specific area of the image, other well organized contrast features can be substituted. This upgrade will make it possible to predict the accuracy of the scene motion extraction subsystem by interpreting the strength of the contrast features selected for tracking.

2 Partition and local maximum operator

The partition and local maximum operator controls the selection of feature points from the size contrast metric image and the spatial distribution of those points. Currently, the user supplies the partitioning grid size to the operator. The grid (Figure 6.0-4) is an effective approach for controlling the spatial distribution of features. The feature point selection process is easily adaptive to range. To increase the number of selected points required for long range images, the grid density is simply increased. The grid size selection process could be made autonomous by using ground truth information about range to set the grid parameters. The recessed boundary of the grid from the edge of the image assures that each selected feature has an opportunity to be tracked. If a feature is too close to the edge of the image, a full correlation window cannot be placed about it.

The partitioning technique has one major drawback in that features are forced to be selected in windows that are void of any significant contrast. Window interpretation, which is discussed in the size-contrast evaluation section, would alleviate this problem. The optimum location for this upgrade is within the local maximum selection operator (Figure 6.0-5). This operator currently selects the location of maximum metric response in each window without regard to feature credibility. The statistical examination of each window prior to point selection would avoid nominating meaningless features that cannot be tracked.

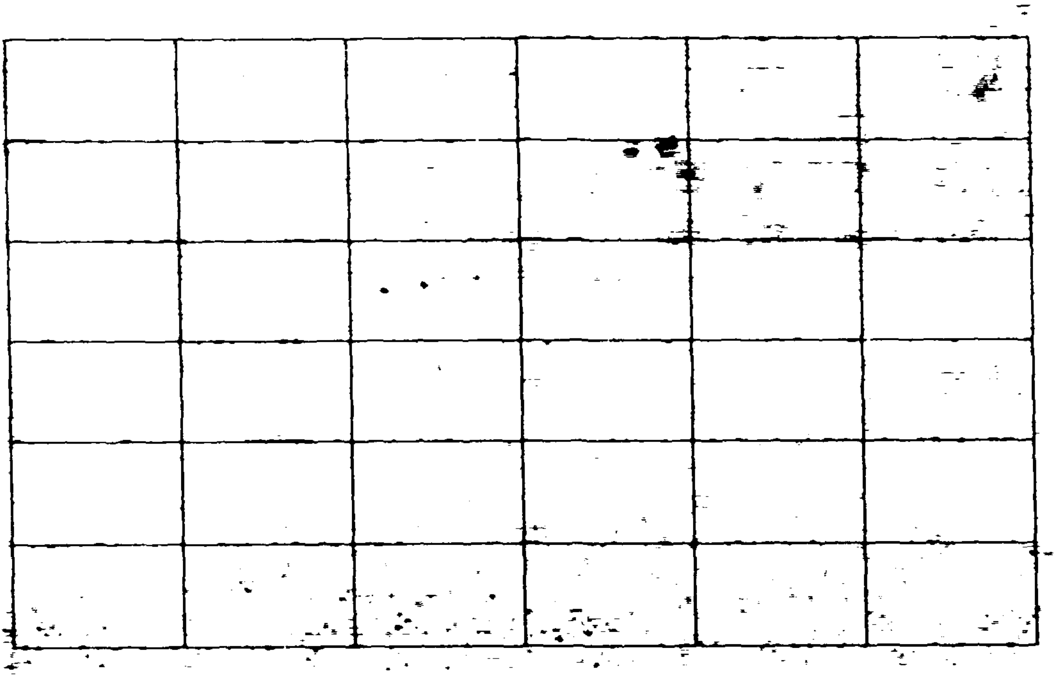

Figure 6.0-4. Size-Contrast Metric Image with Grid Partition

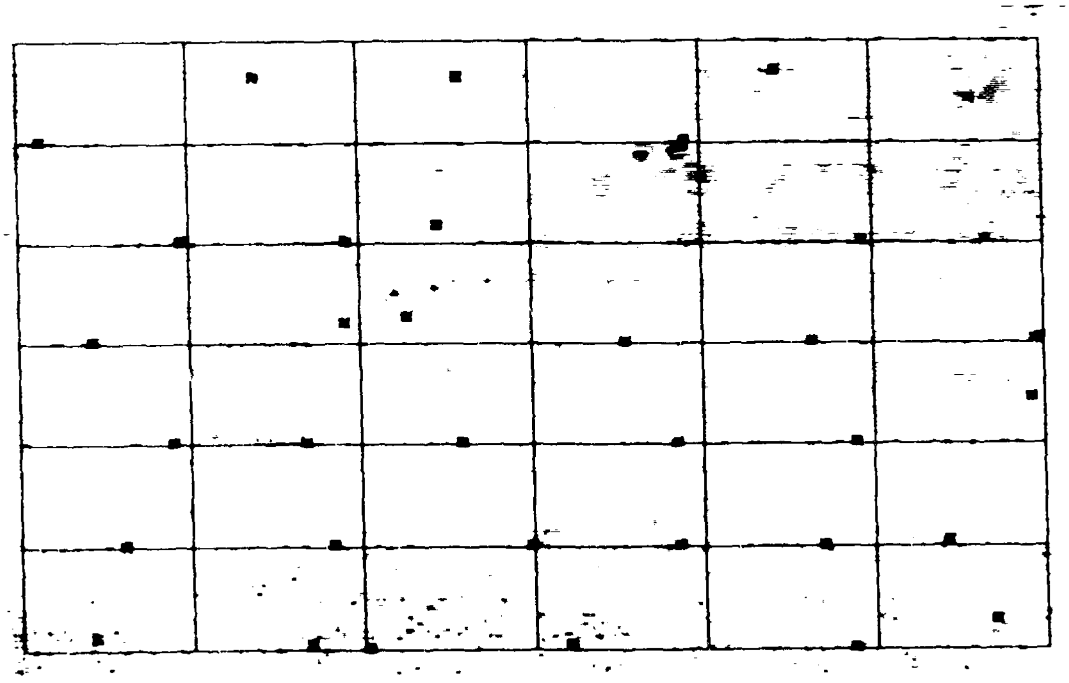

Figure 6.0-5. Local Maximum Metric Selection (36 Interest Points)

3 Full intensity area correlation

Frame to frame feature matching (tracking) is accomplished through the application of a full intensity (all 8 bits) area correlator. Accurate feature tracking is imperative for successful of multi-frame integration. Misalignment of subframe windows due to feature registration errors degrades the multiframe integration. Instead of reducing noise and improving signal quality, registration errors add additional degenerative effects.

The correlation process is the most difficult and time-consuming operator in the motion extraction subsystem. The correlation operator is applied iteratively to each feature point over an area defined as the search area (Figure 6.0-6).

For 36 feature points and a search area of 25 by 25 pixels, 22,500 applications of the correlator are required. The number of applications does not take into account the mathematical computations necessary to compute each correlation measure. The accumulation of correlation measures over each search window represents a correlation surface (Figure 6.0-7).

The organization of the correlation surface determines the degree of similarity between each contrast feature in the last and current frame. A close examination of four search areas (Figure 6.0-8) shows the variations in behavior of the correlator for different contrast features. The ideal correlation surface would depict a singular peak representing the location of great similarity (correlation 1).

The success of intensity-based area correlation is totally dependent on the characteristics of the features being matched. In the close-range test set, the correlation operator very accurately determined the frame to frame positional changes of the two

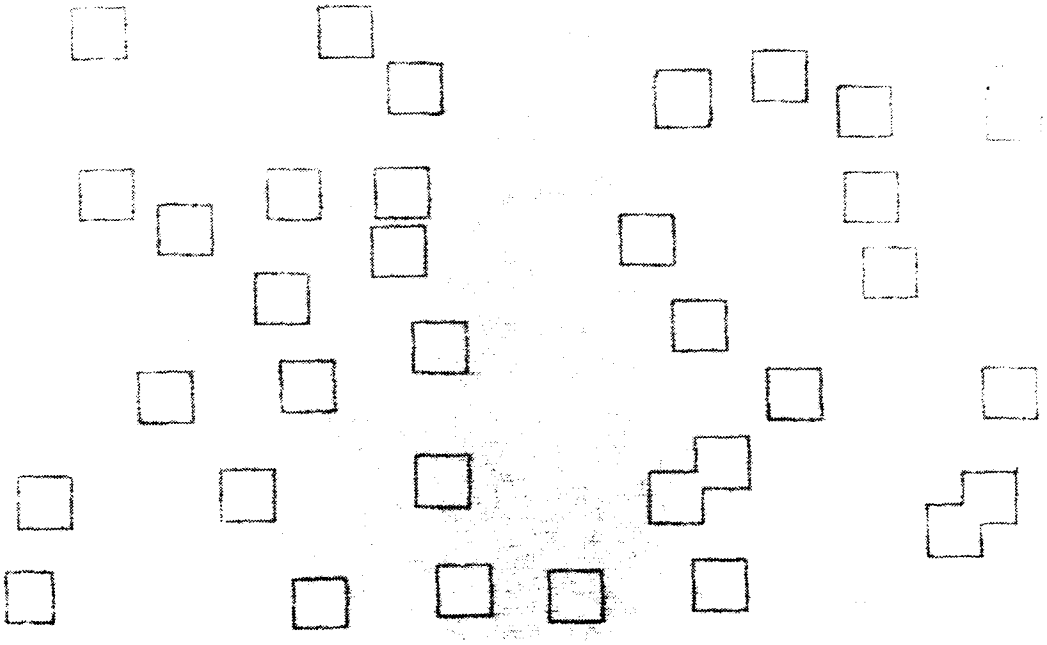

Figure 6.0-6. Area Correlation Search Windows

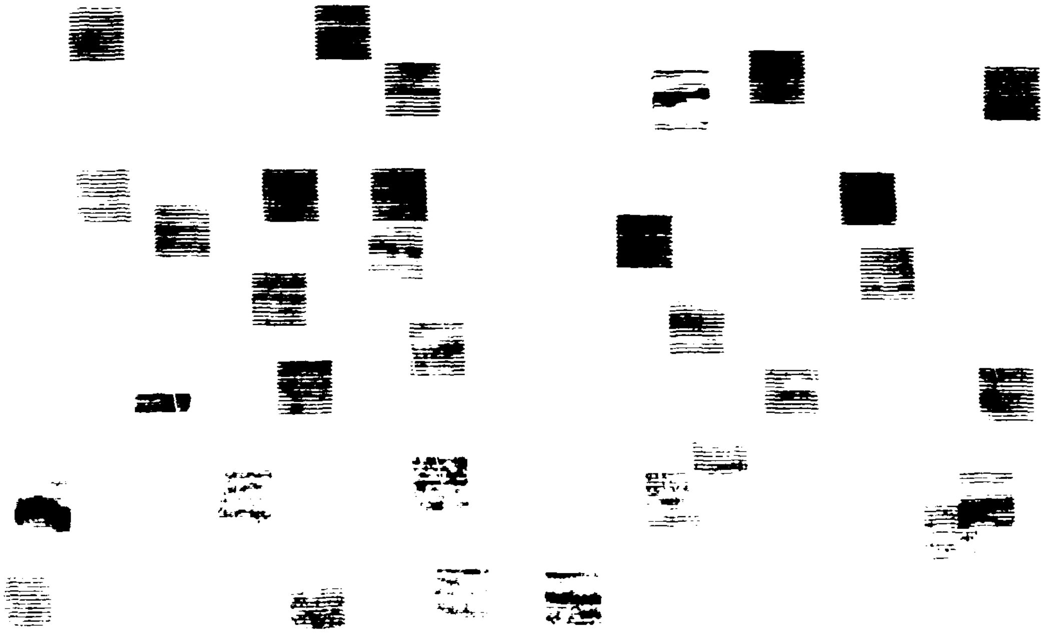

Figure 6.0-7. Correlation Surface for Point Matching

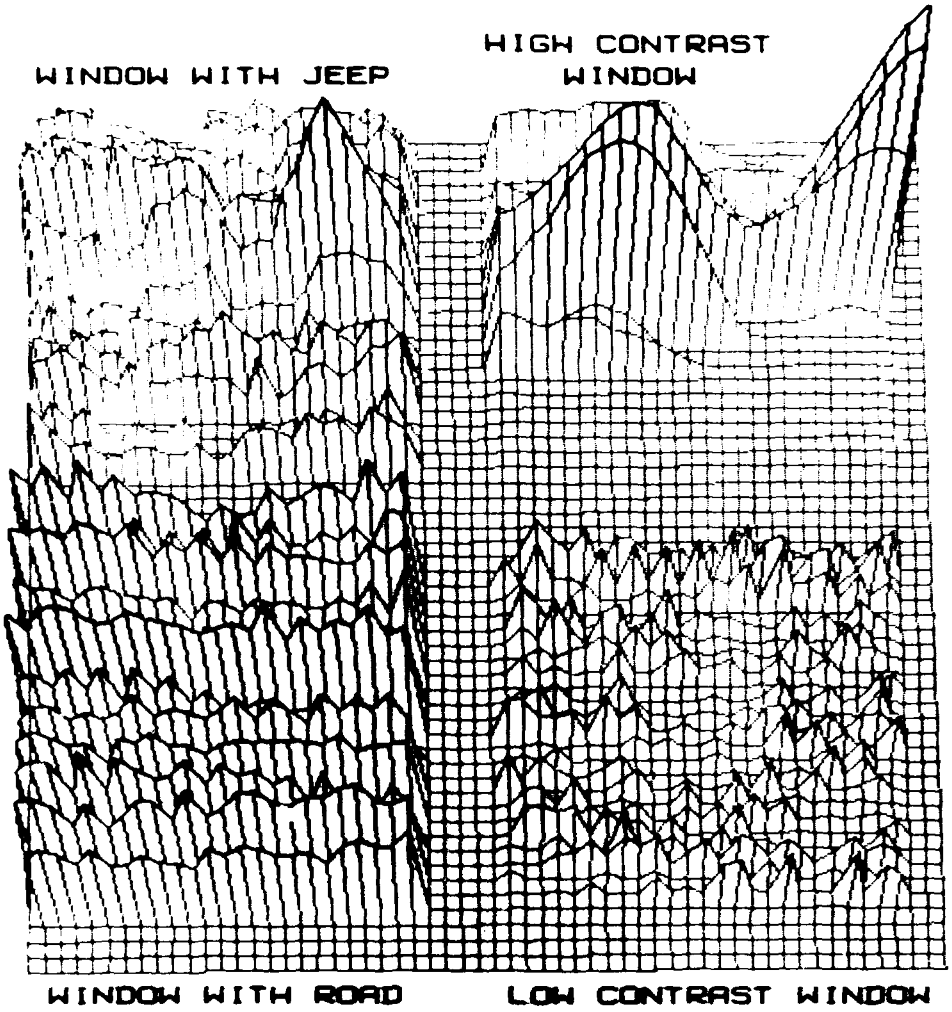

Figure 6.0-8. Correlation Surface of Various Image Features

vehicles. In the latter two test sets, the features were so poorly represented that accurate correlation was not possible. In fact, the manualy derived correlation history, which was required to process these two test sets, was extremely difficult to obtain and was only partially accurate.

Although the intensity-based area correlation has inherent weaknesses, it is still one of the better feature-matching techniques.

AD-A190 965 ADAPTIVE SEGMENTATION EVALUATION(U) MARTIN MARIETTA AEROSPACE ORLANDO FL R PATTON 24 SEP 87 OR-19130 DAAL02-85-C-0084 2/2

UNCLASSIFIED F/G 20/6 NL

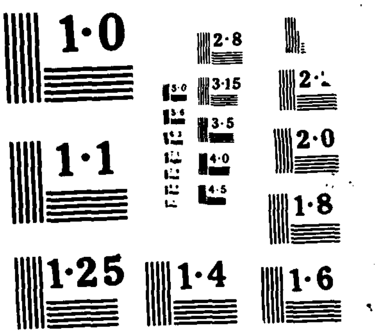
1·0
2·8
3·15
3·5
4·0
4·5
2·0
1·1
1·8
1·25
1·4
1·6

When intensity area correlation fails due to poor feature representation, other techniques such as peak intensity matching, feature vector-based matching, and segmentation centroiding also fail.

A viable solution to poor correlation is to switch between multiframe processing and independent-frame processing, based on the success of the correlators. Most correlation problems occur with long-range poor-contrast images. As the sensor closes on the scene or as contrast conditions improve, multiframe processing can be instituted.

4 Optical flow noise filter

The affine transform is used to identify and to remove feature points that do not accurately represent the frame to frame positional changes of scene context. These feature points are unreliable for use in multiframe integration processing. Discrimination between valid and invalid feature points is accomoplished by building a model of the scene motion and by comparing the history of each feature mode. To initially create a reliable model, a sufficient number of valid points must exist.

We were unable to evaluate the effectiveness of the affine as a noise filter because none of the three data sets generated enough valid feature points for the affine to create a model of the scene motion.

Assessment of the Multiframe Integration

The experiments conducted on the three test sets were used to assess the performance of the data smoothing techniques used for multiframe integration. The primary filter used for multiframe data smoothing for the three test data sets was the lxlxn median. The lxlxn mean and lxlxn mode-median filters did not produce significantly different results to warrent continued testing. All of the tests consisted of running the rule directed segmenter on the raw data, multiframe smoothed data (1x1xn median), and conventionally filtered data (3x3x1 median, independent frame filter) generated for each test data set. We conducted a comparative study of the rule directed segmenter performance results and the behavior of a set of features computed on the data types.

The experiments conducted on data set 1 provided the best overall results. A comparison of the rule directed segmenter applied to the three data types for data set 1 accentuated the primary strengths of multiframe smoothing. Both conventional and multiframe filtering improved segmentation results over that of the raw data results. The primary difference was in the behavior of the features computed on the three data types. The features computed on the raw data and conventionaly filtered data contained random fluctations and wide distributions, which are typical for FLIR data. The features computed on the multiframe smoothed data were better clustered and showed increased signal qualities. The improved feature organization and higher response is an indication of the increase in data stability and noise reduction. These properties have two important consequences. First, the improved signal quality greatly reduces the need for special purpose processing by each ATR component to overcome image ambiguities found in the raw data. Second, features that represent higher levels of structural detail usually masked by noise can be computed for improved object discrimination and classification performance.

The experiments conducted on the other data sets had similar results. Both of the test data sets used during these experiments consisted of low contrast images void of any significant context. These conditions made it necessary to manually derive the scene motion information needed for frame to frame registration of the detected vehicles. The scene motion information was estimated to be 75 percent reliable. Nevertheless, the overall results of the data smoothing process were positive. Improvements in the structural characteristics of the vehicles were evident from an examination of the features computed on the three data types. These results for low contrast images characterized by scene motion information demonstrate that data smoothing is successful under less than ideal conditions.

Multiframe Integration Using Edge Maps

The initial research using multiframe smoothing consisted of registering and integrating subimages of raw data placed about a detected vehicle. All subsequent processing was performed on the smoothed subimages. Additional research was conducted on integrating edge maps generated by applying the composite edge operator to the raw images. The edge maps were handled in the same manner as the raw data images. The process consisted of registering and integrating subimages of edge map information place about a detected vehicle. Test data for set 3 contained one jeep, one APC, and one truck, all at long range (over 6 kilometers). This data was used for the experiments. The basic idea was to use multiframe data smoothing to stabilize the edge map operated on by the segmentation algorithm. The edge map integration process consisted of registering a set of five edge magnitude subimages (Figure 6.0-9) and applying the 1x1x5 median. The direction associated with the selected edge magnitude was retained as the direction for the edge point.

A comparison of the raw- and smoothed edge images (Figure 6.0-10) shows the benefit of multiframe edge map integration. The properties of stability and improved organization depicted in the smoothed edge images are consistent with those seen in the raw-data smoothing results. The implication from these experiments is that data smoothing is an effective data enhancement function when used as a pre-processor or as an imbedded algorithm function.

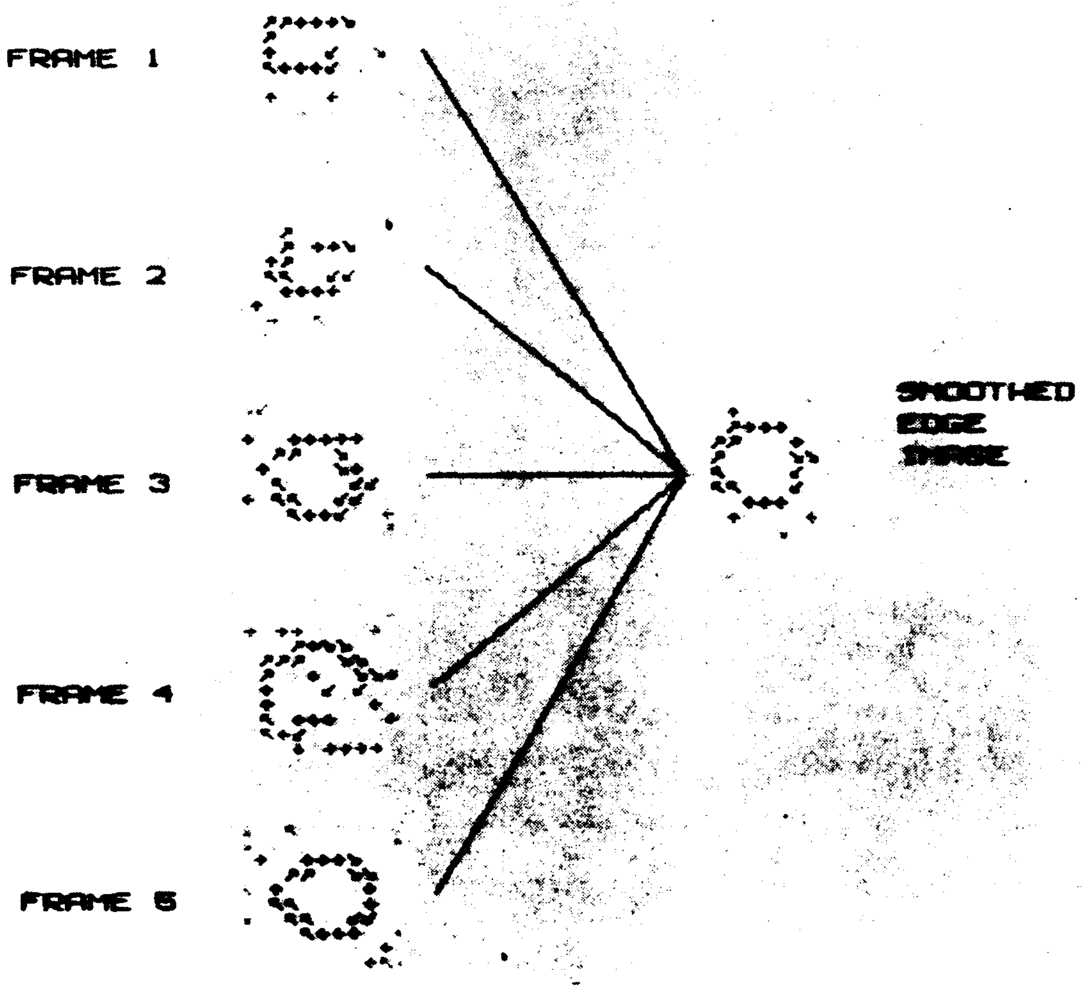
FRAME 1
FRAME 2
FRAME 3
FRAME 4
FRAME 5
SMOOTHED
EDGE
IMAGE

Figure 6.0-9. Multiframe Edge Smoothing (Jeep at 6000 Meters)

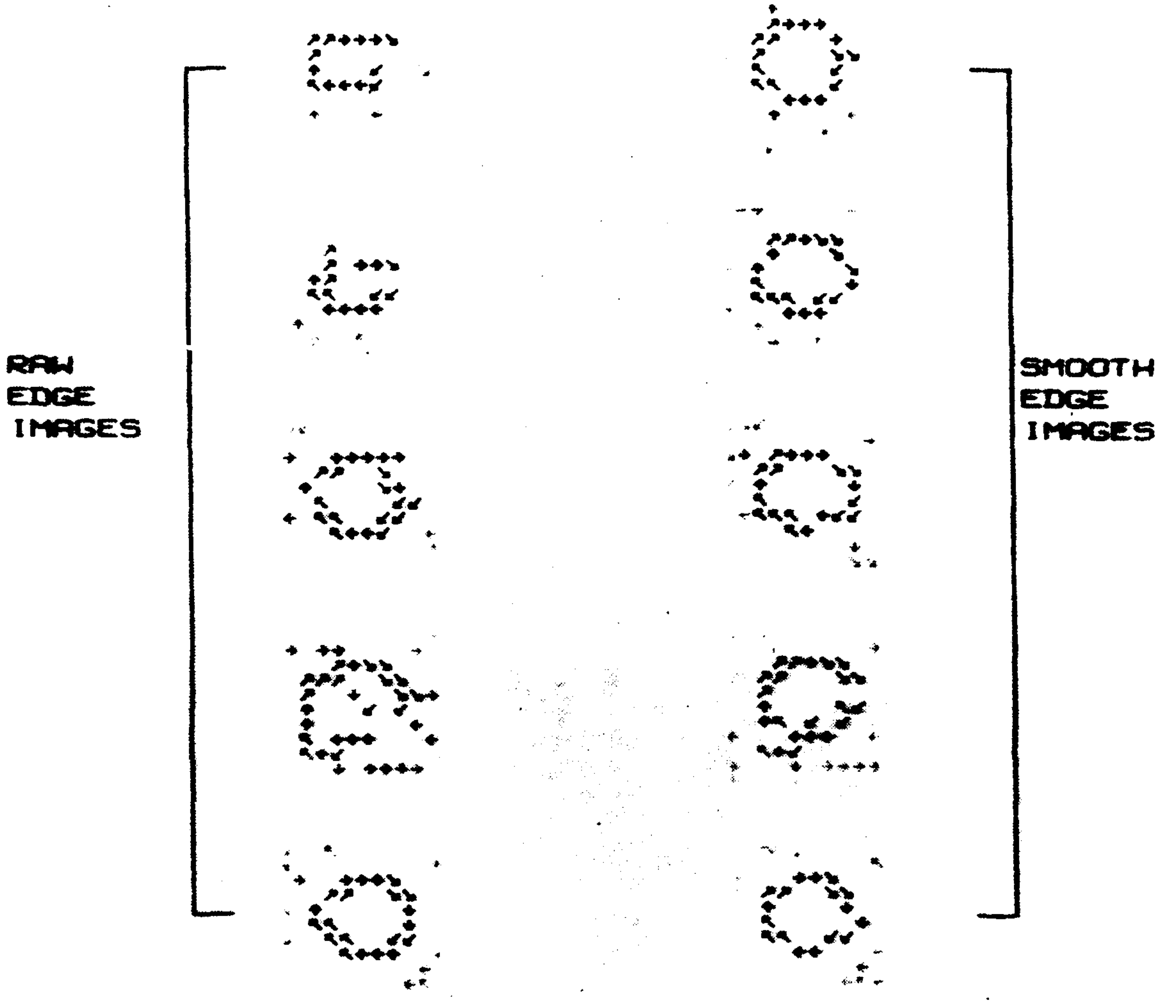
RAW
EDGE
IMAGES
SMOOTH
EDGE
IMAGES

Figure 6.0-10. Comparison of Independent and Multiframe Edge Smoothing

END
DATE
FILMED
5-88
DTIC